ELECTRON PARAMAGNETIC RESONANCE

(Studies of CuO, Ba-Cu-O and Eu-Cu-O
Systems and Eu-Ba-Cu-O Superconductor)

DISSERTATION SUBMITTED IN PARTIAL FULFILMENT
OF THE REQUIREMENTS FOR THE AWARD
OF THE DEGREE OF

Master of Philosophy
IN
PHYSICS

BY
ALEX PUNNOOSE

DEPARTMENT OF PHYSICS
ALIGARH MUSLIM UNIVERSITY
ALIGARH (INDIA)
1992


DS 2409


DS2409

PROFESSOR

DEPARTMENT OF PHYSICS
ALIGARH MUSLIM UNIVERSITY
ALIGARH 202002 (India)
Telc No. : 9001
Tel. No. : 564 230 *AMU IN*

30 June 1992

CERTIFICATE

Certified that the work presented in this dissertation entitled **ELECTRON PARAMAGNETIC RESONANCE** [Studies of CuO, Ba-Cu-O and Eu-Cu-O systems and Eu-Ba-Cu-O Superconductor] is the original work of **Mr. Alex Punnoose**, done under my supervision.

[**R.J. SINGH**]
Professor of Physics.

ACKNOWLEDGEMENTS

It gives me great pleasure to express my sincere and profound gratitude to my supervisor **Prof. R.J. Singh**, Department of Physics, Aligarh Muslim University, Aligarh, for his invaluable guidance and constant inspiration throughout my studies.

I express my sincere thanks to **Prof. Israr Ahmad** (former Chairman) and **Prof. B.N. Khanna**, Chairman, Department of Physics, Aligarh Muslim University, Aligarh, for extending various facilities and excouragements. Thanks are also due to my teachers, staff members and non-teaching staff of this Department.

I take this opportunity to express my special gratitudes to **Prof. B.B. Tripathi**, Department of Physics, I.I.T., New Delhi, **Dr. G.V.S. Murthy**, School of Physics, Hyderabad University, **Dr. Afaq Ahmad**, Department of Chemistry, Aligarh Muslim University, Aligarh, and **Mr. S.V. Sharma**, Advanced centre for Material Science, I.I.T, Kanpur for their various kind of helps during my studies. I am also highly thankful to **Dr. C.K. Sarkar** and **Miss Kalpana Santra**, Department of Electronics and Telecommunication Engineering, Jadavpur University, Calcutta, for providing

thin films for my studies.

I am grateful to **Dr. Mohd. Umar**, Lecturer, University Polytechnic and **Dr. M.I. Haque**, Lecturer, Dawakhana Tibbiya College, of the Aligarh Muslim University, Aligarh, for various helps and stimulating discussions. Cheerful cooperation and friendly interactions with my colleagues **Mr. Jilson Mathew** and **Mr. B.P. Maurya** and with all other friends are also gratefully acknowledged.

I am thankful to the **Co-ordinator**, DSA/COSIST, for providing financial supports during this work. **Mr. Mohd. Owais Khan**, deserve no less appreciation for neat and clean typing of this dissertation.

Finally I wish to put on record, the constant encouragements, inspiration, and support I received from my **mother, brother, sisters** and my well wishers throughout my studies, without which I would not have come to this level.

ALEX PUNNOOSE

30 June 1992

PREFACE

Even after six years of the discovery of High Temperature Superconductivity, the research in this field continues to arouse the interest of the world wide scientific community. A complete understanding of the phenomenon, their peculiar features and the microscopic mechanism etc., are not fully successful yet. There is a wide speculation that the magnetism in these materials, especially that associated with the Cu-O chains and layers has an important role in the superconducting mechanism. Electron Paramagnetic Resonance is a very powerful technique for studying the magnetism associated with the Cu spins present in these systems, as well as the local environment about it. A better understanding of these, will indeed help to unravel the clues behind the mechanism of High Temperature Superconductivity.

The magnetism of copper ions in the high-T_c oxides appears to be much complicated, in the literature. It was surprising to note that a proper understanding of the magnetic complexities even in the more simpler compound, copper oxide which is the most important ingredient of all the high-T_c superconductors, is also missing. Thus it was planned to investigate the basic ingredients of all the

high-T_c superconductors, singly and in binary, ternary, quartnery etc., combinations after subjecting it to different chemical and thermal treatments and by observing how the EPR signal is modified at each step and finally becomes absent in the superconducting phase. The present work deals with the EPR study of copper oxide (CuO), Ba-Cu-O and Eu-Cu-O systems and the $EuBa_2Cu_3O_{7-d}$ high-T_c superconductor.

In chapter 1, an introduction to the basic theory of electron paramagnetic resonance, the various parameters governing this technique and its potential applications are discussed concisely. A brief note on the experimental set up for EPR and its operation is also included.

Chapter 2, is aimed at introducing the phenomenon of superconductivity. A brief out line of the conventional superconductors, their basic properties, and important mechanisms are given, along with BCS theory of superconductivity in a little detailed way. Since the present study is concentrated on the high-T_c superconductors, the structures of the four major families of high-T_c oxide systems, their special features, different methods of preparation etc., are discussed in great length. A qualitative picture of the various pairing mechanisms based on BCS theory and a detailed discussion on the

Resonating Valence Bond Theory are also presented. Due to the current interest, a brief note on the occurence of superconductivity in alkali doped C_{60} Fullerenes is incorporated.

The third chapter is a review of the present status of EPR investigations on high-T_c superconductors, based on a detailed literature survey. The results of EPR studies of these compounds right from their discovery till date are presented and are compared with the EPR observations of many of their related and parent non-superconducting impurity phases. The different theoretical explanations for the observed EPR silence of copper in the high temperature superconducting compounds are discussed.

The results of the EPR investigations carried out by us on copper oxide bulk powder after subjecting to different heat treatments is presented in chapter 4. The study is further extended to CuO thin films deposited on different substrates.

In chapter 5, the results of the EPR studies of BaO-CuO, Eu_2O_3-CuO binary combinations and the EuBaCuO superconductor are presented. The result of the resistance studies of the BaO-CuO binary system is also included and is compared with the results of the EPR studies.

* * * * * *

CONTENTS

* * * * * * *

* * * * * * *

1.1 INTRODUCTION

In 1936, Gorter [1,2] demonstrated that a paramagnetic salt when placed in a high frequency alternating magnetic field, absorbed energy and that this was influenced by the application of a static magnetic field either parallel or perpendicular to the alternating magnetic field. Later in 1945, Zavoiski of U.S.S.R. [3,4] obtained the first electron paramagnetic resonance spectra. At the same time observation of EPR spectra by Cummerow and Halliday of U.S.A. [5] also reported. Since then this phenomenon has become a technique of immense importance in physical and bio sciences, medicine and various other desciplins.

1.2 PARAMAGNETIC RESONANCE PHENOMENON

It is well known that a paramagnetic ion has a magnetic moment and therefore its ground state is degenerate. If this ion is placed in a strong static magnetic field the degeneracy is lifted and the energy levels undergo a Zeeman splitting. Application of an oscillating magnetic field of appropriate frequency will induce transitions between the Zeeman levels and energy is absorbed from the electromagnetic field. If the static magnetic field is slowly varied, the absorption

shows a series of maxima. The plot between the absorbed energy and the magnetic field is called the electron paramagnetic resonance spectrum.

A system of charges exhibits paramagnetism whenever it has a resultant angular momentum. Such paramagnetic system includes elements containing 3d, 4d, 4f, 5d, 5f, 6d etc., electrons, atoms having an odd number of electrons like hydrogen, molecules containing odd number of electrons such as NO_2, NO etc., and free radicals which posses an unpaired electron like CH_3, DPPH etc., are among the suitable candidates for EPR investigation. Trapped electrons or holes in colour centers and conduction electrons in semiconductors and metals are also can be studied using this technique. Substances which are not paramagnetic can be investigated by disrupting the normal bonds and producing paramagnetic species in them by subjecting it to high energy radiation [6], mechanical stress [7-10], thermal excitation etc.

If an electron has both spin and orbital motion, the total angular momentum $\vec{J}$ is obtained by the sum of its orbital momentum $\vec{L}$ and spin momentum $\vec{S}$, i.e. $\vec{J} = \vec{L} + \vec{S}$ where $\vec{J}$ has the possible values from $|L-S|$ to $|L+S|$ differing by unity. The associated magnetic moment of the electron will be

$$\vec{\mu} = g \beta \vec{J}$$

Where β is the Bohr magneton and g is known as the spectroscopic splitting factor. Classically the energy of a magnetic moment in magnetic field $\vec{B}$ is given by

$$E = \vec{\mu} . \vec{B} \tag{1.2}$$

and corresponding quantum mechanical Hamiltonian is

$$H = g\beta \vec{J} . \vec{B} \tag{1.3}$$

If the magnetic field is applied along the z-axis, components of $\vec{B}$ along x and y-directions will become zero and B_z=B, so that scalar product becomes

$$H = g\beta J_z \vec{B} \tag{1.4}$$

The eigen values of equation (1.3) are just the multiplets of ($g\beta\vec{B}$) of the eigen values of J_z. Corresponding to M_J values, there will be 2J+1 energy levels which are equally spaced and their energies are given by,

$$E = g\beta \vec{B} M_J \tag{1.5}$$

Where M_J=J,J-1,....-J+1, -J

Application of microwave radiation of frequency ν, having energy $h\nu$, perpendicular to the direction of static magnetic field $\vec{B}$, results in magnetic dipole transitions between adjacent levels such that $\Delta M = \pm 1$. The resonance condition is given by

$$E_M - E_{M'} = g\beta \vec{B} = h\nu \tag{1.6}$$

The value of g would be equal to 2.0, if the electron is completely free. Value of g usually differs from 2.0, because the electron is not entirely free and is still

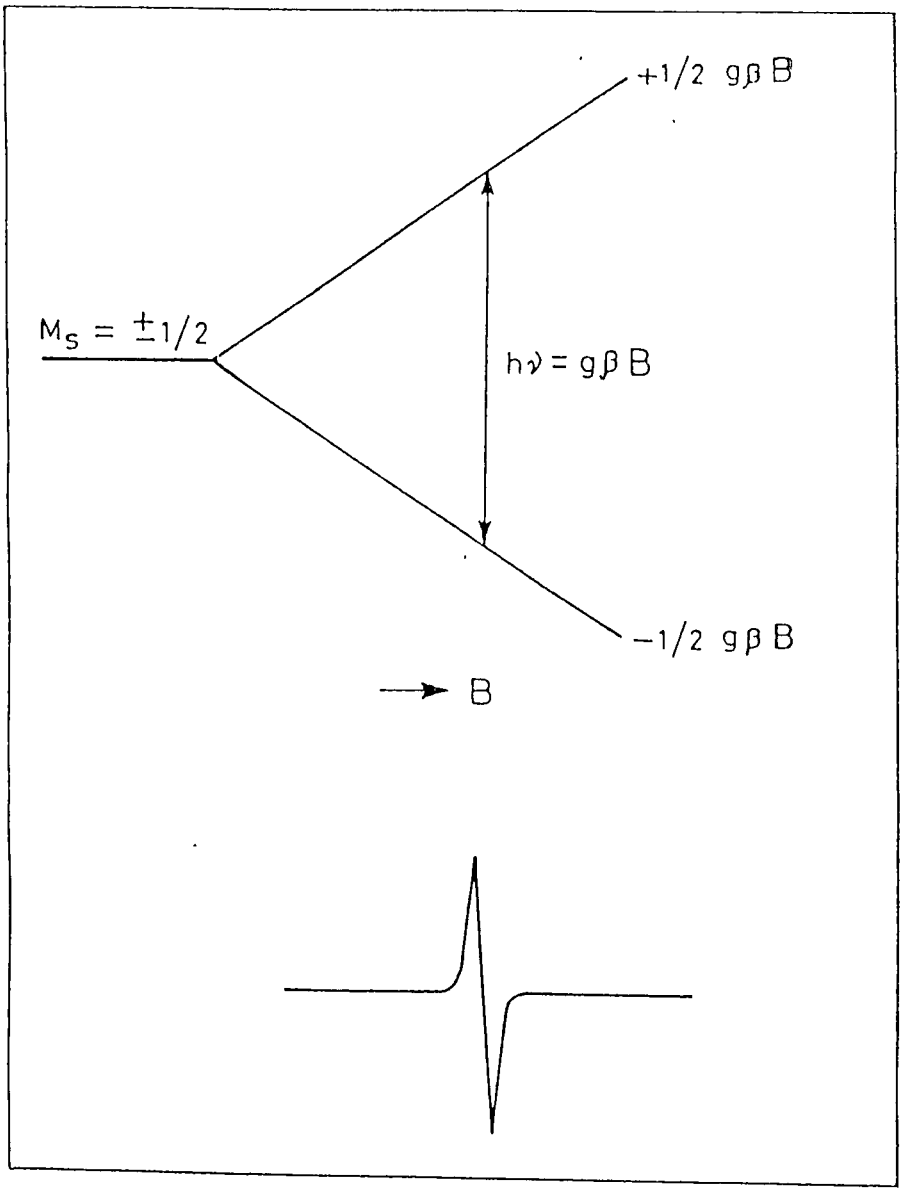

Fig. 1.1 Energy level diagram showing Zeeman splitting for free electron spin system.

affected by the binding forces [11,12]. Probability of these transitions are given by the square of the matrix element connecting M^{th} and $(M+1)^{th}$ levels as

$$P_{M_J \leftrightarrow M_{J\pm1}} = \text{Constant } [J(J+1)-M_J(M_{J\pm1})]^{\frac{1}{2}} \qquad (1.7)$$

This shows that different $M_J \leftrightarrow M_{J\pm1}$ transitions will have different intensities.

1.3 CRYSTAL FIELD EFFECTS

Splitting of energy levels in EPR occurs under the effect of two types of fields, namely the internal crystalline field and applied magnetic field. While studying a paramagnetic ion in a diamagnetic crystal lattice, two types of interactions are observed, i.e. interactions between the paramagnetic ions called dipolar interaction and interactions between the paramagnetic ion and the diamagnetic neighbours called crystal field interaction. For small doping amount of paramagnetic ions in the diamagnetic host, the dipolar interaction will be negligibly small. The latter interaction of paramagnetic ion with diamagnetic ligands modify the magnetic properties of the paramagnetic ions. According to crystal field theory, the ligands influence the magnetic ion through the electric field which they produce at its site and their orbital motion get modified. The crystal field interaction is affected by the electrostatic screening by the outer electronic shells. Depending upon its magnitude

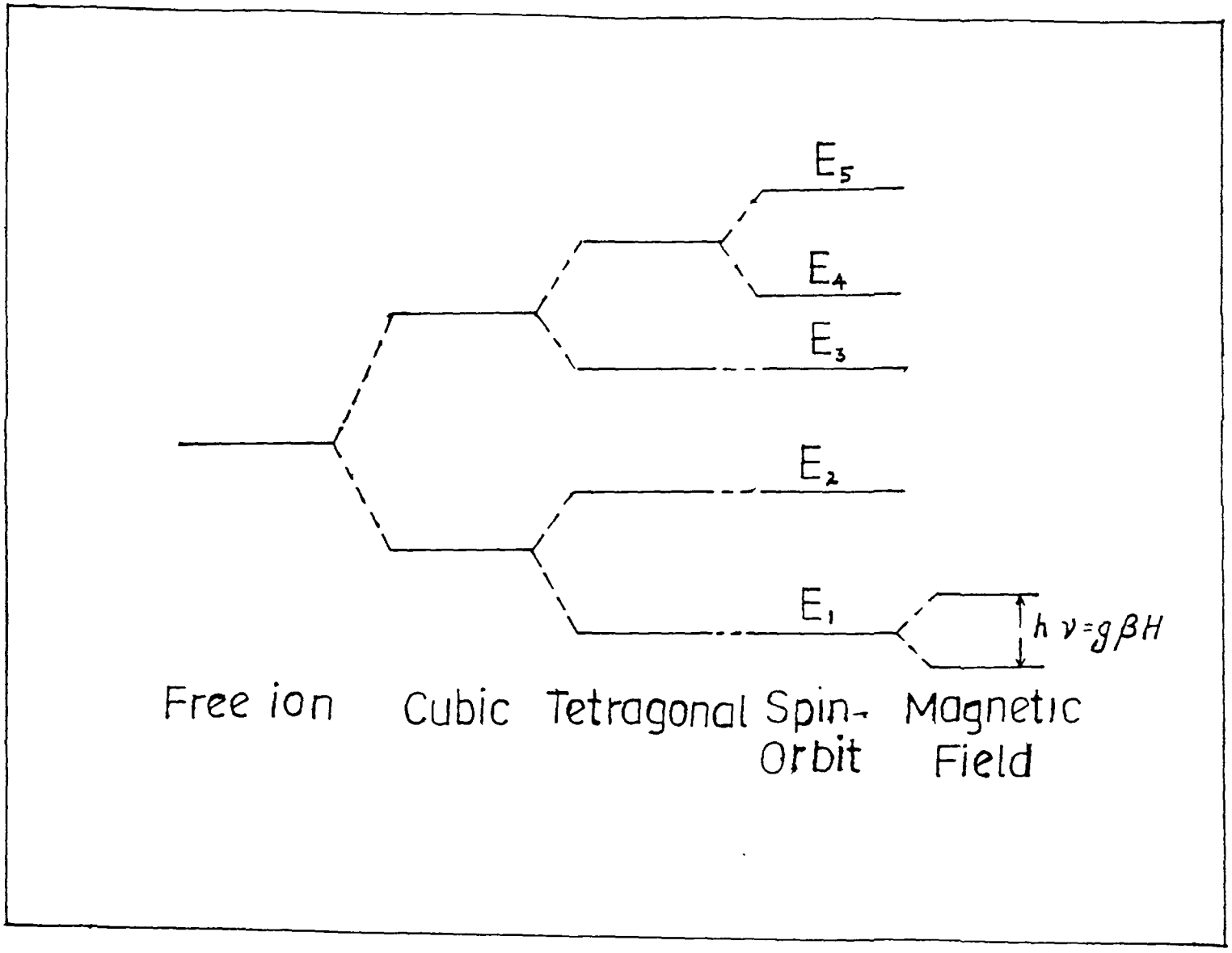

Fig. 1.2 Electronic splitting of energy level of Cu^{2+} in different crystal fields.

relative to other interactions, the crystalline field interaction is generally classified into three categories.

(a)**Weak Crystal Field**

The crystal field interaction will be weaker than the spin-orbit coupling in this case. Rare earths and actinide compounds are good examples of this type. It is due to the fact that the paramagnetic shell of the electrons, i.e. 4f or 5f, lies fairly deep within the ion and is shielded from the crystal field by closed shells of 5s and 5p or 6s and 6p electrons, respectively.

(b) **Intermediate Crystal Field**

When the crystal field interaction is greater than spin orbit interaction but is less than the coulombic interaction between electrons. The best example of these are hydrated salts of the iron group. This situation can be described by considering the orbital motion as clamped by crystal field and making it unable to respond to an applied magnetic field. This is known as quenching of orbital angular momentum. In this case, the magnetic properties are all due to spin which is affected only weakly by crystal field through spin-orbit coupling.

(c) **Strong Crystal Field**

When the crystal field interaction is of the order of the energy of mutual interaction between electrons. For the ions of 4d and 5d transition groups, there is a tendency

of covalent bonding due to which the orbitals of paramagnetic ion and neighbouring ligands overlap appreciably. In this case due to strong covalent bonding, the crystal field assumption actually does not hold.

1.4 RELAXATION PROCESSES

The effect of microwave radiation absorption will eventually be to equalize the population of two levels. When the population in the two levels becomes equal, it will not be possible to detect EPR absorption signal from the system as there would be no net transfer of energy from the radiation to the spins. But in practice we would be able to detect EPR signals due to interactions of spins with the environment. The population difference between two levels is maintained by relaxation processes. The upper level is replenished by oscillating magnetic field, but depleted by relaxation processes and an equilibirium difference of population is maintained. The two types of relaxation processes involved are the spin-lattice and spin-spin relaxation.

1.5 SPIN-LATTICE RELAXATION

The process in which energy flows from the spin system to the lattice is called spin-lattice relaxation process. The mean time taken in the transfer of energy to the lattice is called spin-lattice relaxation time T_1. For spin-lattice

relaxation, there are mainly three mechanisms which are the direct, Raman and Orbach processes.

In direct process, relaxation occurs through transfer of energy from a single spin to a single vibrational mode of the crystalline lattice which has essentially the same frequency [13]. When relaxation is by the direct process, then $T_1 \propto 1/B^2T$, and is independent of spin concentration [14]. The direct process is important only at low temperature.

In Raman process, a phonon is inelastically scattered in the process of flipping a spin. Energy is conserved and this process is strongly temperature dependent with $T_1 \propto 1/T^7$ for $T<\theta_D$ and $T_1 \propto 1/T^2$ for $T>\theta_D$, where θ_D is the Debye temperature [15,16]. This process is important at high temperatures.

In Orbach process, there are two transitions one after the other which occur via an intermediate state. Here the relaxation rate is given by $1/T_1 \propto e^{-\Delta/KT}$, where Δ is the energy gap between the upper level and the intermediate state.

1.6 SPIN-SPIN RELAXATION

It contains all the mechanisms by which the spin can exchange energy amongst themselves, rather than giving it back to the lattice [17,18]. In this process, the two main types of interactions have been identified, which are the dipole-dipole and exchange interactions.

(a) **Dipole-Dipole Interaction**

This arises from the influence of magnetic field of one paramagnetic ion on the dipole moments of the neighbouring, like ions. The local field at any given site will depend on the arrangements of the neighbours and the direction of their dipole moments. Thus the resultant magnetic field on the paramagnetic ion will be the vector sum of the external field and the local field. This resultant field varies from site to site giving a random displacement of the resonance frequency of each ions and thus broadening the line widths.

(b) **Exchange Interaction**

In many paramagnetic compounds in which the separation of the magnetic ions is less than about 0.5 nm, exchange interaction between the neighbours exceeds the purely dipole interaction. This effects in two forms as isotropic exchange and anisotropic exchange.

If the spins are identical, the line is narrowed in the centre and extended in the wings. The width at half maximum is reduced and the phenomenon is known as exchange narrowing, and the line shape approximates to a Lorentzian.

On the other hand, the anisotropic exchange interaction generally arises if the magnetic ions have anisotropic g-tensors, even if the exchange interaction between the true spins of the ions is itself anisotropic. Anisotropic exchange interaction will give rise to broadening of the resonance line.

1.7 LINE WIDTH

There are many interactions which influence the line width. However, the Heisenberg uncertainity principle sets the ultimate minimum width $dEdt \geq \hbar$ with $\hbar = h/2\pi$,where dE is the uncertainity in the energy level E and dt is the uncertainity in the time spent by the electron in energy level E. Using $h\Delta\nu$ for dE, the uncertanity in the resonance frequency corresponds to a half band width $\Delta\nu \geq 1/2\pi dE = 1/2\pi T_r$ where T_r corresponds to the relaxation time.

The various sources of line broadening includes dipole-dipole interaction between like spins, spin-lattice relaxation, interaction of spins with radiation field, motion of unpaired spins in the microwave field, diffusion of the spin system excitation through the paramagnetic sample, hyperfine interactions, anisotropy of the splitting of the spin levels, dipolar interaction between spins with different Larmour frequencies and inhomogeneties in applied d.c magnetic field.

1.8 FINE STRUCTURE

When a paramagnetic ion is doped in a diamagnetic host system, then the surrounding diamagnetic ions will give rise to an electric field at the site of the paramagnetic ion. This electric field internal to the spin system can lift the degeneracy of the energy levels and generate a fine structure

which appears when the splitting is small enough so that the levels are populated and the resonance transitions are within the energy range of EPR [19]. Interactions such as spin orbit coupling, electron spin-spin coupling, and the Stark effect of an asymmetrical crystalline electric field are usually responsible for the fine structure.

1.9 HYPERFINE AND SUPERHYPERFINE STRUCTURES

Hyperfine interactions are mainly magnetic dipole interactions between the electronic magnetic moment and the nuclear magnetic moment of the paramagnetic ion. The quartet structure in the EPR of divalent copper ion (see figure 1.3) and octect in the EPR vanadyl ion are the results of hyperfine interactions. The origin of this can be understood simply by assuming that the nuclear moment produces a magnetic field B_N at the magnetic electrons and the modified resonance condition will be $\Delta E = h\nu = g\beta|B+B_N|$ (1.8) where B_N takes up 2I+1 values, where I is the nuclear spin.

There may be an additional hyperfine structure also due the interaction between magnetic electrons and the surrounding nuclei called superhyperfine structure [20]. The effect was first observed by Owens and Stevens in ammonium chloroiridate [21] and subsequently for a number of transition metal ions in various hosts [22-24].

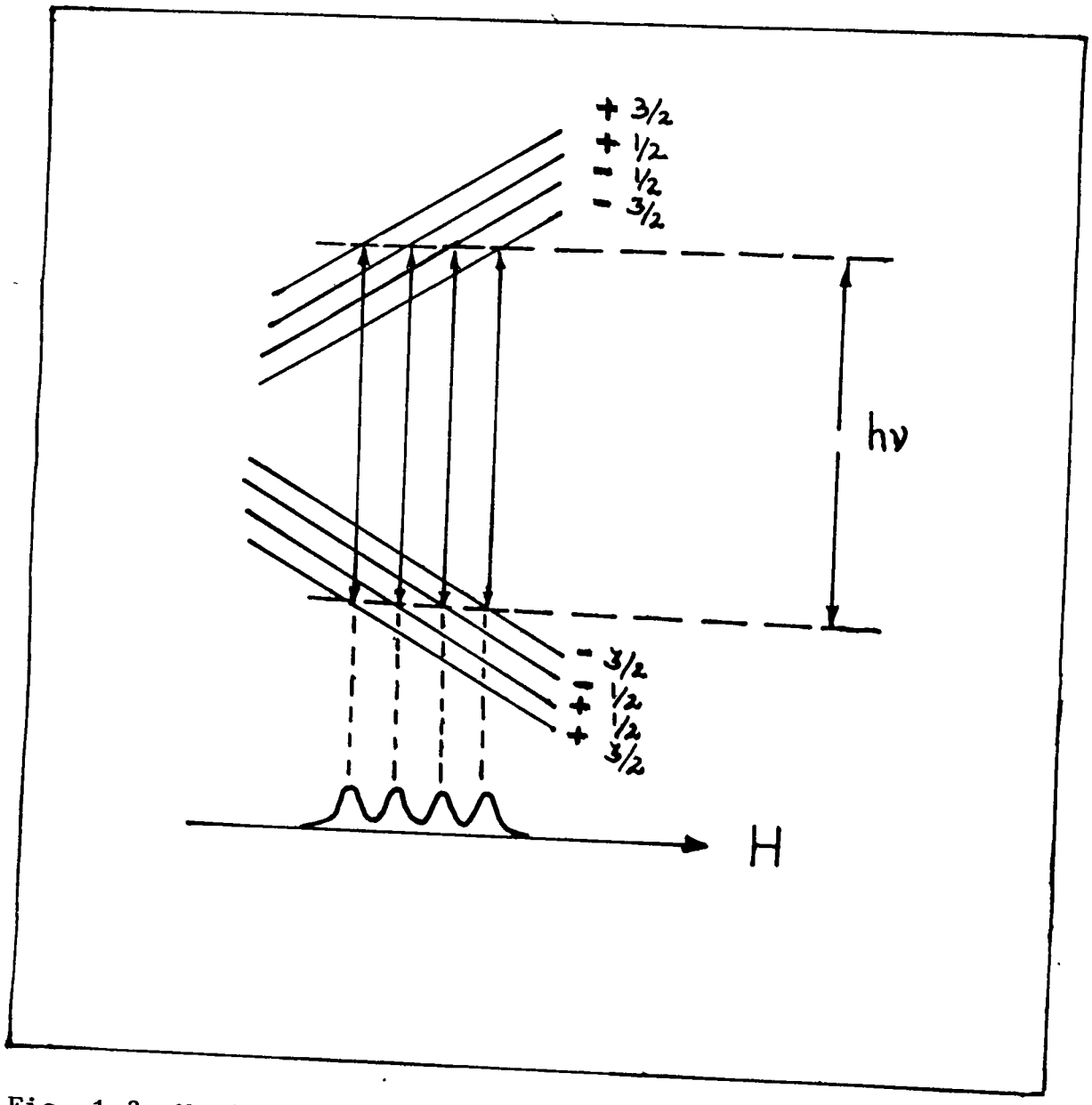

Fig. 1.3 Nuclear hyperfine splitting of energy levels of Cu^{2+}.

1.10 THE SPIN HAMILTONIAN

In EPR, the unpaired electron is not isolated or free. It frequently interacts with a variety of nuclei and electrons in various degrees. So the magnetic field $\vec{B}$ becomes the sum of numerous components. The observed spectrum contains contributions from many electrons residing in many different local fields. Quantum mechanically it is conventional to express the state of affairs in terms of Hamiltonians. Abragam and Pryce initially and numerous others subsequently described the electronic interactions which contribute to the total energy of the ion by the following Hamiltonian [19,25]

$$H=H_o+ H_{cr}+H_{so}+H_{ss}+H_z+H_{hf}+H_q+H_n+H_e \qquad (1.9)$$

Where

H_o = electronic energy = 10^4-- $10^5 cm^{-1}$ (optical region)

H_{cr} = crystal field energy = 10^3 -- 10^4 cm^{-1} (IR or Optical)

H_{so} = electronic spin-orbit interaction energy= $10^2 cm^{-1}$

H_{ss} = electronic spin-spin interaction energy = 0--$1cm^{-1}$

H_z = Zeeman energy due to interaction of electron with external field = 0--$1cm^{-1}$

H_{hf} = dipole-dipole coupling between the electron and nuclear magnetic moments = 10^{-1}--$10^{-2} cm^{-1}$

H_q = quadrupole interaction energy = $10^{-2} cm^{-1}$

H_n = nuclear Zeeman energy due to interaction of nuclei with external field = 10^{-3} -- $10^{-4} cm^{-1}$

H_e = energy of exchange effects between two types of electrons.

The first three Hamiltonian terms namely, the electronic, crystal field, and spin-orbit energies correspond to transitions in the visible and IR regions and are not observed in EPR. Practical EPR spectroscopy concerns itself mainly with the fine structure H_{ss}, Zeeman splitting H_z, and hyperfine interaction H_{hf}, as the nuclear Zeeman and quadrupole interactions are usually small.

The best way to consider all the energy contributions is to express them in the following form including the nuclear Zeeman and quadrupole terms

$$H_s = \beta.\vec{S}.g\vec{B} + \vec{S}.D.\vec{S} + \vec{S}.A.\vec{I} - \beta_N \vec{B}.g_N.\vec{I} + \vec{I}.Q.\vec{I} \qquad (1.10)$$

Where $\vec{S}$ and $\vec{I}$ are the electronic spin and nuclear spin operators respectively. The first term represents Zeeman interaction with the applied field $\vec{B}$. The presence of orbital momentum is taken into account by allowing the splitting factor 'g' to differ from the spin only value of 2.0023. $\vec{D}$ in the second term represents a quadrupolar coupling to the crystal field. The third term expresses nuclear Zeeman interaction and the fifth expresses the quadrupolar coupling between nuclear spin $\vec{I}$ and the electric field gradient in the ion. These tensors are diagonalized in a system of orthogonal axes, known as principal axes. In principal axes system, the above equation can be written as

$$H_s = \beta[g_xB_xS_x + g_yB_yS_y + g_zB_zS_z] + D[S_z^2 - 1/3\,S(S+1)] + E[S_x^2 - S_y^2]$$
$$+ A_xS_xI_x + A_yS_yI_y + A_zS_zI_z + Q'[I_z^2 - 1/3\,I(I+1)] + Q''[I_x^2 - I_y^2] \qquad (1.11)$$

where $D=D_z-1/2(D_x+D_y)$; $E = 1/2(D_x-D_y)$ (1.12)

$Q' = Q_z-1/2(Q_x+Q_y)$; $Q'' = 1/2(Q_x-Q_y)$ (1.13)

and g_x, g_y, g_z and A_x, A_y, A_z are components of $\vec{g}$ and $\vec{A}$ tensors respectively along principal axes.

1.11 EPR AS A PROBE OF PHASE TRANSITIONS

In the recent years there has been increased emphasis on the use of electron paramagnetic resonance as a tool to study structural as well as magnetic phase transitions [26]. For structural phase transitions the approach involves introducing into the soild a paramagnetic probe ion in low concentrations either by irradiation or doping and monitoring the EPR spectrum in the region of phase transitions as a function of temperature, pressure or stress. In the case of magnetic materials, the intrinsic ions of the lattice may be used to investigate the phase transition provided the resonance is not so broadened as to be undetectable. The approach has been used to study ferroelectric, antiferroelectric, ferromagnetic and antiferromagnetic transitions as well as phase transitions that do not involve net changes in susceptibility.

(a) Structural Phase Transitions

In case of a second order phase transition, axial zero field splitting will depend on the temperature and the dependence near the critical temperature Tc is given by

$$D = aT + b(Tc - T)^{\frac{1}{2}} \quad (1.14)$$

where a and b are constants. Thus the zero field splitting D will deviate from linearity near Tc. A first order phase transition will generally cause an abrupt change in the zero field splitting at Tc. In first order phase transition the change in line intensity near Tc will be abrupt, where as in second order transition there will be a gradual change in the resonance intensity as Tc is approached. In second order transition, a temperature dependent broadening of the linewidth of the resonance may occur near Tc.

(b) **Magnetic Phase Transitions**

Earlier EPR investigations on the broad resonance in three dimensional magnetic materials indicated that the line widths and the intensities of the resonance behaved anomalously [26] near Curie temperature. Kawasaki [27] predicted the behaviour of EPR linewidth in a uniaxial antiferromagnetic material near Tc to be

$$\Delta H \approx (T - Tc)^{-P} \qquad (1.15)$$

where $P = 3/2$

In ferromagnetic materials, the EPR line widths are predicted to narrow following the relation [28-31]

$$\lambda \Delta H = [T/(Tc - 1)]^{-P} \qquad (1.16)$$

where λ is the magnetic susceptibility. The exponent P was determined to be 2/3.

In the quasi one and two dimensional magnetic lattices, due to their reduced dimensionality, the modified Kawasaki's

theory predicts P in the above equation (1.15) to be of 1.5 [31,32]. In two dimensional materials, the linewidth should be anisotropic having an angular dependence ($3\ Cos^2\phi-1$), where ϕ is the angle between the d.c magnetic field and the plane of magnetic interaction [33]. It was also noted that there was a gradual change in the g-values as Tc is approached.

In high dimensional spin systems, the development of short range order is considered as associated with the onset of fluctuations that occur near Tc. This will result in change in the g-values and will affect the line widths considerably. In one dimensional magnetic systems EPR line width is found to be anisotropic and is having a ($1-Cos^2\phi$) dependence as predicted by the theory of one dimensional system by Tazuke and Nagata [34]. Shifts in g-values were also accounted for, by spin fluctuations [35]. The direction of g-shifts in the linear one dimensional magnetic systems depends on the orientation of the d.c magnetic field with respect to the chain axis.

1.12 EPR INSTRUMENTATION

The various components of an EPR spectrometer is given below.

(a) **Source**

The different components of the source are as follows

(i) **Klystron or Gunn diode oscillator:** In most of the EPR spectrometer the source is a klystron or a Gunn diode

oscillator which is operating in the microwave band region of 3 cm wavelength. An automatic frequency control (AFC) can be used to measure the stability of the frequency so that the oscillation frequency of the Gunn oscillator matches the resonance frequency of the sample cavity resonator.

(ii) **Isolator:** It is a non-reciprocal device which minimises variations in the frequency of microwaves produced by the Gunn diode oscillator. The variations occur in the frequency due to the backward reflections in the region between the Gunn diode oscillator and the circulator. Isolator is a strip of ferrite material.

(iii) **Wave meter:** The wavemeter is put in between the isolator and attenuator to know the frequency of microwaves produced by Gunn oscillator. The wavemeter is usually calibrated in frequency units instead of wavelength.

(iv) **Attenuator:** Between the wavemeter and circulator there is an attenuator which adjusts the level of the microwave power incident upon the sample. It possesses an absorption element and corresponds to a neutral filter in light absorption measurements.

(b) **Circulator or Magic-T:**

The microwave radiations produced by Gunn diode oscillator are allowed to pass through the isolator, wavemeter and attenuator and finally enter the circulator through a wave guide by a loop of wire which couples with the oscillating

magnetic field and sets up a corresponding field in the wave guide. The microwave radiations enter the arm 1. Arm 3 is connected to resonant cavity and sample. Arm 2 generally is having a terminating load, and is used to absorb any power which might be reflected from the detector arm 4.

(c) **Sample Cavity**

The heart of an EPR spectrometer is the resonant cavity cantaining the sample. It is usually equiped with an ultra violet ray irradiation aperture, cooling device, a 100 KH_z field modulation coil etc.

(d) **Magnet System**

The resonant cavity is placed between the pole pieces of an electromagnet. This provides a homogeneous magnetic field and can be varied over a wide range. The excitation power supply supplied a highly stabilized excitation current to the electromagnet.

(e) **Crystal Detectors**

The most commonly used detector is a silicon crystal which acts as a microwave rectifier. This converts microwave power into a direct current output.

(f) **Autoamplifier and Phase Sensitive Detector**

After detection by the crystal detector, the signal undergoes narrow-band amplification. But the amplified signal contains a lot of noise. The reduction in noise is achieved by rejection of all noise components except those in a very

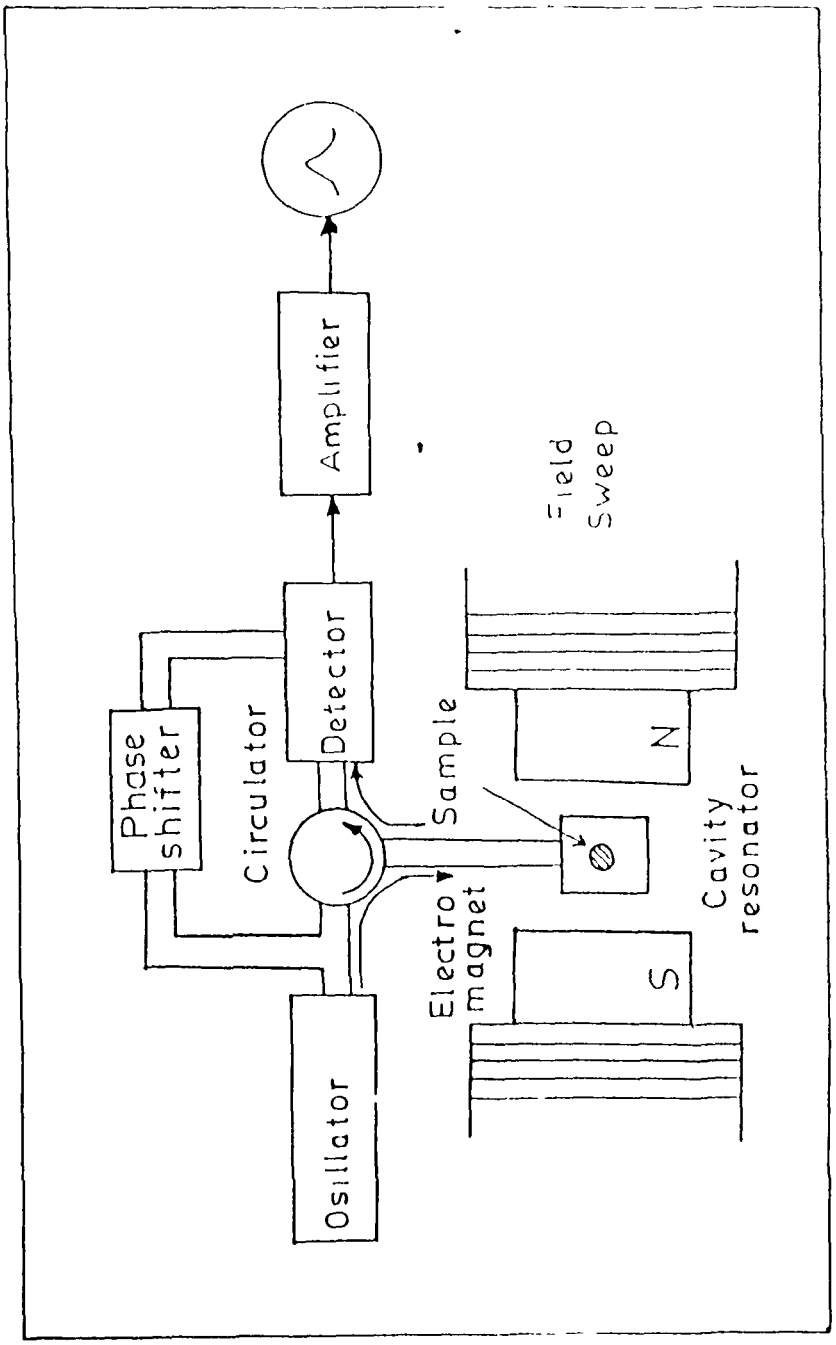

Fig. 1.4 Block diagram of a paramagnetic resonance spectrometer.

narrow band by the operation of the phase sensitive detector.

(g) **Oscilloscope and Pen Recorder**

Finally, the signal from the phase sensitive detector and sweep unit is recorded by a pen recorder. The oscilloscope provides a facility to check the signals before recording.

The block diagram of an EPR spectrometer is shown in figure 1.4. The sample is placed in a quartz tube and is kept at the centre of the cavity. The electromagnet produces a wide range of magnetic field B. Then the sample is subjected to a microwave magnetic field of constant frequency and which is perpendicular to B. The magnitude of B is changed by varying the electromagnet excitation current and when the resonance condition is fulfilled, part of the microwave energy is absorbed into the sample. With the result, the cavity resonator Q-value changes. This Q-variation is detected, amplified and recorded.

1.13 EPR SPECTROMETER USED

The present investigations were carried out on a new ESR spectrometer (JES-RE2X, JEOL,JAPAN) in the X-band with 100 KHz field modulation. All experiments were performed at room temperature. Other details on the specification of the EPR spectrometer used are as follows [36].

Reference frequency : 8.8 -- 9.6 GHz

Sensitivity : 1×10^{14}/T

Resolution	: 47 mG
Microwave power range	: 0.1 μW- 200mW
Cavity mode	: TE_{011}, Cylindrical
Detection Method	: Homodyne crystal detection
Magnetic field Modulation	: 0.0002-2mT (100 KHz)
	0.0002-1mT (50 KHz)
	0.0002-0.2mT (25 KHz)
Maximum magnetic field	: 1300mT
Recorder	: DYT type
Chart width	: 360 mm
Oscilloscope	: 228mm persistance type

REFERENCES

1. C.J. Gorter, Physica **3** (1936) 503.
2. C.J. Gorter, Physica **3** (1936) 1006.
3. E. Zavoisky, J. Phys. (USSR) **9** (1945) 211.
4. E. Zavoisky, J. Phys. (USSR) **10** (1946) 191.
5. R.L. Cummerow and D.Halliday, Phys. Rev. **70** (1946) 433.
6. D.J.E. Ingram, spectroscopy at radio and microwave frequencies, Butterworths, London, (1955).
7. T.Kushida, G.B.Benedek and N.Bloembergon, Phys. Rev. **104** (1956) 1364.
8. G.B.Bednek, E.M.Purcell, J. Chem. Phys. **22** (1954) 2003.
9. W.M. Walsh, Phys. Rev. **114** (1959) 1485.
10. W.M. Walsh, Phys. Rev. **122** (1961) 762.
11. I.Fidone and K.W.H Stevens, Proc. Phys. Soc. **73** (1959)116.
12. G.B. Watkins, Phys. Rev. **110** (1958) 986.
13. J.A.Giordmaine, L.E.Alsop, F.R. Nash and C.H.Townes, Phys. Rev. **109** (1958) 302.
14. G.E.Pake, Paramagnetic Resonance, Benjamin, New York (1962).
15. W.Low, Paramagnetic Resonance in Solids, Solid State Physics Suppl. **2** (1960) 150.
16. A.V.Jaganadhan, Ph.D.Thesis, I.I.T, Kanpur, India (1969).
17. J.H.Van Vleck, Phys. Rev. **74** (1948) 1168.
18. M.H.L.Pryce and K.W.H. Stevence, Proc. Phys. Soc. **A63** (1950) 36.
19. Reymond. S. Alger, Electron Paramagnetic Resonance: Techniques and Applications (Interscience) New York (1968).
20. M. Umar, Ph.D. Thesis, Department of Physics, Aligarh Muslim Unversity, India, (1985).

21. J. Owens and K.W.H Stevens, Nature **171** (1953) 836.

22. S.Ogawa, J. Phys. Soc. Jap. **15** (1960) 1475.

23. J.E. Drumheller, J.Chem. Phys. **38** (1963) 770.

24. T.L. Estle and W.C. Holton, Phys. Rev. **150** (1966) 159.

25. A. Abragam and B.Bleaney, Electron Paramagnetic Resonance of Transition ions,(Oxford University Press , Clarendon), Oxford (1970).

26. F.J. Owens, Charles. P.Poole Jr., and Horacio. A. Farach, Magnetic Resonance of Phase Transitions (Academic Press) New York (1979)

27. Kowasaki. K, Prog. Theor. Phys. **39** (1968) 285.

28. Toyata. E, and Hirakawa. K, J. Phys. Soc. Jap. **30** (1971) 692.

29. Petrov. M.P. and Kizhaev S.A. Sov. Phys -Solid State, **11** (1970) 1968.

30. Mori. H, and Kawasaki. K, Prog. Theor. Phys. **28** (1962) 971.

31. Dillon. J.F., and Remeika, J.P. in Magnetic Resonance and Relaxation (North-Holland) Amsterdam (1967).

32. Richards P.M. Solid State Commun. **13** (1973) 253.

33. Huber H and Seehra. M.S., Phys. Lett. **43A** (1973) 311.

34. Tazuke. Y and Nagata K, J. Phys. Soc. Jap. **38** (1975) 1003.

35. Nagata. K, and Tazuke. Y, J. Phys. Soc. Jap, **32** (1972) 337.

36. Operation Mannual of the JES-RE2X, JEOL EPR spectrometer.

2.1 INTRODUCTION

In 1911, H. Kamerling Onnes [1] found that at 4.15K, the d.c. electrical resistance of mercury dropped abruptly to zero. With that finding, the branch of superconductivity was born. After that, 60 years of continuous efforts could raise this transition temperature (T_c) only to 23.2 K for Nb_3Ge. Later, on April 17, 1986, a brief article of "Possible High-T_c Superconductivity in Ba-La-Cu-O System" by J.G. Bednorz and K.A. Muller [2] announcing the discovery of superconductivity in that system with T_c in the range 30 K, begun the era of high temperature superconductivity. Within a year, La-Sr-Cu-O system with T_c close to 40 K at atmospheric pressure [3-5] and upto 52 K under high pressure [6] were prepared. Soon after, the Yttrium barium copper oxide system was discovered with superconductivity transition temperature in the range 90-95 K [7]. By 1988, the bismuth and thallium based systems raised the transition temperature further to 125 K [8-10], the highest T_c recorded till now. As a result of these developments, superconductivity has become one of the most active area of research in physical sciences in the last few years. The rising of T_c during the last 80 years is shown in Table 2.1.

2.2 CONVENTIONAL SUPERCONDUCTIVITY

(a) Background.

After the discovery of superconductivity in mercury by Kamerling Onnes in 1911, the phenomenon was observed in a

Material	T_c(K)	Year of Discovery
Hg	4.1	1911
Pb	7.2	1913
Nb	9.3	1930
Nb_3Sn	18.1	1954
$Nb_3(Al_{0.75}Ge_{0.25})$	20-21	1966
Nb_3Ga	20.3	1971
Nb_3Ge	23.2	1973
$Ba_xLa_{5-x}Cu_5O_{5(3-y)}$	30-35	1986
$(La_{0.9}Ba_{0.1})_2CuO_{4-d}$, at 1 GPa	52.5	1986
$YBa_2Cu_3O_{7-d}$	90-95	1987
BiSrCaCuO	105-120	1988
TlBaCaCuO	110-125	1988
K_xC_{60}	18	1991
Rb_2CsC_{60}	31.3	1991.

Table 2.1 Superconductivity records through the years

number of other elements also [11-13]. Majority of these elements are members of various transition series [14]. Of the transition elements most commonly found in the newer high-T_c ceramic superconductors, lanthanum is superconducting with a moderately high T_c of 4.88 K for the fcc form and 6.3 K for the hcp from, yttrium becomes superconducting only under pressure (T_c = 2 K) and copper is not known to superconduct. The non-transition elements oxygen and strontium in these compounds do not superconduct, barium and bismuth only does so under pressure, and thallium is a superconductor with T_c = 2.4 K.

Transition elements combine with a number of other elements to form superconducting materials, that usually have higher transition temperatures than any of their constituents. These materials include alloys, intermetallides, semiconductors, layered compounds, polymers etc. For these materials, T_c is often found to be sensitive to their stoichiometry. The highest transition temperature of the older superconductors were obtained with what are called the A-15 intermetallic compounds of the general formula A_3B. Nb_3Ge is an example of this group. 'A' atom is always a transition element and sometimes 'B' atom also.

Superconductivity is also observed in a number of ternary compounds containing one of the group VI elements such as S,Se,Te or O. There are many superconducting ternary molybdenum sulfides and selenides called cheveral phases [15]

with the general formula $A_xMo_6B_8$ where 'B' is a chalcogenide S, Se or Te and 'A' can be practically any element. Superconductivity and magnetic order are known to coexist in cheveral phase compounds. Of the many oxide compounds in which conventional superconductivity was detected includes $SrTiO_3$[16-18], $LiTi_2O_4$ [19], $BaPb_{1-x}Bi_xO_3$ [20-22] etc. The mixed valence system $BaPb_{1-x}Bi_xO_3$ containing Bi^{3+} and Bi^{5+} has shown a highest T_c of 13 K. It is this finding which actually led, Bednorz and Muller to experiment on the mixed valence (Cu^{2+} and Cu^{3+}) lanthanum copper oxides containing alkaline earths and led to the biggest breakthrough in physics of the present decade.

(b) **Basic Features**

(i) **Zero Resistivity and Critical Current Density:** Disappearence of the electrical resistance is the most striking aspect of superconductivity, which takes place at the critical temperature T_c. For homogeneous single crystals of pure metals, the transition width is narrow, but it gets broadened for polycrystalline or impure materials. For such cases it is customary to consider the onset temperature of superconductivity, which is generally taken to be the temperature where the resistance has dropped by 10%. When the transition is complete, the resistance becomes indistinguishable from zero. Because of this, the induced currents in a closed superconducting ring takes several thousands of years to decay and hence they are termed as persistent currents.

Superconductors allow flow of electric current under zero voltage. However beyond a certain critical value, called the critical current density Jc, the material developes resistance and show voltage drop and superconductivity ceases.

(ii) **Meissner Effect, Critical Fields and Susceptibility:** Meissner and Ochsenfeld [23] observed that, if a superconducting specimen in a magnetic field is cooled through its transition temperature, the magnetic flux gets expelled from the specimen at and below T_c. This property is known as Messiner effect and helps to unambiguously establish superconductivity.

But below T_c, superconductivity can be quenched by applications of an external field Hc known as critical field. Hc increases with decreasing temperature as

$$Hc = H(0)\ [1 - (T/T_c)^2]$$

Thus for a superconductor at $T<T_c$, magnetic flux $\vec{B} = 0$, or $\vec{B} = \vec{H} + 4\pi\vec{M} = 0$ or $M = -H/4\pi$

and $\chi = -1/4\pi$

where $\vec{M}$ is the magnetization per unit volume and χ is the magnetic susceptibility. Then the superconductor in a field H<Hc behaves like a perfect diamagnetic substance. Materials which exhibit complete Meissner effect are called Type-I superconductors or soft superconductors. For some materials, the superconducting electrical properties persist beyond the Meissner regime, until a much larger magnetic field called

upper critical field Hc2 is applied. The field Hc1 upto which Meissner effect is maintained is called lower critical field. Such materials are called type-II superconductors.

(iii) **Specific Heat and Thermal Properties**: Specific heat measurements in superconductors show a discontinuity at T_c, characteristic of a second order transition.

At low temperatures, the specific heat of a normal metal is expressed by

$$C = \alpha T^3 + \gamma T$$

where the first term represents lattice contribution and second term, the electronic part. Experimental observations have shown that the electronic specific heat in the superconducting state exhibits an exponential relation with temperature.

The entropy is found to be much lower in the superconducting state. This is explained as due to the more ordered state of electrons in the superconducting phase.

Analogues to specific heat, the thermal conductivity of normal metals is expressed as K = Ke + Kl, where Ke and Kl denote electronic and lattice parts. The electronic part is primarily affected by two scattering processes, namely the scattering by impurities and defects and by phonon, the former becoming predominent at low temperatures. In the superconducting state, the electron pairs cannot carry thermal energy nor can they scatter phonons. Thus the electronic

conduction diminishes rapidly below T_c, but at the same time the conduction by phonons is enhanced as they are no longer scattered. In pure superconductors, the decrease in electronic part Ke outweighs the increase in Kl and hence the overall thermal conductivity in superconducting state is reduced, but in highly impure metals, the reverse occurs.

(iv) **Characteristic Length Parameters:** There are three important characteristic length parameters that takepart in determining the properties of superconductor, namely the penetration depth λ, coherence length ξ and Ginzberg-Landau parameter κ.

When an external magnetic field is applied to a superconductor, even though it cannot enter into the whole specimen due to Meissner effect, it actually penetrates into the specimen, a short distance. This penetration is found to be effective at the surface of the specimen over a distance where the external d.c magnetic field has decreased to 0.368(1/e) of its value outside and this distance is called penetration depth. For the classical superconductors, λ has been found to be of the order of 5×10^{-6} cm.

Coherence length [24], ξ of a superconductor is defined as the range of the wave function that describes the superconducting state, i.e. the distance over which electron coherence occurs. In a spatially varying magnetic field, the energy gap cannot change appreciably over this distance. Based

on several types of experimental evidences, Pippard [25] proposed this coherence as a fundamental property of a superconductor.

The ratio of the penetration depth λ to the coherence length ξ is defined as the Ginzburg-Landau parameter κ. Superconductors are classified as type I or type II depending on whether the parameter κ is less than $1/\sqrt{2}$ or greater than $1/\sqrt{2}$ respectively.

(v) **Electromagnetic Absorption and Energy Gap:** When electromagnetic waves of frequency ν are incident on a superconductor they get absorbed, if $h\nu \geq 2\Delta$ and consequently the phenomenon offers the most direct technique for measuring the energy gap of superconductors. For superconductors with $T_c \sim 1K$, with $2\Delta_o = 3.5\ K_B T_c$, ν is in the microwave region, while for $T_c \sim 10K$, it is in the far infrared range. For instance Biondi and Garfunkel [27] measured energy gap of Al, (with $T_c = 1.8$ K) by studying microwave absorption. But Richard and Tinkham [28] studied the gap in La, Sn etc., with $T_c >> 1K$, using infrared absorption. The energy gap found to be decreasing continuously to zero as the temperature is reduced to the transition temperature T_c [29].

(vi) **Isotope Effect:** It has been observed that the critical temperature T_c of superconductors varies with isotopic mass. The first observations were made by Maxwell [30] and by Reynold, et al, [31]. In mercury they found that T_c varies

from 4.185°K to 4.146°K as the average isotopic mass M varies from 199.5 to 203.4 atomic mass units. The same phenomenon was observed in Zn, Cd, Sn, Pb etc., also. The experimental results within each series of isotopes followed a relation of the form given by $M^{\alpha} T_c$ = Constant or $T_c \propto M^{\alpha}$. It is seen that value of α = 0.5 in most of the conventional superconductors. Since the amplitude of lattice vibrations also varies as $M^{-0.5}$, the isotope effect suggested that the mechanism of superconductivity might involve phonons.

(vii) **Flux Trapping and Flux Quantization:** When a normal metallic ring is placed in a magnetic field perpendicular to its plane and the temperature is lowered, the metal becomes superconducting and magnetic flux is expelled from it. If the external field is then removed no flux can still pass through the superconducting metal. Since the total trapped flux must remain constant in the hollow of the ring, it has to be maintained by the circulating supercurrent in the ring itself, in the form of persistent currents. In sufficiently thick rings, the flux trapped is quantized in units of

$$\phi_o = hc/2e = 2.07 \times 10^{-7} \text{ Gauss. cm}^2$$

In a cylindrical sample with inner hollow cross sectional area 'a', if the external field H_{ext} is applied when $T > T_c$ and the sample is cooled below T_c, similar flux trapping in the hollow of the cylinder and flux exclusion from the superconducting material takeplace. Because of quantization of the flux in units of ϕ_o, the flux ϕ trapped in

the hollow varies with H_{ext} in the form of steps since one must satiesfy the relation

$$\phi = H_{ext}\ a = n\ (hc/2e)$$

where n is an integer.

(c) **Mechanisms of Conventional Superconductivity**

Superconductivity has always been a very fascinating but difficult problem for theoreticians. Although a number of models were suggested for the phenomenon, the mechanism based on the concept of pairing of electrons of opposite spins and momenta near the Fermi surface, given by Bardeen, Cooper and Schrieffer [32] called BCS theory appears to be the most acceptable one. Here the different model suggested for the conventional superconductivity will be discussed very briefly and then the BCS theory in more detail.

In the initial stages of superconductivity era, C.J. Gorter and H.B.G. Casimir [33] put forward the two fluid model to explain the phenomenon. In this model the superconducting state is assumed as an assembly of conduction electrons which can be considered as being composed of two interpenetrating fluids, a fluid of normal electrons which behaves in the same way as the conduction electrons of the normal metal and a fluid of superconducting or superelectrons which has zero entropy and which experiences no resistance to flow. As the metal is cooled below T_c, a certain fraction x of electrons

becomes superelectrons, the value of x depending on the temperature. Since these electrons have zero resistance, they will short circuit the normal electron stream and so the specimen as a whole exhibits zero resistance. The model was successful in explaining the thermal properties such as specific heat, thermal conductivity etc, but could not explain the magnetic properties as well.

Based on the two fundamental properties, Meissner effect and zero resistivity of superconductors, F and H. London [34] introduced a more phenomenological model for superconductivity. The zero resistivity consideration for superconductors can lead to an acceleration equation for electrons. The motion of electrons in the perfect conductor under the influence of an electric field E is given by the equation

$$mdv/dt = -eE,$$

where v is the velocity of electrons.

If the density of electrons moving is n, then the current density j = nev leads us to the condition

$$dj/dt = ne^2E/m$$

By applying the Maxwells equations for a superconductor in an applied external field H_a, this equation will give us

$$(mc^2/4\pi ne^2)\nabla^2(H - H_o) = H - H_o.$$

where H is the sum of the applied field H_a and magnetic field H_b of the current j. H_o denotes the field at time t = 0. This

result admits the particular solution $H = H_o$, which is contrary to Meissner effect. To eliminate H_o and thus to explain the Meissner effect, F and H. London [34] proposed the following equations for a superconductor,

$$\text{Curl } j = -(ne^2/mc)\, H$$

and

$$j = -ne^2 A/mc$$

and are called London equations. When applied to type I superconductors, they have considerable success in macroscopic description of the electrodynamic behaviours.

For a superconductor extending in the x-direction, H varies as

$$H = H_o \exp(-x/\lambda)$$

where $$\lambda = (mc^2/4\pi ne^2)^{\frac{1}{2}}$$

and is a measure of the penetration depth of the field. Experiments shown that the measured values of λ in pure metals are about five times larger than the London value. Also the pure metals showed only weak field dependence of λ, when the field was increased from zero to H_c. These observations could not be accounted by London theory. London also argued that the flux penetration over depth λ would make a superconductor in a field $H < H_c$, to split into a fine mixture of normal and superconducting regions. The surface energy between these regions is found to be negative by the London theory, but Meissner effect indicates that the surface energy should be positive.

In 1950 V.L. Ginzburg and Landau [35], using the two fluid model, proposed the superconducting state as a macroscopic quantum state described by a macroscopic wave function Ψ, which acts as an order parameter for the transition from the normal state (Ψ=0). At any superconducting normal interface, the variation of Ψ is characterised by a new length called Ginzburg-Landau parameter $K = \frac{\lambda}{\xi}$. Far away from the interface, Ψ is a non-zero constant in the superconducting region and zero in the normal region.

Although the phenomenological approach of Ginzburg and Landau could not explain all the basic features of superconductivity, it expressed a better picture of superconductors under magnetic fields and fluctuation effects near T_c. Their equations have been able to predict the Meissner effect and have shown that between the normal and superconducting regions of a material, the surface energy is positive.

(d) **The BCS Theory**

In spite of all these phenomenological models for understanding the phenomenon, efforts were underway, since early fifties to find a microscopic explanation of superconductivity. This got much enhancement by the discovery of isotope effect [31] suggesting the involvement of phonons in the superconducting mechanism and reports on the experimental observation of energy gap.

In 1957, Bardeen, Cooper and Schrieffer put forward the BCS theory of superconductivity, based on an effective interaction between electrons resulting from the electron-phonon interaction. This interaction is attractive when the energy difference ΔE between the electronic states involved is less than the phonon energy $\hbar w$. The strength of the electron phonon interaction is sharply peaked when the electrons are in states of equal and opposite momentum and of opposite spins. When Fermi energy E_F is much larger than $\hbar w$, the two electrons will be deep down in the Fermi sea and are so constrained by the Pauli principle that they cannot take advantage of the attraction. But if the two electrons are in the Fermi surface, they will tend to form a bound pair in momentum space, by taking advantage of the attractive interaction V(w) and are called "Cooper pairs". This produces a ground state well separated from the upper excited states by a gap in energy. The simplest approximation is to assume that $V(w) = V$ for electron energies within the range $E_F \pm E_D$, and $V = 0$, beyond this range. Here E_D is the Debye energy $k_B\theta_D$, characteristic of lattice vibration and θ_D is the Debye temperature. Under these conditions, BCS theory predicts the energy gap and transition temperature as

$$E_g = 4E_D \exp(-1/\lambda_c)$$

and

$$T_c = 1.134\ \theta_D \exp(-1/\lambda_c)$$

where $\lambda_c = V\ N(E_F)$ is called electron-phonon coupling constant

and $N(E_F)$ is the density of states at the Fermi level. From these equations

$$E_g/k_BT_c = 3.528$$

In the next higher order approximation the repulsive screened coloumb potential V_c taken into account. Defining a dimensionless coloumb constant $\mu = \langle V_c \rangle N(E_F)$, the coloumb interaction pseudo potential μ^* given by

$$\mu^* = \mu/[1+\mu \log(E_F/E_D)]$$

which on introducing to the expression for T_c gives

$$T_c = 1.14\ \theta_D \exp[-1/(\lambda-\mu^*)]$$

In addition to T_c and E_g, other important predictions of BCS theory includes the discontinuity in the electronic contribution to the specific heat at the transition temperature given by

$$(C_s-C_n)/C_n = 1.43$$

where s and n denote superconducting and normal states, respectively, magnetic flux quantization with $\phi_o = hc/2e$ and the isotope effect. In terms of BCS theory, coherence length is the distance in real space over which the motion of the pair is correlated under the attractive interaction. London penetraction depth as well as London equations are natural consequences of the BCS theory.

2.3 HIGH-TEMPERATURE SUPERCONDUCTIVITY

With Bednorz and Muller's pioneering discovery [2] of high transition temperatures in the range 30K for metallic oxygen deficient compounds of the lanthanum-barium-copper oxide system, a new field of high-T_c superconductivity is originated. Less than a year later the $YBa_2Cu_3O_{7-d}$ class of superconductor was discovered with T_c of 85-95K, above liquid nitrogen temperatures [6-8]. By the beginning of 1988, the Bi-Sr-Ca-Cu-O and Tl-Ba-Ca-Cu-O systems with T_c in the 110-125K range were reported [9,10].

Even though the basic phenomenon in both conventional and high-T_c superconductors are the same, these new oxide compounds shows many serious differences in their properties and structure. Due to their extreme structural complexities and much contradictory results on many of their properties, a complete understanding of these compounds were not successful till now. The present picture indicates clearly that the high-T_c superconductivity needs a unique mechanism, probably much different from that of their conventional counterparts.

2.4 STRUCTURE OF HIGH- T_c SUPERCONDUCTORS

The systems which exhibit high-T_c superconductivity belong generally to four families of copper oxide, namely La-M-Cu-O (where M=Ca,Sr or Ba), RE-Ba-Cu-O (where RE=Y and most of the rare earth ions), Bi-Sr-Ca-Cu-O and Tl-Ba-Ca-Cu-O.

In this section, the structures of these four systems are considered. The numerical vaules of structural parameters show some variation in the literature and most prevalent values are quoted here

(a) **La-M-Cu-O System**

Substitution of an alkaline earth ion M such as Ca, Sr or Ba for La in La_2CuO_4 allowed a series of oxides with a rather wide range of T_c and of formula $La_{2-x}M_xCuO_{4-d}$ [37]. The homogeneity range of these phases depends on the nature of the alkaline earth ion. For Ca and Ba, it is $0 \leq x \leq 0.20$ and for Sr it follows $0 \leq x \leq 1.33$. The symmetry of the cell and parameters depend on the value of x, oxygen content and temperature used during synthesis. Substitution of Ca, Sr or Ba stabilizes the tetragonal structure of La_2CuO_4 at room temperature, when x in $La_{2-x}M_xCuO_{4-d}$ is greater than 0.05. It changes to an orthorhombic structure around 180K [39] and becomes superconducting composition. For the tetragonal form, typical lattice dimensions are a = b = 3.77Å , and c = 13.18Å (11) and it contain two formula units per unit cell [40,41]. Lattice parameters of the orthorhombic form are a=5.363Å , b=5.409Å and c=13.17Å [11], with four formula units per unit cell. This system contains CuO layers square planar coordination of copper ions stacked equally spaced and perpendicular to the c-axis. Structure of the La-Sr-Cu-O compound is shown in figure 2.1

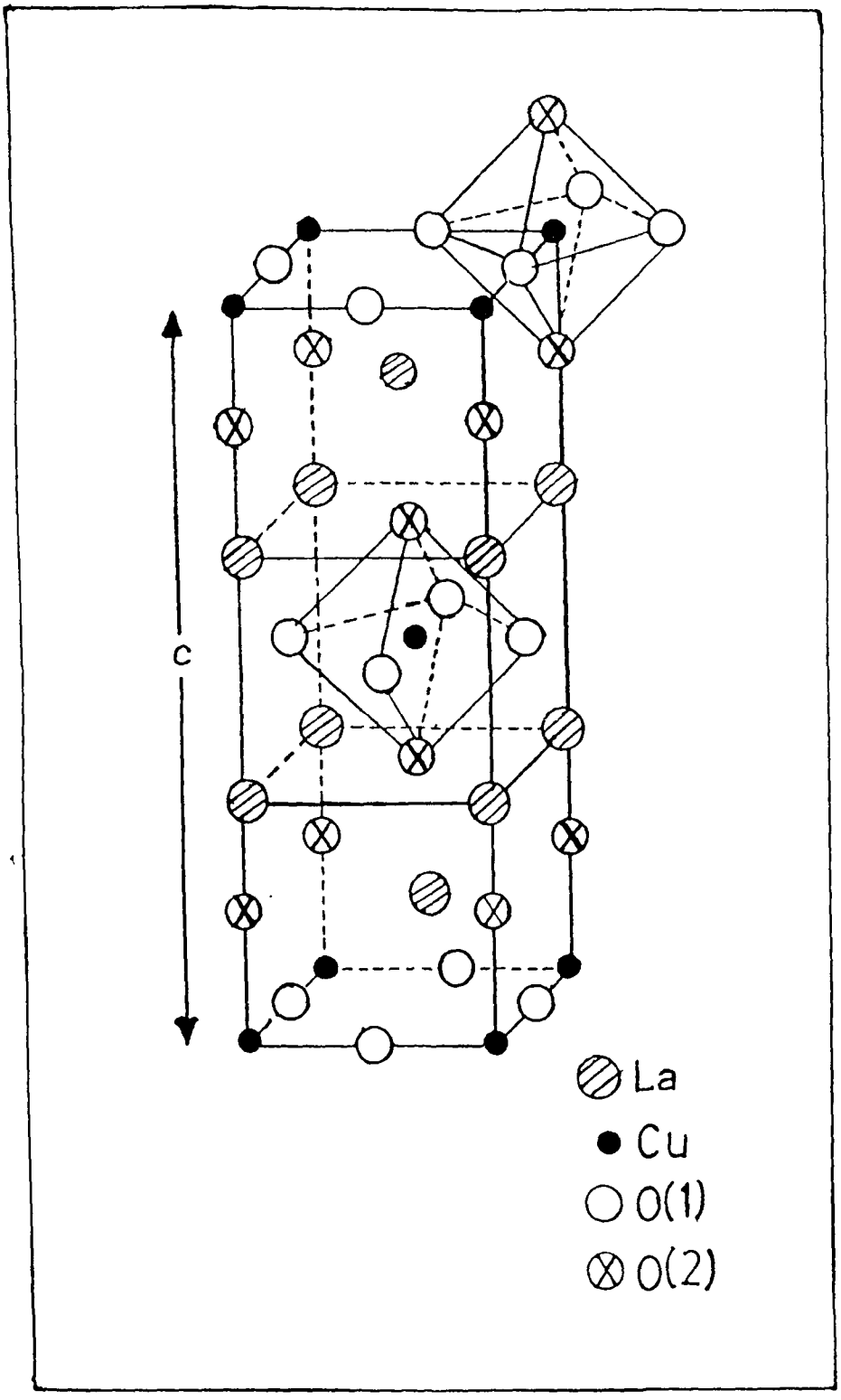

Fig. 2.1 Structure of LaSrCuO superconductor.

Partial substitution of La in $La_{2-x}M_xCuO_{4-d}$ by other rare earth ions such as Pr, Nd, Gd, and Eu showed lowering of T_c [42], but structural features are nearly maintained. Small substitutions of Cu by Ni or Zn reduced T_c markedly [43,44].

(b) RE-Ba-Cu-O System

Superconductivity above liquid nitrogen temperature in this system was first reported [7] in the composition $Y_{1.2}Ba_{0.8}CuO_4$ which was prepared by analogy with the $La_{2-x}Ba_xCuO_4$ composition. $YBa_2Cu_3O_{7-d}$ has shown the highest T_c (=95K)in this system. For $0<d<0.6$, the structure remains orthorhombic above which it changes to the tetragonal form. Upto d = 0.2, T_c remained nearly constant at 90K and from 0.2 to 0.5, it drops to a value around 60K. Above 0.6, it transform to the non-superconducting tetragonal form. In the tetragonal structure [45-47], the unit cell dimensions are a=3.9018A°, and c=11.9403A° and contain one formula unit per unit cell. Lattice parameters for the orthorhombic phase are a=3.827A°, b=3.882A° and c=11.682A° and the number of formula units per unit cell remained unchanged [45,48-50].

In the superconducting $YBa_2Cu_3O_{7-d}$, 2/3 of the Cu ions form CuO_4 planar groups derived from a square pyramidal coordination for Cu while 1/3 of the Cu ions form one dimensional chains of squashed CuO_4 planar groups with no links in the a-direction [51]. The structure is given in the

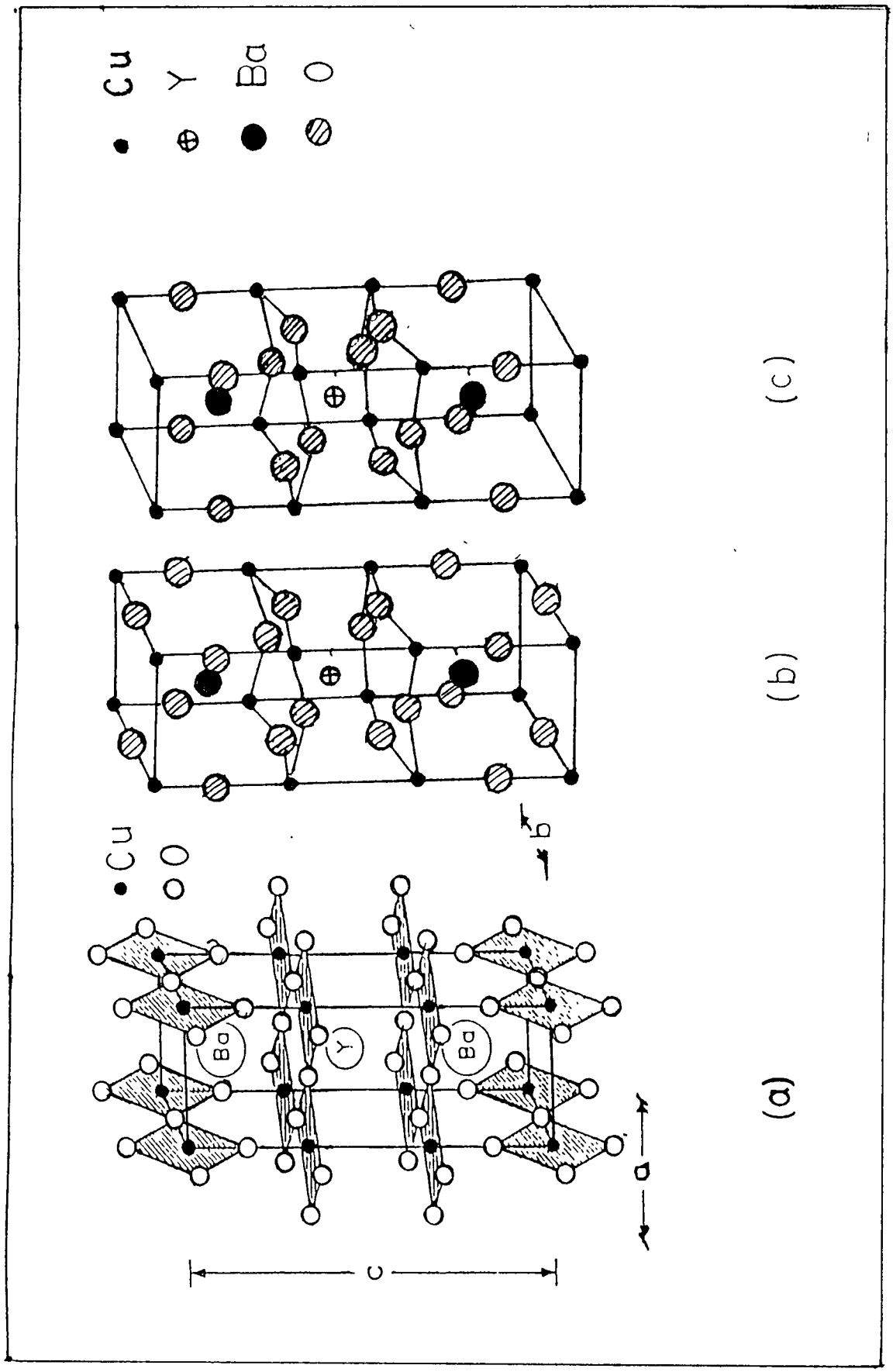

Fig. 2.2 (a) and (b) show structure of $YBa_2Cu_3O_{7-d}$ superconductor. In (a) Cu-O planes and chains are illustrated. (c) shows crystal structure of non-superconducting $YBa_2Cu_3O_6$.

figure 2.2, which shows the corner linked CuO_4 planar groups connected as sheets in the ab planes and as chains parallel to b-axis. In the tetragonal phase the Cu-O chains along b-axis is completely missing.

All the superconducting oxides of the formula REBaCuO (with RE=Nd,Sm, Eu, Gd, Dy, Ho,Er, Tm, Yb, and Lu) have the orthorhombic structure of YBaCuO and show $T_c \sim 90K$. Oxides of this composition formed by Ce, Pr and Tb are not superconducting and possess different structures. Partial substitution of Cu by Zn, Fe and Ni found to lower T_c much.

(c) Bi-Ca-Sr-Cu-O System

This system is found to form a series of compounds with a general formula $Bi_2Sr_2Ca_{n-1}Cu_nO_{2n+4+y}$ where n=1,2,3. The important ones among these are the 2212 phase with T_c=80K and composition $Bi_2Sr_2CaCu_2O_y$ (i.e.,n=2) [8] and the 2223 phase with T_c=110K and composition $Bi_2Sr_2Ca_2Cu_3O_y$ (i.e., n=3) [52,53]. Detailed structural studies indicate that the structure can be either an orthorhombic or a tetragonal provoskite layer type. For the 2212 phase with orthorhombic structure [54], the lattice parameters are a=5.420Å , b=5.376Å and c=30.72Å and for tetragonal structure [55], the parameters are a=b=3.818Å and c=30.6Å .

The structure can be described as containing double sheets of corner shared squar planer CuO_4 units (see figure

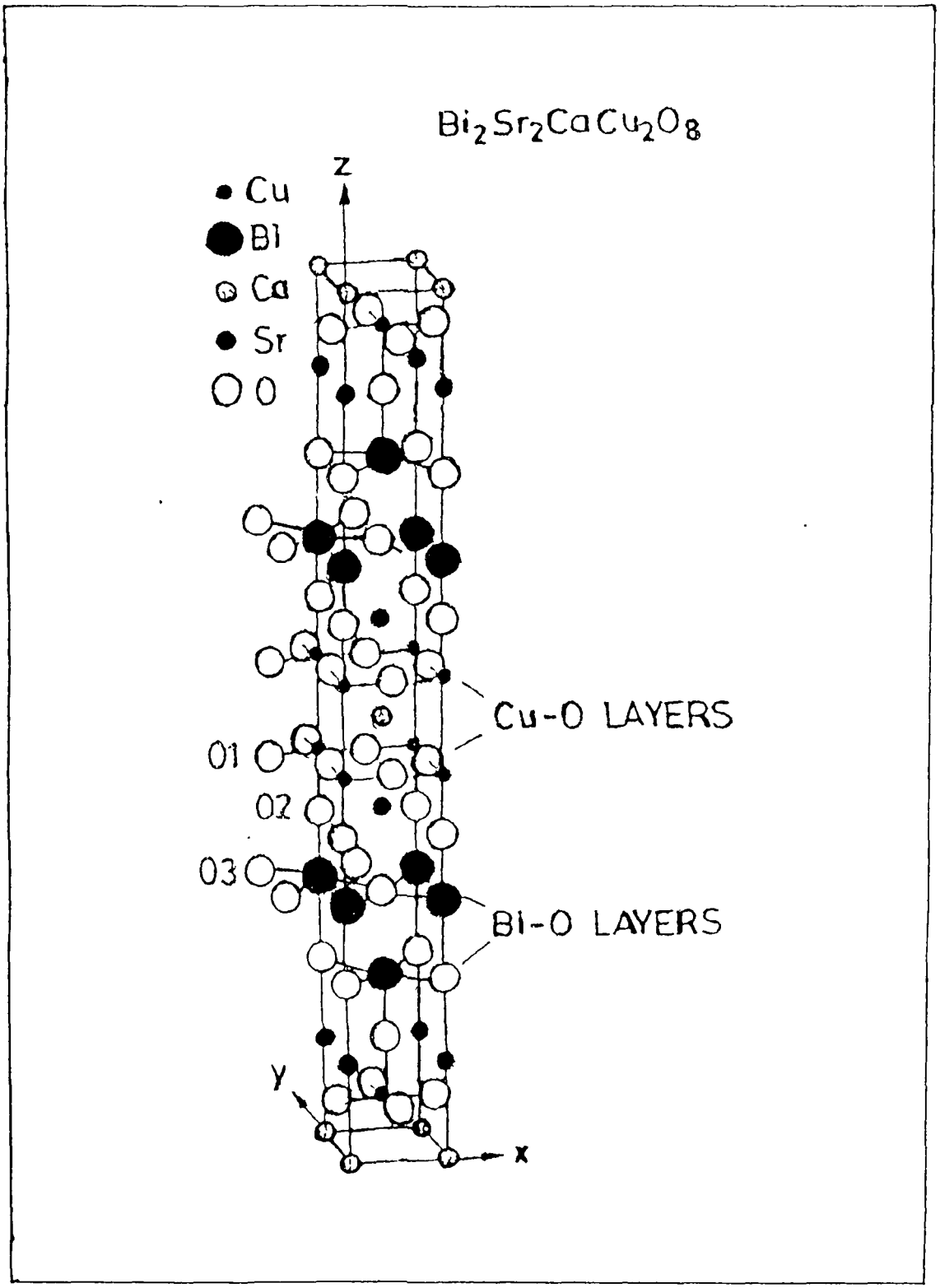

Fig. 2.3 Structure of $Bi_2Sr_2CaCu_2O_8$ superconducting compound.

2.3). Sr-O layers reside just above and below the Cu-O sheets. Planes containing Ca ion lie between the Cu-O sheets. In comparison to RE-Ba-Cu-O compounds, these Bi-cuprates do not have Cu-O chains and rare earth elements. The T_c value shows an increase with number of CuO_2 planes.

In addition tothis basic structure, the Bi-system also shows a superlattice modulation [55-58] which is attributed to the insertion of extra oxygen into the structure. The nominal value for d in the $Bi_2Sr_2CaCu_2O_{8+d}$ is found to be 0 15 which indicate the possibility that part of Cu to be present in +3 oxidation state.

(d) Tl-Ba-Ca-Cu-O System.

The Tl containing superconductor was first discovered by Sheng and Herman [59]. Most of the structural characteristics of the Tl-based system are similar to the Bi-system. A number of compositions were reported for this system of which $TlBa_2Ca_2Cu_3O_9$ (with T_c=100 to 110K) called 1223 phase, $Tl_2Ba_2Ca_2Cu_3O_{10}$ (T_c=120-125K) phase, abbreviated 2223 are the important ones. For the 1223 phase, the cell parameters are a=3.8429Å and c=15.1871Å [60] and for the 2223, these are a=3.822Å and c=36.26Å . Similar to Bi-based system, the Tl-based compounds also contains many copper oxide layers arranged perpendicular to the c-axis. In the different compositions of Tl-Ba-Ca-Cu-O system, the T_c increases with increase in number of $Cu-O_2$ layers.

2.5 PREPARATIVE METHODS

(a)**Bulk Synthesis**

The most widely used preparative method today is the conventional ceramic one [62,63] which comprises the following steps.

(i) Weighing the appropriate amounts of the starting materials.

(ii) Mixing these powders to get a homogeneous mixture.

(iii) Calcining the homogeneous mixture to get the related material.

(iv) Grinding the calcined and reacted powder to get the desired particle size.

(v) Shaping the ground powder by pressing, extrusion etc.

(vi) Sintering the shaped material

(vii) Annealing in oxygen or air with a slow cooling to room temperature to get the superconducting specimen.

For the YBaCuO superconductor the strating materials are Y_2O_3, $BaCO_3$ and CuO, calcination temperature is 880°C to 900°C and sintering temperature is around 920°C to 950°C. In case of Bi-based superconductor [55], Bi_2O_3, $SrCO_3$, $CaCO_3$ and CuO are used as the starting materials. Calcination temperature should be 800°C to 850°C and sintering at 870°C to 880°C.

For preparation of better quality products, solution techniques are used. Solution techniques permit reaction at

lower temperature. The solution derived materials have a narrower transition width. There are mainly two solution methods namely, the sol-gel process and freeze drying process.

In sol-gel powder preparation [62], an aqueous solution of the salts, generally nitrates, of the starting materials is prepared. It is then emulsified with the help of water immiscible organic compounds such as heptane. Generally some emulsifying agents such as polyoxyethylene ethers of fatty alcoholes would be required to get a stable solution. Emulsion is formed by ultrasonic agitation. The metal hydroxides in the emulsion droplets are then coprecipitated using suitable organic amines. The hydrous oxides of the cations will precipitate to form an amorphous gel by the amines. This gel is dried to get a fine grained, homogeneously mixed powder in the correct ratio. The further processing of the materials such as reaction grinding shaping, sintering and annealing were done as in the ceramic process.

In the freeze-drying technique [62,63] a solution containing salts of the starting materials are taken in the appropriate ratio. The solution is sprayed into a tray containing liquid nitrogen. The frozen beads of the solution have to be vacuum dried at room temperature or slightly higher temperature. This gives a fine grained homogeniously mixed salt in the right ratio. Then the mixture is slowly heated to decompose the salt to the oxides. The further steps are the same as that of ceramic technique.

(b) Film Preparation

The important techniques used for film preparation are electron beam evaporation technique, molecular beam epitaxy growth, R.F. sputtering, D.C. Magnetron sputtering and pulsed laser evaporation technique. In electron beam evaporation [64,65], component elements (for example, Y,Ba and Cu in case of YBaCuO superconductor) are evaporated from three electron beam sources in an oxygen partial pressure of 10^{-4} to 10^{-3} Torr. The substrate used for the deposition is usually $SrTiO_3$, kept at 400°C. In the molecular beam epitaxy growth [66], single crystal $YBa_2Cu_3O_{7-d}$ films were deposited from three separate sources simultaneously, i.e., Y from an electron beam heated evaporator and Ba and Cu from effusion cells, in presence of a molecular oxygen overpressure of 10^{-5} Torr. In R.F. sputtering [67], specimen films were deposited on Al_2O_3 or MgO single crystal substrates in argon atmosphere by using a R.F. diode sputtering apparatus. Discs of the bulk superconducting specimen was used as the target. The substrate temperature during deposition is 1050°C. In D.C. megnetron sputtering [68] also, the method is similar to R.F. sputtering. For obtaining thin films from pulsed laser evaporation [69] technique, a pellet of bulk spepcimen is subected to pulsed excimer laser evaporation and films were deposited on suitable substrates.

2.6 NOVEL FEATURES OF HIGH-T_c SUPERCONDUCTORS

(a) Resistivity and Critical Current Density

The superconducting transition temperatures for all the high-T_c superconductors (HTSC) were reported to vary over a range due to the various nominal composition and differences in the synthesis procedures adopted. It has been noted by many workers that the normal state resistivities of these HTSC are rather high compared to the metallic system, but exhibit remarkable linear dependence on temperature over a wide temperature range down to the neighbourhood of T_c [70,71]. The oxide superconductors are highly anisotropic in many of their properties, including resistivity. Bi-Sr-Ca-CuO is the most anisotropic one whereas Tl-Ba-Ca-Cu-O shows the least anisotropy among the copper oxide superconductors [11]. The resistivity (ρ) is much higher when measured along c-axis ($\rho_\perp$) than it is along the ab planes ($\rho_\parallel$). The measured ratios of $\rho_\perp/\rho_\parallel$ are about 20 for LaSrCuO [72], 50 for YBaCuO [73], and 10^5 for BiSrCaCuO [74].

The critical current density Jc in all the high-T_c superconductors is quite low in bulk polycrystalline samples and is in the range from 10^3 to 10^4 amp/cm^2 [75,76]. But in thin films, higher Jc values of the order of 10^6 to 10^8 amp/cm^2 were reported for all the HTSC system [77-80].

(b) Meissner Effect and Critical Fields

Flux expulsion studies on the new high-T_c cuprate

superconductors have shown that Meissner effect is not complete in these compounds [81,82]. This incomplete Meissner effect was regarded earlier as due to poor sample quality. But later studies on more pure and single phase systems also, the fractional Meissner effect remained same. All the HTSC are type II with lower and upper critical fields [11]. The upper critical field H_{c2} shows an anisotropy with H_{c2} along c-axis, i.e., $H_{c2\parallel}$ is many times greater than that along the ab plane ($H_{c2\perp}$). For LaSrCuO $H_{c2\parallel}/H_{c2\perp} \gtrsim 5$ and for YBaCuO and BiSrCaCuO, the ratio is approximately 10 [83-85].

(c) **Specific Heat and Thermal Properties**

Specific heat measurements show a jump at the transition temperature for all the HTSC. At low temperatures the specific heat carries a linear term in addition to the T^3 dependence for all the high-T_c oxides [86,87], with exception of BiCaSrCuO system. But in a few recent studies, a non-zero linear contribution in the Bi-based compound also is reported [88]. The discontinuity in specific heat at T_c is found to be strongly diminished by the application of an external field [89]. The thermal conductivity measurements have shown that conductivity in HTSC is much lower than that of metals or conventional superconductors. There is a remarkable sudden increase in thermal conductivity associated with the onset of superconductivity [90,91]. Below T_c, it reaches a maximum around 60K for LaSrCuO, YBaCuO and BiCaSrCuO and above T_c, the variation is quite linear [92].

(d) **Characteristic Length Parameters**

Both coherence length and penetration depth are found to be highly anisotropic in HTSC [93]. The coherence length, which is related to H_{c2} as $\phi_o = 2\pi \xi^2 H_{c2}$, where ϕ_o is the flux quantum associated with the superconductor, is extracted from H_{c2} measurements on different HTSC appears to lie in the range $25 < \xi_{ab} < 40A°$ and $3 < \xi_c < 7A°$ [85,93]. From critical field measurements, the penetration depth estimated for these materials are $\lambda_{ab} \sim 900A°$ and $\lambda_c \sim 8000A°$ [94]. From muon spin rotation experiments, an average λ of 2500A° is yielded for LaSrCuO [95] and of 1500A° for YBaCuO [96]. The Ginzburg-Landau parameter κ is found to be of the order of 100 [11].

(e) **Electromagnetic Absorption and Energy Gap**

Infrared and tunnelling experiments show the existence of a gap in the electronic energy spectrum, but the value of the gap ratio $2\Delta/k_B T_c$ deviates considerably from the BCS value of 3.5 [97]. The gap ratio is found to be of the order of 5 in YBaCuO, LaSrCuO and BiCaSrCuO superconductors, suggesting strong coupling in these compounds. The oxide superconductors exhibit a much wider spread in energy gap values which probably reflects their great diversity in composition, oxygen content and grain size distribution [11].

(f) **Isotope Effect**

The traditional test for phonon mediated mechanism for superconductivity is the isotope effect, where by for an

element, T_c is related to the atomic mass through the relation

$$T_c M^{\alpha} = \text{constant}$$

with $\alpha = \frac{1}{2}$ for electron phonon coupling in elemental superconductors. But in HTSC, the values of α differs considerably. In LaSrCuO, ^{18}O substitution produces an isotope effect with $0.1 < \alpha < 0.35$ [98,99]. However in YBaCuO and other rare earth substituted compounds, isotope effect is found to be almost absent [100,101] for substitutions for O, Ba and Cu. Isotope shifts of transition temperature of superconductors were used widely to characterize details of the coupling mechanism between electrons and phonons. As a general result, the isotope effect on T_c is smaller than expected from a simple BCS theory.

(g) **Flux Quantization and Tunneling**

Flux quantization studies in YBaCuO and other HTSC using an rf SQUID magnetometer shown integral number of flux quanta jumping in and out of the ring. The results indicated a value of hc/2e for the flux quantum ϕ_o, the denominator confirms that the carriers in the superconducting state are pairs of electrons, presumably cooper pairs [11]. The results of tunneling experiments also established that the superconducting condensate is produced by carriers with two units of charge 2e.

2.7 MECHANISMS OF HIGH TEMPERATURE SUPERCONDUCTIVITY

The discovery of high temperature superconducivity in layered copper oxide perovskites has stimulated a lot of theoretical effects along various directions to search for the microscopic mechanism responsible for this novel phenomenon. The theoretical approaches can broadly be devided in two main catagories, namely, those describing the normal phase as a Fermi liquid and viewing the superconducting transition as a pairing of two Fermionic quasiparticle like in the BCS approach and those considering the normal phase as a non Fermi liquid and describing the superconducting transition as a charged Boson condensation.

The models under the pairing approach with normal metallic phase as a Fermi liquid can again be subdivided on the basis of the nature of interaction causing the pairing. The pairing interaction can be charge fluctuation induced or spin fluctuation induced. The former includes phonons, charge transfer exciton and plasmon mediated attractive interaction. The latter includes antiparamagnon mediated, antiferromagnetic indirect exchange induced and spin bag mediated attraction. The models predicting charged Boson condensation starting from a non-Fermi liquid, have so far been primarily of two types, namely the Resonating Valence Bond (RVB) type and Bipolaronic type.

(a) **BSC Like Pairing Mechanisms**

The theories involving conventional mechanism of phonon exchange have been proposed to explain the high transition temperatures in the copper oxide superconductors [102,103]. Based on Eliashbeg [104] formalism corresponding to the strong electron phonon coupling, Weber [105] has argued that at least in 40K, La-based oxide, the superconductivity can be explained by the usual phonon exchange mechanism. Conventional superconductors form Cooper pairs through electron-phonon interaction, in which the weak coupling constant, λ_c is significantly less than 1. But in the newer copper oxides, band structure calculations indicate for both LaSrCuO [106,107] and YBaCuO [108] a λ_c value of 2.5 which indicate the possibility of strong coupling in these compounds. Since in these compounds a small isotope effect is observable, several workers consider that the phonon mechanism may have an important role in the phenomenon. Several serious attempts have been made by many, to explain the high-T_c using the strong coupling phonon exchange mechanism.

For HTSC, it has been suggested that Cooper pairs might form through exciton mechanisms. The attraction between the paired electrons can be obtained from the virtual movement of electrons or by the exchange of excitors. Verma et al, have considered the exchange of pure electronic intra cell charge transfer excitons in Cu-O layers [11]. Superconductivity is

shown to arise from the exchange of these charge transfer excitons. In the case of copper oxide superconductors, this exciton produces essentially a localised charge fluctuation of the form $Cu^{+2}O^{-2} \rightarrow Cu^{+1}O^{-1}$, which is almost unscreaned, because of low carrier densities in these materials. It has a much higher characteristic energy ($\sim$0.5 ev) than the usual Debye energy ($\sim$0.03 ev) of the phonons and is therefore capable of producing much higher T_c, provided electron-exciton attactive coupling is not very small.

The high-T_c in the copper oxide superconductors are also suggested to be arising from the combination of strongly coupled phonons and plasmons [109,110]. IR and Raman studies [111,112] on YBaCuO and LaSrCuO systems indicated plasmons in these compounds and a mechanism was proposed involving an attractive interaction between plasmons in a band composed mainly of Cu $d_{x^2-y^2}$ and oxygen 2p orbitals and electrons in a lower band formed copper d_z and oxygen 2p orbitals.

At least in the case of La-based and Y-based copper oxide compounds antiferromagnetic spin order has been observed close to the superconducting transition in the phase diagram. In $La_{2-x}M_xCuO_4$ there seems to be no superconductivity for x greater than 0.3. But in the absence of doping, in La_2CuO_{4+y}, one finds an antiferromagnetic ordering with Neel temperature T_N=220K. Similarly for $YBa_2Cu_3O_{7-d}$, superconductivity is observed for $0 \leq d \leq 0.5$ but for $d > 0.5$ it undergoes

antiferromagnetic (AF) ordering. This proximity of the superconducting phase to the antiferromagnetic phase has motivated many workers to put forward models invoking magnetic pairing mechanisms for superconductivity. Neutron and Raman studies show that appreciable two dimensional AF correlation perisists even in the superconducting phase with spin correlation length falling down from 200A° around T_N in undoped materials to 10 to 20A° in superconducting phase.

Emery [113] considered the holes as residing on oxygen 2p states and not on Cu 3d states because the short range repulsion is better screened by oxygen than it is by copper. The attraction between these holes can produce a BCS gap of s-wave symmetry and also a high value of T_c. This effective attraction between the holes on oxygen sites mediated by spin fluctuation of the frustrated spins on Cu sites in the doped phase producing superconductivity is suggested in many other reports also [114].

Schrieffer, et al, proposed a model assuming the magnetic ordering in the insulating phase to be a commensurate spin density wave type occuring due to the nesting property of the Fermi surface in a copper oxide layer, which leads to a gap Δ_{SDW} in the single particle electronic excitation spectra. As holes are introduced by doping, the Fermi surface loses the nesting property locally and amplitude of Δ_{SDW} is also reduced locally in vicinity of the holes. This can cause a pair of

holes to be bound inside a spin bag with a reduced amplitude of both SDW and Δ_{SDW} within th bag. This attraction potential leads to an s-wave pairing and a large T_c.

(b) **Resonating Valence Bond Theory**

Stoichiometric La_2CuO_4 is a Mott insulator of spin ½ AF material [102]. Doping this material by substitutional Sr or Ba for about 3% destroys the magnetic order leading to a spin liquid state. The new disordered magnetic phase is called the quantum spin liquid phase. Oxides such as La_2CuO_4, NiO, MnO and several AF insulators will be conducting metals according to simple band picture. But such a picture fails when we have one electron per orbital, and the strong electron repulsion prevents electrons from gaining the delocalization energy and localise one electron per orbital. When we take into account screening, the dominant electrostatic interaction is the onsite coloumb repulsion, i.e., the Hubbard U. When the delocalization energy is small compared to the onsite Coloumb repulsion U, the electron changes into a Mott insulator phase [116]. Mott insulation represents a break down of the band model in which a non-metallic state is realized despite the existence of incompletely filled atomic shells. Any excitation involving charge transfer needs an energy equal to the difference between the Hubbard U and the delocalization energy. This energy is called Mott-Hubbard gap. Even though the charge excitations have a finite gap, the spin fluctuation

have no gap to overcome. The spin fluctuations, which are the low lying states, are described by an effective Hamiltonian, usually referred to as the Heisenberg exchange Hamiltonian H. In terms of the original electron operators, this Hamiltonian is

$$H=-\tfrac{1}{2}J\Sigma b^{+}_{ij}\, b_{ij}$$

where

$$b^{+}_{ij}=(C^{+}_{i}C^{+}_{i}-C^{+}_{i}C^{+}_{j})$$

C^{+}_{i} creates an electron at the orbital site i. The exchange described by this Hamiltonian is called superexchange [117], well known in insulating oxides. It has been established that a spin $\frac{1}{2}$ Heisenberg AF has long range order at low temperature, in 3-dimension. In one dimension quantum fluctuations destroy long range order converting it into a Resonating Valence Bond State (RVB). RVB state is a wuantum liquid of singlet pairs [118].

These singlets which have been created in zero momentum state gives phase coherence among various singlet configurations appearing in the RVB wave function. As Anderson [119] noticed, this phase coherence is exactly the one that appears in a superconducting BCS state. It was observed that oxides which are $s=\frac{1}{2}$ Heisenberg AF rarely have long range magnetic order [118]. Their low temperature magnetic properties are often anomalous. It was argued [120] that when less than 1% of holes are introduced in an AF Mott insulator, the long range order is destroyed and the insulator

is converted into a RVB liquid.

Compounds such as La_2CuO_4, $YBa_2Cu_3O_{6.5}$ etc., which are parent systems of the LaBaCuO and YBaCuO superconductors are considered to be Mott insulators [116]. When doping is done or oxygen content is changed, electrons are removed from such Mott insulators, and a fraction of the pre-existing singlet pairs get charged. In these doped systems, the charge carriers are now holons, having a charge +e. A holon is essentially an empty site with the rest of the elctrons single bonded and resonating among various valence bond configurations in a coherent way. They behave like bosons and superconductivity results from the Bose condensation of these holons. When such an empty site is filled with one electron, we get a spinon which is a neutral fermion. A spinon is an unpaaired spin in a sea of resonating singlet paris.

Further due to strong singlet correlation within the CuO planes, single electron tunneling is less probable than tunneling of a pair electrons. This explains the observed flux quantization of hc/2e in the high temperature superconductors.

2.8 SUPERCONDUCTIVITY IN C_{60} FULLERENES

The very recent discovery [121,122] of superconductivity in alkali doped C_{60} Fullerenes have raised much scientific interest. The existance of soccer ball

structure for different clusters of carbon atoms such as C_{60}, C_{240}, C_{540} etc., were discovered during mass spectroscopic analysis of carbon soot and were designated as Fullerenes after Buckminster Fuller. It was found earlier that C_{60} molecules crystallize into FCC or body centered tetragonal latices and their resistivity could be greatly reduced by addition of small amounts of monovalent alkali elements which occupy interstitial sites. The C_{60} molecule comprises of 12 pentagons of sp^3 hybridization and 20 hexagons of sp^2 hybridization, with a soccer ball radius of 5A° approximately. In FCC phase (with a=14.2A°), there are two inequivalent interstitial sites with octahedral and tetrahedral symmetries respectively, whereas in the tetragonal phase (more accurately orthorhombic with a=25.01A°, b=25.58A° and c=10.0A°) there are three inequivalent sites for alkali element A, corresponding to the stoichiometry A_3C_{60}. the compound A_6C_{60} has BCC structure, the A atoms occupy the edge sites or cube faces located in between the two C_{60} molecules occupying the corner sites.

The resistivity verses x plots for the compound A_xC_{60} show a minima at x=3 for A=Na,K,Rb and Cs. Occurence of superconductivity in these alkali doped Fullerenes was first observed in potassium doped Fullerene, K_xC_{60}, with T_c=18K by Hebard et al [122] in 1991. Later Holezer et al [123] obtained a T_c of 30K in Rb doped Fullerene Rb_xC_{60}. Till now

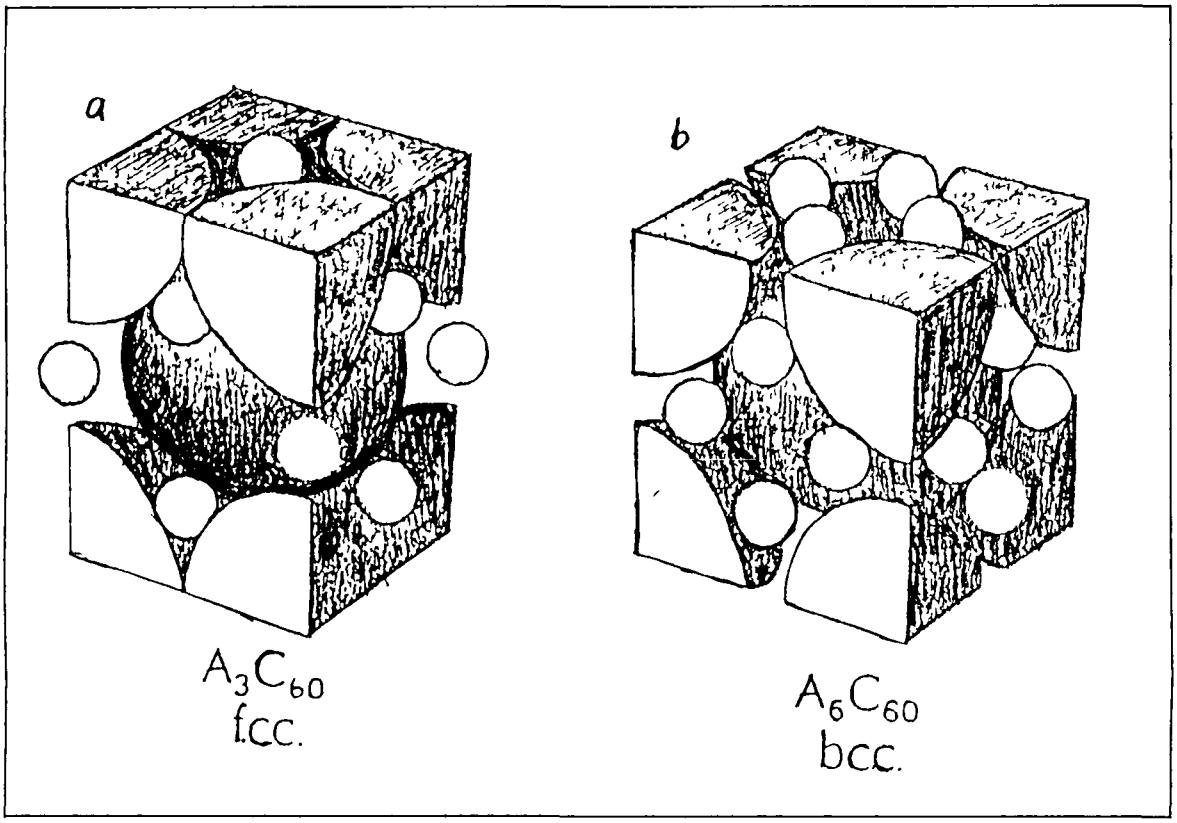

Fig 2.4 Structure of Alkali (A) doped C_{60} Fullerenes (a)A_3C_{60}, (b) A_6C_{60}.

the highest T_c in this system is reported to be 31.3K in Rb_2CsC_{60} [124].

Studies on various properties and structure of these novel superconducting system is underway. A better understanding of superconductivity in these alkali doped Fullerenes may help to raise the T_c still further.

2.9 CONCLUSIONS

There is a general consensus concerning most of the physical properties of these copper oxide materials. But the theoretical literature concerning the high temperature superconductivity is not as voluminous as the experimental one. Many theoretical models, based on the BCS pairing and also on the Boson condensation in non-Fermi liquid were suggested. But a mechanism which can fully explain the phenomenon and various features associated with it is yet to be solved out. At present the three persistent and most important problems in this field are

(i) how to raise the T_c further

(ii) what is the mechanism responsible for high temperature superconductivity and

(iii) how to convert these ceramic superconducting materials to usable forms such as film, discs, wires, tapes etc., without any loss in their properties.

REFERENCES

1. H. Kamerling Onnes, Akad. Van Wetenschappen **14** (1911) 113,818.
2. J.G. Bednorz and K.A. Muller, Z.Phys. B **64** (1986) 189.
3. R.J. Cava, R.B. Van Dover, B.Batlogg and E.A. Rietman Phys. Rev. Lett. **58** (1987) 408.
4. H. Takagi, S.I. Uchida, K.Kitazawa and S.Tanaka, Jpn. J. Appl. Phys. **26** (1987) L1.
5. J.M. Tarascon, et al, science, **235** (1987) 1373.
6. C.W. Chu, et al, Science **235** (1987) 567.
7. M.K. Wu, et al, Phys. Rev. Lett. **58** (1987) 908.
8. C.W.Chu, et al, Phys. Rev. Lett. **60** (1988) 941.
9. C.Michel, et al, Z. Phys. B **68** (1987) 421.
10. H.Maeda, et al, Jpn. J. Appl. Phys. **27** (1988) L209.
11. C.P. Poole Jr, T.Datta and H.A. Farach, Copper Oxide Super conductors [wiley NY] 1988.
12. C.Kittel, Introduction to Solid State Physics, Vol.III 1966.
13. J.C.Phillips "Physics of High-T_c Superconductors"[Academic, NY](1989).
14. B.T. Mathias, T.H. Geballe and V.B. compton, Rev. Mod. Phys. **35** (1963) 1.
15. O.Fisher, Appl. Phys. **16** (1978) 1.
16. A. Baratoff and G. Binning, Physica B **188** (1981) 1335.
17. B.Binning, et al, Phys. Rev. Lett. **45** (1980) 1352.
18. C.K.Chu, et al, Phys. Rev. Lett. **58** (1987) 405.

19. D.C. Johnston, et al, Mat. Res.Bull. **8** (1973) 777.

20. A.W. Sleight, J.C. Gillson and R.E. Bierstedt Solid State Commun. **17** (1975) 27.

21. A.W. Sleight, ACS Symp. (1987) P.2.

22. L.R. Gilbert, R. Messier, and R. Roy, Thin Solid Films **54** (1978) 129.

23. W.Meissner and R. Ochsenfeld, Naturwiss **21** (1933) 787.

24. M.Tinkham, Introduction to superconductivity, Krieger, Florida (1985).

25. Pippard A.B., Proc. Roy. Soc. **A203** (1950) 210.

26. R.Meservey and B.B. Schwartz in "Superconductivity" R.D.Parks (Ed), Marcel Dekker, New York (1969) 174.

27. M.A.Biondi and M.P.Garfunkel, Phys.Rev.**116** (1959)853.

28. P.L.Richards and M.Tinkham, Phys.Rev. **119** (1960) 575.

29. D.H. Douglass, Jr.and L.M.Falicov, Prog.in Low Temp. Phys. **4** (1964) 97.

30. E. Maxwell, Phys. Rev. **78** (1950) 477.

31. Reynolds, et al, Phys. Rev. **78** (1950) 487.

32. J. Bardeen, L.N. Cooper and J.R. Schrieffer Phys. Rev.**108** (1957) 1175.

33. G.Gorter and H.B.G Casimir, Physica **1** (1934) 306.

34. F.London and H. London, Proc.Roy. Soc.(London)AI **49** (1935) 72.

35. V.C. Ginzburg and L.D. Landau, Sov. Phys. JETP **20** (1950) 1064.

36. J. Bardeen, L.N. Cooper and J.R. Schrieffer Phys. Rev. **106** (1957) 162,1175.

37. C. Michel and B. Raveau, Rev. Chim. Min. **21** (1984) 407.

38. R.J. Cava, et al, Phys Rev. Lett. **58** (1987) 1408.

39. P.Day, et al, J. Phys. C: Solid State, **20** (1987) 1429.

40. G. Burns, F.H. Dacol and M.W.Shafer, Solid State Commun **62** (1987) 687.

41. M. Onoda, et al, Jpn. J. Appl. Phys. **26** (1987) L363.

42. C.N.R. Rao, in "High Temperature Superconductivity" S.V.Subramanyam and E.S.Rajagopal (Ed.) (1989)69.

43. P.Ganguly, et al, Solid State Commun. **62** (1987) 807.

44. J.M. Tarascon, et al, ACS Symp. Series (1987) P351.

45. J.D. Jorgensen, et al, Phys. Rev. B **36** (1987)3608.

46. I.K.Schuller, et al, Solid State Commun.**63** (1987) 385.

47. R.M. Hezen, et al, Phys. Rev. B **35** (1987) 7238.

48. F.Beech, et al, phys. Rev. B **35** (1987) 8778.

49. M.A. Beno, et al, Appl. Phys. Lett. **51** (1987) 57.

50. H. You, et al, Solid State Commun **64** (1987) 493.

51. W.I.F. David, et al, Nature **327** (1987) 310.

52. N.Kijima, et al, Jpn. J.Appl. Phys. **28** (1988)L787.

53. D.Shindo, et al, Jpn.J . Appl. Phys. **27** (1988) L1018.

54. R.M. Hazen in "Properties of High Temperature Superconductors" Ginzburg (Ed.) [World Scientific, Singapore] (1990).

55. J.M. Tarascon, et al, Phys. Rev. B **37** (1988) 9382.

56. M.A. Subramanian, et al, Science **239** (1988) 1015.

57. C.N.R. Rao, et al, Pramana J. Phys. **30** (1988) 495.

58. S.A. Sunshine, et al, Phys. Rev. B **38** (1988) 893.

59. Z.Z. Sheng and A.M. Herman, Nature, **332** (1988) 138.

60. O.N. Sirvastava, in "Studies of High Temperature Superconductors" Anand Narlikar (Ed.) [Nova Science, New York], Vol.3 (1989).

61. A.P.B. Sinha, in "High Temperature Superconductors" S.V. Subramanyam and E.S. Rajagopal (Ed.) (1989).

62. Many articles in "Chemistry of High Temperature Superconductors",ACS Symposium Series (1987) 351.

63. Several articles in Proced. of Intl. Conf. on High Temp. Supercond. and Mat. and Mech. of Supercond., Feb 29- March 14, Interlaken Switzerland (1988).

64. R.B. Laibowitz, et al, Phys. Rev. B. **35** (1987)8821.

65. P. Chaudhari, Phys. Rev. Lett. **58** (1987) 2684.

66. S.B. Ogale, et al, Phys. Rev. B **36** (1987) 13.

67. N.Terada, Jpn. J. Appl. Phys. **26** (1987) L508.

68. S.J. Lee, Appl. Phys. Lett. **51** (1987) 1194.

69. X.D.Wu, et al, Phys. Rev. B **36** (1987) 18.

70. R. Micnas, J. Ranninger and S. Robaskiewicz, Phys. Rev. B **36** (1987) 4051.

71. M.Gurvitch and A.T. Fiory, Phys. Rev. Lett. **59** (1987) 1337

72. Y. Hidaka, et al, Jpn. J. Appl. Phys, **26** (1987) 1377.

73. S.W. Tozer, et al, Phys. Rev. Lett., **59** (1987) 1768.

74. S. Martin, et al, Phys. Rev. Lett., **60** (1988) 2194.

75. S. Jin, R.C. Sherwood and T.H. Tiefel in Proc. of Intl. Fonf. Critical Currents in High Temp. Superocnd., Colorado, USA (1988).

76. J. Palca, Nature, **330** (1987) 511.

77. S.L.Furcone and Y.M.Chiang, Appl. Phys. Lett., **52** (1988) 2180.

78. A.B. Harkar, et al, Appl. Phys. Lett. **82** (1988) 2186.

79. P. Chaudari, et al, Phys. Rev. Lett., **58** (1987) 2684.

80. J. Kwo, et al, Phys. Rev. B **36** (1987) 4039.

81. J.C. Philips in "Physics of High-T_c Superconductors" [Academic, New York] (1989) 273.

82. E.L. Venturi, et al, MRS Anaheim Symp. (1987) P.97.

83. Y.Hidaka, et al, Jpn. J. Appl. Phys. **26** (1987) L377.

84. Y. Tajima, et al, Phys. Rev. B **37** (1988) 7956.

85. J. Beille, et al, Physica C **156** (1988) 448.

86. G. Nieva, et al, Phys. Rev. B **16** (1987) 8780.

87. A. Junod, A. Bezinge and J.Muller, Physica C **152** (1988) 50

88. S.J. Collocott, et al, Physica C **156** (1988) 292.

89. N.E. Phillips, et al, J. Appl. Phys, **26** (Suppl) (1987)1115

90. J.C. Cohn, S.D. Pearson and C.Uher,Phys. Rev. B **38** (1988) 2892.

91. V. Bayot, et al, Solid State Commun, **63** (1987) 983.

92. S.D. Peacor and C.Uher, phys. Rev. B **39** (1989) 11559.

93. Yasuhiro Iya, in "Studies of High Temperature Superconductors" Anand Narlikar (Ed.) Vol.2 (Nova Science, New York] (1989).

94. A. Umezava, et al, Phys. Rev. B **38** (1988) 2843.

95. G.Aeppli, et al, Phys. Rev. B **35** (1987) 7129.

96. Y.J. Uemura, et al, phys. Rev. B **38** (1988) 909.

97. S.N. Behera, in "Studies of High Termperature Superconductors" Anand Narlikar (Ed.), Vol.2 [Nova Science, New York] (1989).

98. B.Batlogg, et al, Phys. Rev. Lett., **59** (1987) 912.

99. T.A. Faltens, et al, Phys. Rev. Lett., **59** (1987) 915.

100. B.Batlogg, et al, Phys. Rev. Lett., **58** (1987) 2333.

101. L.C. Bourne, et al, Phys. Rev. B **36** (1987) 3990.

102. L.F. Matheiss, Phys. Rev. Lett., **58** (1987) 1028.

103. H. Kemimura, Jpn. J. Appl. Phys. (Suppl.) **26** (1987) 1092.

104. G.M. Eliashberg, Sov. Phys. JETP **11** (1960) 696.

105. W.Weber, Phys. Rev. Lett., **58** (1987) 1371.

106. L.C.Bourne, et al, Phys. Rev.Lett., **58** (1987) 2337.

107. D.A. Papeconstantopoulos, et al, Jpn. J.Appl. Phys. (Suppl.) **26-3** (1987) 1091.

108. A. Mawdsley, et al, Nature **328** (1987) 233.

109. J. Ruvald, Phys. Rev. B **35** (1987) 8868.

110. Z. Kersin, Phys. Rev. B **35** (1987) 8716.

111. Z.Schlesinger, et al, Phys. Rev. B **36** (1987) 5275.

112. S. Perkowitz, et al, Solid State Commun, **64** (1987) 721.

113. V.J. Emery, Phys. Rev. Lett., **58** (1987) 2794.

114. A. Birgenean R.J. and M.A. Kastner; Intl. J. Mod. Phys. B **1** (1988) 649.

115. J.R. Schrieffer, S.G. Wen and S.C. Zhang, Phys. Rev. Lett.,**60** (1988) 944.

116. G.J. Hyland in "Studies on High Temperature Superconductors" Anand Narlikar (Ed.) Vol.1 [Nova Science, New York] (1989).

117. P.W. Anderson, Solid State Phys. **14** (1963) 99.

118. P.W. Anderson, Mat. Res. Bull. **8** (1973) 153.

119. P.W. Anderson, Science **235** (1987) 1196.

120. P.W. Anderson, G. Baskaran, Z.Zou and T. Hsu, Phys. Rev.Lett., **58** (1987) 2790.

121. Several papers presented in Intl. Conf. M^2S-HTSC III Kanazava, Japan, July (1991).

122. Hebard A.F., et al, Nature **350** (1991) 600.

123. K.Helozer, et al, Science **253** (1991) 1154.

124. R.M. Fleming, et al, Nature (in press).

[redacted]

[redacted]

[redacted]

3.1 INTRODUCTION

Since the discovery of high temperature superconductivity in La-Ba-Cu-O system by Muller and Bednorz in 1986 [1], there have been immense experimental as well as theoretical attempts to elucidate the mechanism of the phenomenon and to understand the peculiar properties exhibited by these copper oxide superconductors. The magnetic properties of these high-T_c superconductors [HTSC] have been studied in great detail and there have been many theoretical suggestions and experimental indications that magnetism plays an important role in underlying superconducting mechanism [2-6]. In all the high-T_c materials Cu-O layers were found to occur and the understanding of the magnetic interactions in the copper oxygen layers still remains as an unresolved problem [7].

Electron paramagnetic resonance, in principle, is a very powerful technique to get detailed informations about the magnetism and the local environment surrounding the paramagnetic ions, especially about Cu^{2+} ions in the high-T_c materials, and their interactions between themselves and with other paramagnetic ions such as rare earths and doped paramagnetic ions such as Mn^{2+}, Fe^{2+} etc. Upto now extensive research has been carried out on the EPR spectrum of Gd^{3+} ions in high-T_c superconductors either in $GdBa_2Cu_3O_{7-d}$ or compounds

with gadolinium partially substituting, since Gd^{3+} EPR spectra are easily observable upto room temperature because of its long spin lattice relaxation time [8-12]. Great interest has been focussed on the EPR spectrum of Cu^{2+} ions, which is attributed by many authors to impurity phases formed in the high-T_c compounds during their preparation, while others believe that it is due to the original superconducting phase [13-19]. Due to this, a large variety of non-superconducting parent and related compounds were studied extensively to ascertain whether the EPR signals originate from the actual high-T_c superconducting compounds or from some impurity phases.

3.2 EPR STUDIES OF PARENT AND RELATED SYSTEMS OF HTSC

Eventhough copper ions are amongst the most amenable transition metal ions for EPR detection [20], it is interesting to note that EPR silent copper occasionally occurs in nature [21,22]. A good example is copper oxide (CuO] which is supposed to be the most important basic ingredient for all the high-T_c oxides [22]. It is found to be antiferromagnetic with a Neel temperature of 230K [23], but even upto room temperature it does not exhibits any EPR spectrum. In an EPR study by Kindo, et al, [24], using pulsed magnetic field and at 45GHz microwave frequency, a very broad paramagnetic resonance was observed and is attributed to one dimensional

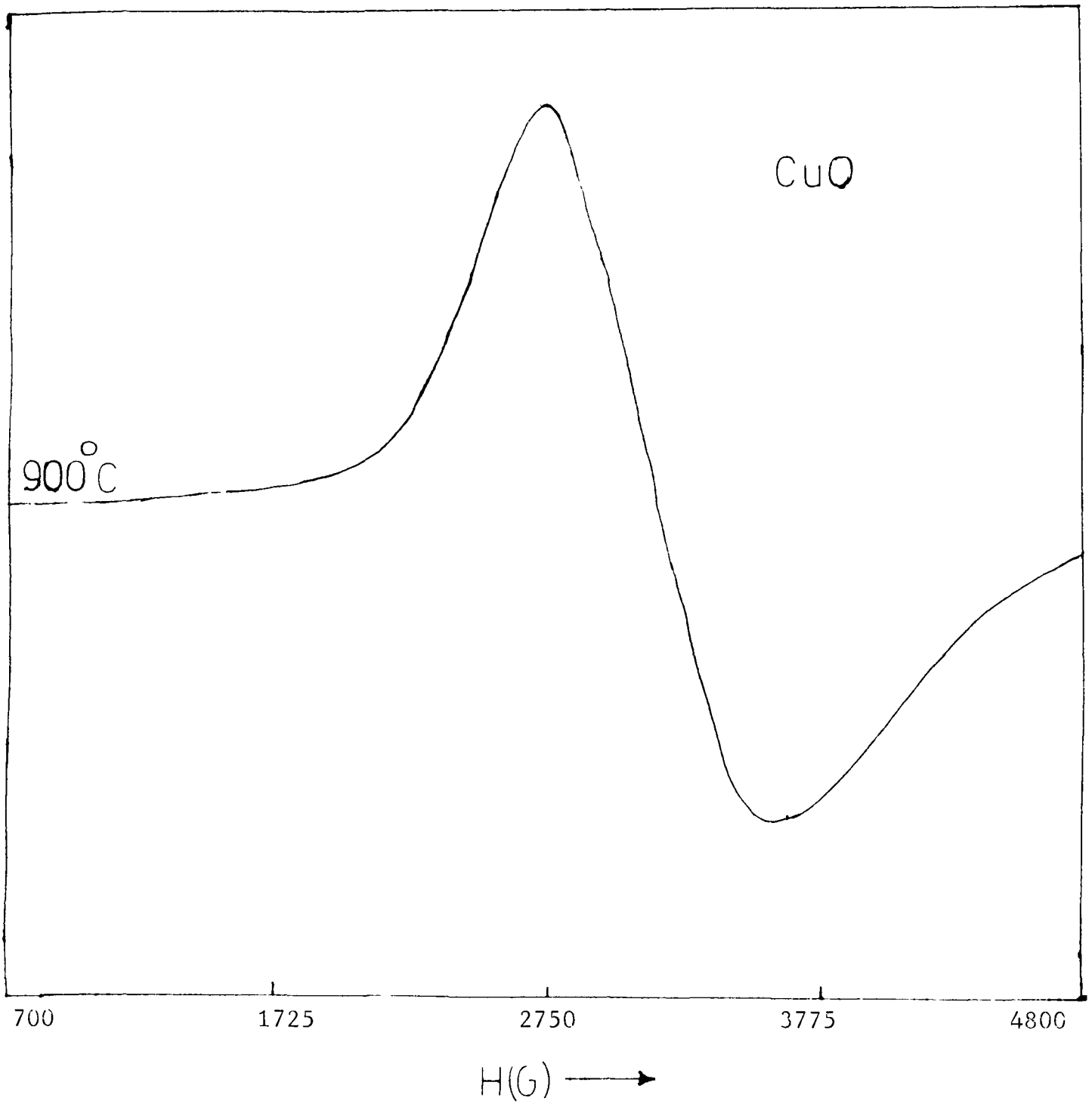

Fig. 3.1 EPR Spectrum of CuO annealed at 900°C [Ref.25,26].

spin correlations. Recently strong paramagnetic signal at g~2 region were obtained in CuO by the authors [25,26], by subjecting it to successive heat treatments. K. Tagaya et al, [27,28] observed strong EPR signals due to superparamagnetic CuO particles which are precipitated out along with high-T_c superconducting compounds during their preparation.

In the BaO-CuO binary system, the most widely studied compound is $BaCuO_2$. In most of the cases, an axially symmetric signal is found to be superimposed on a broad signal in the EPR spectrum [14,29]. In few studies on freshly prepared samples, only the broad signal is obtained, but after exposure to the atmosphere it completely replaced by a very intense and narrow line [30-32]. The broad signal is usually attributed to ferromagnetic order in this compound as is suggested by magnetic susceptibility studies [33], and the sharp one to pure paramagnetic Cu^{2+}. In Ca and Sr cuprates, Ca_2CuO_3 exhibited a well resolved EPR signal with g =2.04 and g =2.26 [34], while $SrCuO_2$, $CaCuO_2$ and $CaCu_2O_3$ are reported to be EPR silent due to strong antiferromagnetic interactions between adjacent copper ions [14,35].

In the R-Cu-O system (where R is a rare earth ion), studies on the compounds with the general formula R_2CuO_4, no Cu^{2+} EPR signal is reported, for R=Pr,Nd,Sm etc [36]. Oseroff, et al, [36] performed an EPR study in these systems from 2K to 600K but could not observe any signal and this

absence is attributed to the two dimensional antiferromagnetic correlations which is strong even upto much higher temperatures. Vier et al, have reported an unusual magnetic field dependent signal in Eu_2CuO_4 which appears to be associated with a resonance mode of the CuO_2 complex [37]. The only rare earth ion which is reported to give an EPR signal in this system is Gd^{3+} in Gd_2CuO_4 [36]. The compound $Y_2Cu_2O_5$ has been studied by many workers [14,16,38]. In all these cases, an exceptionally broad symmetric spectrum with g=2.10 is observed. This exchange averaged, dipolar broadened line is attributed to the ferromagnetic coupling of copper ions observed from magnetic susceptibility data [33,39]. In La_2CuO_4, while Yu and Lii failed to observe any EPR signal, Zhang, et al, [40] observed an EPR signal with hyperfine structure at room temperature and is attributed to Cu^{2+} in a square planar or tetragonaly distorted octahedral site. In oxygen deficient $LaCuO_{3-d}$, Mehran, et al [41] observed an EPR signal due to Cu^{2+} at much higher temperatures of 573K. Upon reducing the temperature, the linewidth increases rapidly. It is assumed that for d=0, all copper ions are in the trivalent states and for d=0, some of the copper ions become divalent and the Cu^{2+}-Cu^{2+} exchange interaction comes into play. The exchange interactions would have to be mediated possibly by oxygen and/or conduction electrons.

In the La-Ba-Cu-O system, for both superconducting and non superconducting phases of $(La_{1-x}Ba_x)_2CuO_{4-d}$ no Cu^{2+} EPR

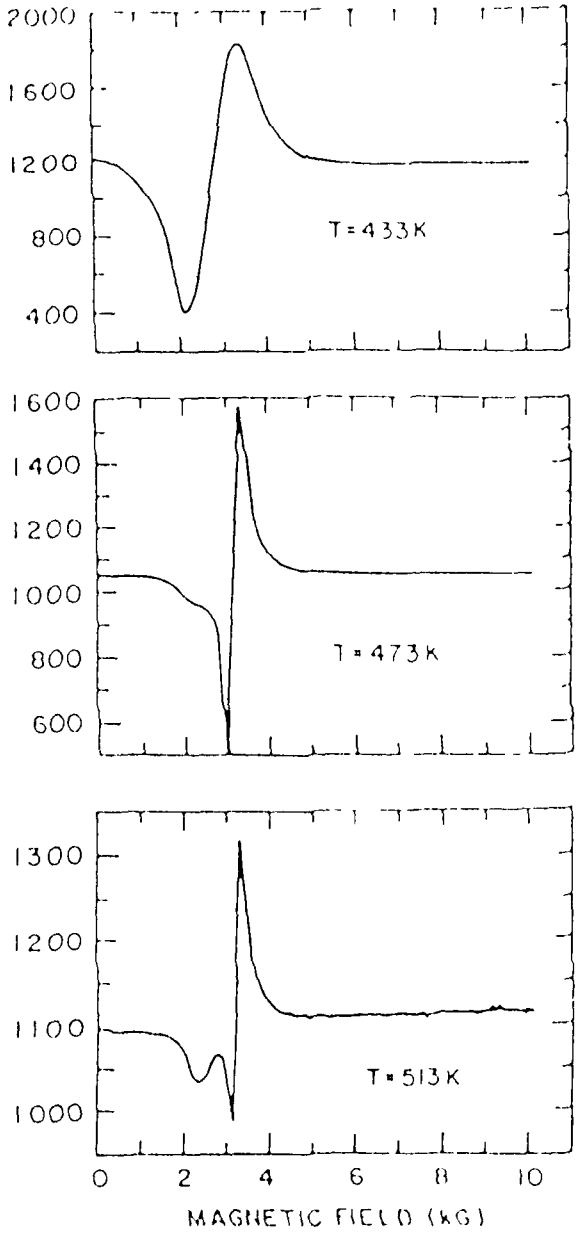

Fig. 3.2 EPR Spectra of $LaCuO_{3-d}$ at different Temperature [Ref. 41].

signals were observed [42]. Similar observations were also reported for the $(La_{1-x}Sr_x)_2CuO_{4-d}$ compounds also [43]. Of the different non-superconducting phases of the R-Ba-Cu-O system, the most studied phase is of the form R_2BaCuO_5 [14,31,38] and $RBa_2Cu_3O_6$ [44]. The R_2BaCuO_5 series of compounds, including Y_2BaCuO_5, exhibits strong EPR signals at room temperature, characteristic of Cu^{2+} in tetragonal environment [38]. The intensity of the signal is found to increase upon cooling from room temperature, which is consistent with indication of antiferromagnetic interactions in this compound [38]. The oxygen deficient $RBa_2Cu_3O_6$ compounds are reported to be EPR silent probably due to strong antiferromagnetic interaction [44,45].

3.3 OBSERVATION OF Cu^{2+} SIGNALS FROM HIGH-T_c SUPERCONDUCTING MATERIALS

Right from the beginning of HTSC, many researchers believe that the dominant valence state of copper ions in the high-T_c superconductors, especially in the most studied $YBa_2Cu_3O_{7-d}$ is Cu^{2+} and therefore it will give an intrinsic signal in the g~2 region in the EPR spectrum [40,46-52]. For example, R.Bartucci, et al, [46] observed an EPR spectrum which was a superposition of two EPR signals with hyperfine structures, in pellets of YBaCuO high-T_c compound all over the investigated temperatures, ranging from 77K to room

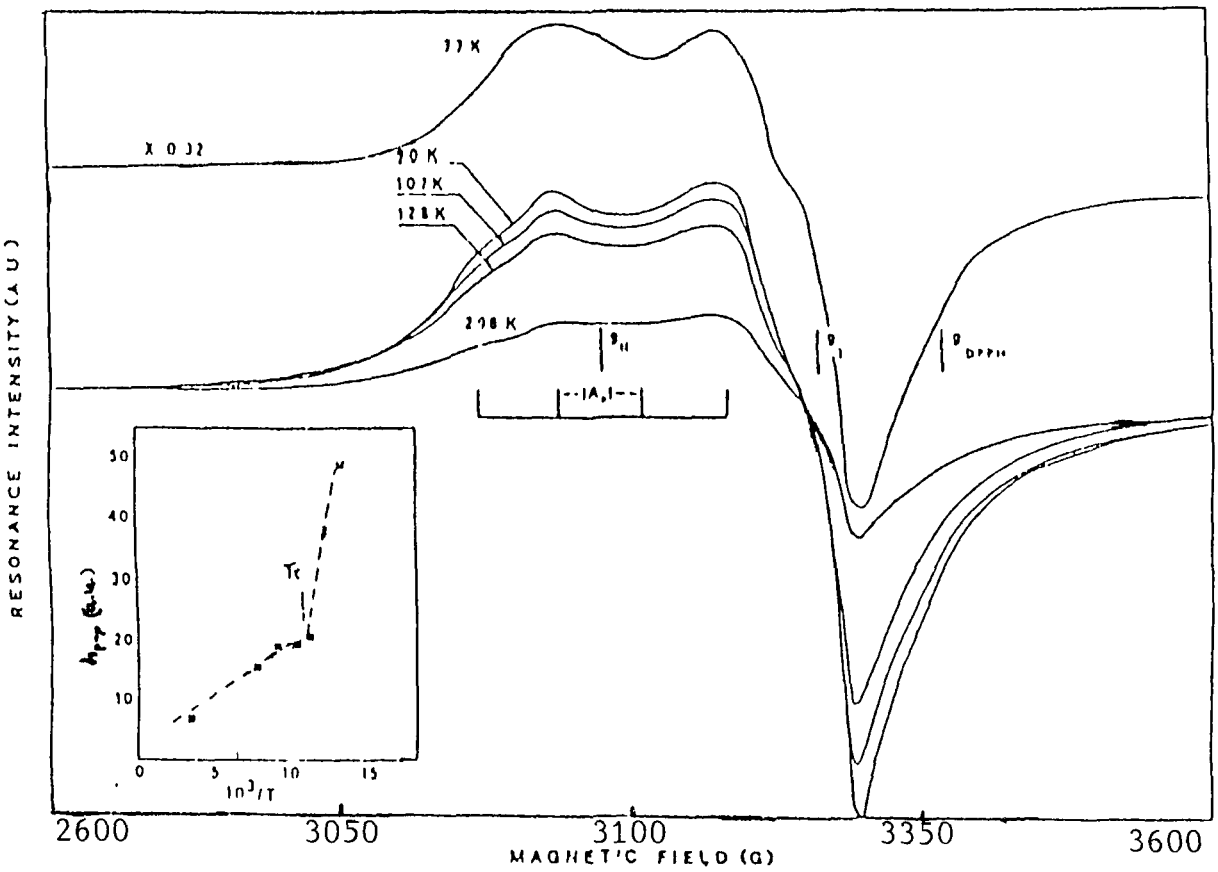

Fig. 3.3 EPR Spectra of Polycrystalline $YBa_2Cu_3O_{7-d}$ pellet detected by Bartucci et al, [Ref. 46]. Inset shows the peak-to-peak intensity of the derivative line shape vs 1/T.

temperature (see figure 3.3) The intensity of the signal increases rapidly below T_c, and the line width also shows a significant increase. They attributed the two signals to two non equivalent Cu^{2+} ion sites namely $Cu^{2+}(1)$ and $Cu^{2+}(2)$ in the compound. It is well known that the perovoskite structure of the orthorhombic superconducting $YBa_2Cu_3O_{7-d}$ formed by one square planar $Cu^{2+}(1)$ complex and two square pyramidal $Cu^{2+}(2)$ environment per unit cell [53-55]. De [56] also observed an EPR signal from YBaCuO superconductor characteristic of Cu^{2+}, both above and below T_c. The signal was attributed to Cu^{2+} ions which either takepart in superconductivity or converts itself to the superconducting phase. The Cu^{2+} ions below T_c seem to have an orthorhombic site symmetry, whereas above T_c, it changes to axial symmetry. Similar EPR observations were reported by other workers also [57,58].

Guskose, et al [59], observed an EPR signal with g=2.312 in superconducting YBaCuO at $T<T_c$ and is attributed to Cu^{3+} ions. It is known that the ground state of $3d^8$ configuration is the orbital F-state which in an octahedral field splits into two triplets and one singlet. The triplet states admixes with the singlet one due to spin orbit coupling and the g-value in this case assumes values in the range from 2.15 to 2.35 [60]. The observed line is therefore attributed to Cu^{3+} origin. Observation of signals due to Cu^{3+} is reported by Sastry also [61].

Owen [62] and several others [13,52,63-65] observed the appearance of an isotropic spectrum below T_c in $YBa_2Cu_3O_{6+x}$ (with $T_c \sim 40K$). Owen attributed it to Cu^{2+} ions in the CuO chains along b-axis of the superconducting phase. The large g-shift and line broadening with decreasing temperature, which was observed over a wide temperature range shows that the resonance is arising from Cu^{2+} in one dimensional chains and the effects are due to the persistance of short range one dimensional antiferromagnetic ordering fluctuations [62]. But Mehran, et al [63], ascribed this signal to be originated from a site which does not have real cubic symmetry.

When EPR silent monophasic YBaCuO pellets were crushed into powder form, it was found to give clear signals in the $g\sim2$ region [66]. Stankowski, et al [66] explained it as due to the structural charge non - equilibirium, resulting in stable fluctuation of $Cu^{3+}+Cu^{1+}\rightarrow 2Cu^{2+}$ in exchange coupled complexes of CuO_5 blocks, as a result of mechanical powdering. After longer pulverisation, CuO_5 complexes get isolated giving rise to the powder like signal at the observed g-values of $g_{\parallel}=2.39$ and $g_{\perp}=2.07$ [66]. Lue [69] argued that the superexchange between the copper spins to give S=0 in the pure orthorhombic structure, will result in the absence of any EPR signal. But this he considered as a volume property and will be weakened as the particle size is reduced, i.e., for the powder case. If oxygen deficiency density is not high, the

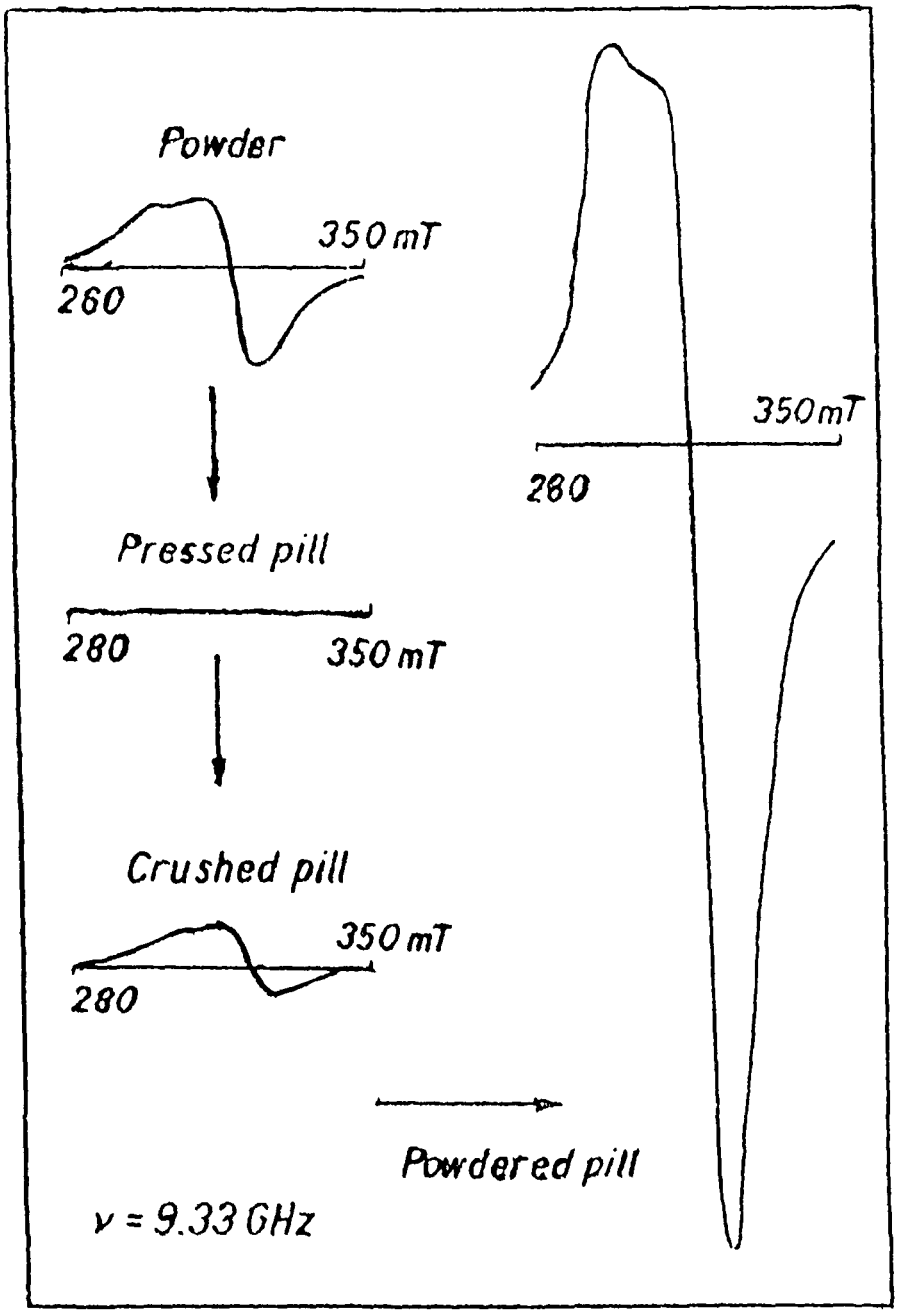

Fig. 3.4 The influence of the mechanical processing of YBaCuO superconducting sample, on the EPR spectra [Ref.66].

spin up and spin down electrons in neighbouring Cu^{2+} ions can experience a collective motion giving rise to spin wave while still superconducting and EPR sensitive. At still higher d, collective motion is interrupted and resulting insulator will give dipolar broadened EPR signal [69]. Indications about such a role of antiferromagnetic spin waves were detected in the EPR study of Ag doped YBaCuO superconducting compound [70,71].

Guskose, et al, [17,72] carried out a detailed EPR investigation on YBaCuO superconductor and a series of high-T_c compounds of the general formula $RBa_2Cu_3O_{7-d}$ with R=La,Pr,Nd,Sm,Eu,Gd,Dy,Ho,Tm,Yb and Lu. Except $LaBa_2Cu_3O_{7-d}$ (T_c=50K) and $PrBa_2Cu_3O_{7-d}$ (non-superconducting) for all other compounds, T_c was in the range of 90-95K. All these compounds have shown conventional EPR spectrum of powder samples with an anisotropic g-tensor, which can be attributed to Cu^{2+} ions in an orthorhombic symmetry. Comparison among different $RBa_2Cu_3O_{7-d}$ samples under similar conditions showed that absolute EPR signal intensities are widely differing [17]. Table 3.1 shows the conductivity and EPR signal intensities for different RBaCuO compounds. The observed change in intensities of EPR lines of Cu^{2+} could be attributed to the so called 'skin effect', according to which the volume of the sample that could be penetrated by microwave radiation decreases when the electrical conductivity increases. The

Compound	relative intensity I/I_o	$(O^{-1}{}_{cm}{}^{-1})$
$YBa_2Cu_3O_{7-d}$	0.0281	500
$LaBa_2Cu_3O_{7-d}$	0.0439	198
$PrBa_2Cu_3O_{7-d}$	0.0081	5795
$NdBa_2Cu_3O_{7-d}$	0.0127	2357
$SmBa_2Cu_3O_{7-d}$	0.0154	1604
$EuBa_2Cu_3O_{7-d}$	0.0129	2285
$GdBa_2Cu_3O_{7-d}$	0.0211	856
$DyBa_2Cu_3O_{7-d}$	0.0090	4687
$HoBa_2Cu_3O_{7-d}$	0.0163	1452
$TmBa_2Cu_3O_{7-d}$	0.0251	603
$YbBa_2Cu_3O_{7-d}$	0.0132	2186
$LuBa_2Cu_3O_{7-d}$	0.0305	409

Table 3.1 Room temperature electrical conductivity and relative intensity of the EPR signals of different 123 superconducting compounds.

relative intensities of the EPR signals are given by

$$I/I_o=\{2\ \exp(-w)+[1+\exp(-2w)]/w\}/[1+\exp(-w)]^2$$

where $w=d/\delta$, d is the thickness of the sample and $\delta=(2/\mu_o\omega\sigma)^{\frac{1}{2}}$ is the skin depth, w the frequency of microwave radiation and σ is the electrical conductivity. Similar results of intensity dependence of EPR on conductivity is found in $YBa_2Cu_3O_{7-d}$ pellets prepared with different values of σ [73,74]. Recently Guskose, et al, extended the EPR investigations to rare earth ions doped SmBaCuO superconductor All the compounds $Sm_{0.5}RE_{0.5}Ba_2Cu_3O_{7-d}$ (with RE=Nd,Eu,Gd,Dy, Ho,Tm,Yb etc.,) are superconducting with T_c in the range of 90-95K. For all case Cu^{2+} EPR signals were observed, the intensity of which showed strong dependence on their electrical conductivity [75]. Based on these observations, it was conjuctured that all high-T_c cuprates contains characteristic Cu^{2+} EPR lines, and any failiure to observe any EPR signal in superconducting oxides by some researchers is doubted to be either due to the high electrical conductivity of their sample so that microwave could not penetrate the whole volume of the sample or due to the small masses of the single crystals [17,74,75].

Similar observations of EPR signals due to Cu^{2+}, which are assumed to be present in the superconducting phases of Tl and Bi-based systems, also were reported. For instance,

Songliu, et al, [76,77] studied the EPR spectrum of $BiSrCaCu_2O_y$ high-T_c superconductor (T_c=110K) over a wide range of temperatures from 96K to 300K. Above T_c two EPR signals were observed, one of which gradually shifts towards higher magnetic field with rising temperature as is illustrated in figure 3.3. At room temperature only one signal is seen and is attributed to Cu^{2+} origin. But on lowering the temperature, an electron from the oxygen ion transferrs to the nearby Cu^{2+} ion subject to Hunds rule. During this transfer it also interacts with the unpaired electron in the oxygen ion. In this case the electron does not get completely transferred to the orbit of Cu^{2+} ion. The first EPR signal in the figure which shifts towards low magnetic field and its g-value increased from 2.24 to 2.78 when temperature is decreased from 310K down to 115K is attributed to the possibility of electrons from oxygen ions occupying the orbit of Cu^{2+} ions on cooling. The second signal may be related to the unpaired electrons from oxygen ions. With decreasing temperature, the probability of electron transferred from oxygen occupying the orbit of Cu^{2+} and thus making, it to have an effective spin of one increased. For copper ions (Cu^{2+}) with spin one, its energy levels would have initial splitting in zero magnetic field, i.e., Stark splitting. The zero field signal observed below T_c could therefore be attributed to the Cu^{2+} with spin

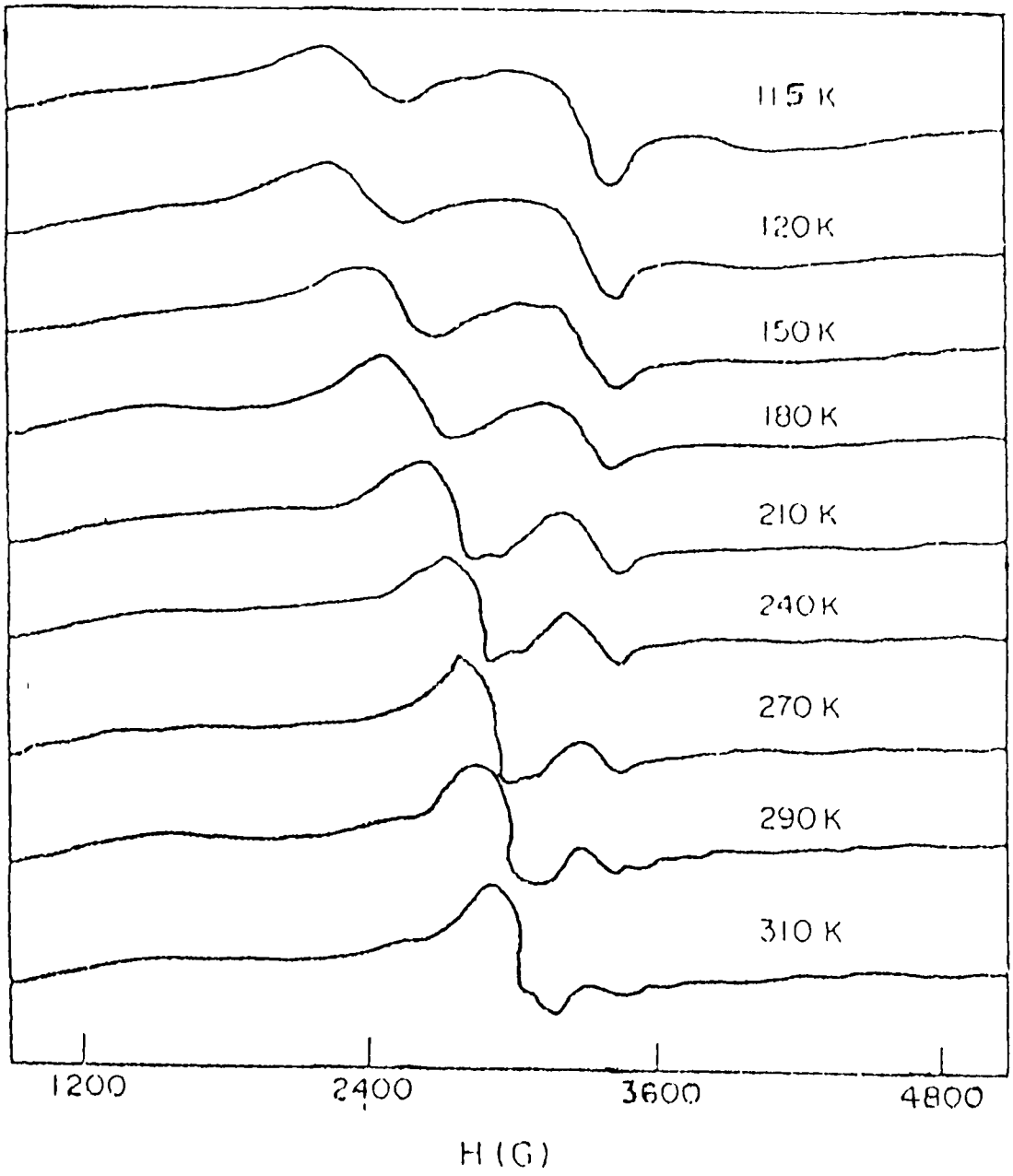

Fig. 3.5 The EPR characteristic spectra of the $BiSrCaCu_2O_y$ sample in the range of temperature from 115K to 310K reported by Songliu et al, [Ref. 76,77].

one. On the other hand the unpaired electron in one oxygen will get paired with the unpaired electron in another oxygen at T_c, thus vanishing the second signal also at T_c. An anomaly in line width and g-value is found near $T=2T_c$ as is observed in most of the other superconducting systems also [77,78-80].

Observation of Cu^{2+} EPR signal from Pb-Bi-Sr-Ca-Cu-O superconducting single crystal was reported by Karim et al, [81] also. The sharp line at $g\sim2.055$ observed in the whole temperature range from 4K to 300K is ascribed to Cu^{2+} ion excitations. The EPR signal got intensified as temperature decreased from 300K to T_c, and then remained constant on further decreasing. The increase in intensity of the signal upto T_c is attributed to the increase in the number of spins involved in the magnetic transitions in accordance with Boltzmann statistics. Below T_c, the flux penetration creates regions of normal electrons. These electrons are responsible for signal below T_c. Area of these fluxoid regions will decrease proportionally and will compensate exactly the increase in spins given by Boltzmann statistics and therefore the intensity of the signal will remain constant. In a recent EPR study on $Bi_2Sr_2CaCu_2O_8$ and $Bi_{2.2}Sr_2Ca_{0.8}Cu_2O_8$ Takekazu,et al [82] also reported the observation of Cu^{2+} signals with g=2.1 attributed to be of intrinsic origin.

Hayashi, et al [83,84] observed EPR signals in both

Bi-based (T_c=108K) and Tl-based (T_c=124K) superconductors. Two kinds of EPR signals were observed at room temperature, one anisotropic and the other an isotropic one with a Lorentzian line shape. At T_c both these signals disappear, but the anisotropic one reappears at low temperatures far below T_c. The isotropic signal is attributed to be originated from the original superconducting phase whereas the origin of the other signal is doubted. The isotropic signal is assigned to Cu ions located over or below an apex oxygen and in that case, a hole should be trapped at the apex oxygen. Modelung energy calculations in high-T_c oxides [85] especially in the Bi and Tl-based systems [86] suggests that holes are doped to the oxygen sites, and the CuO_2 plane remains insulator even under the hole doping to the material. The symmetry around the Cu^{2+} ions in the CuO_2 planes then does not change. Hence it is argued that an isotropic signal is expected in this system.

3.4 EPR SILENCE OF COPPER IN HIGH-T_c CUPRATES

In spite of all these observations, majority of the EPR studies on high temperature superconducting cuprates indicate that Cu^{2+} in the pure superconducting phase is insensitive to EPR. In a number of studies it was seen that most of the EPR signal reported in these compounds are similar to that observed in their related and parent cuprates. At the same

time it was found that such non-superconducting impurity phases are usually formed along with the superconducting phase during their preparation. Many authors argued that any signal reported to be obtained in the superconducting compounds may be arising out of such impurity phases. To ascertain this, several workers [14,38,87] carried out EPR studies on these HTSC, especially the $YBa_2Cu_3O_{7-d}$ and their possible related impurity phases simultaneously. For example Jones, et al, [14] performed a comparative EPR investigation on YBaCuO superconducting samples and various other phases in the Y-Ba-Cu-O phase diagram, such as $BaCuO_2$, $Y_2Cu_2O_5$, Y_2BaCuO_5 etc. The intensity of the Cu^{2+} resonance signal was found to be much weaker in the superconductor, typically with spin count orders of magnitude much below than that expected for any intrinsic Cu^{2+} spin concentrations. Furthermore, the intensity of this weak resonance was strongly dependent upon preparation conditions. Such results were reported by several others also [38,87]. The EPR investigations carried out by Bowden et al, [16] in the $YBa_2Cu_3O_{7-d}$ superconducting phase and their related non-superconducting insulator phases also supported the view that any signal in the EPR spectra of the superconducting compounds has actually originated from the impurity phases formed during preparation. The intensity of the signal observed does not show any pronounced change on passing T_c. These results, together with reports by many

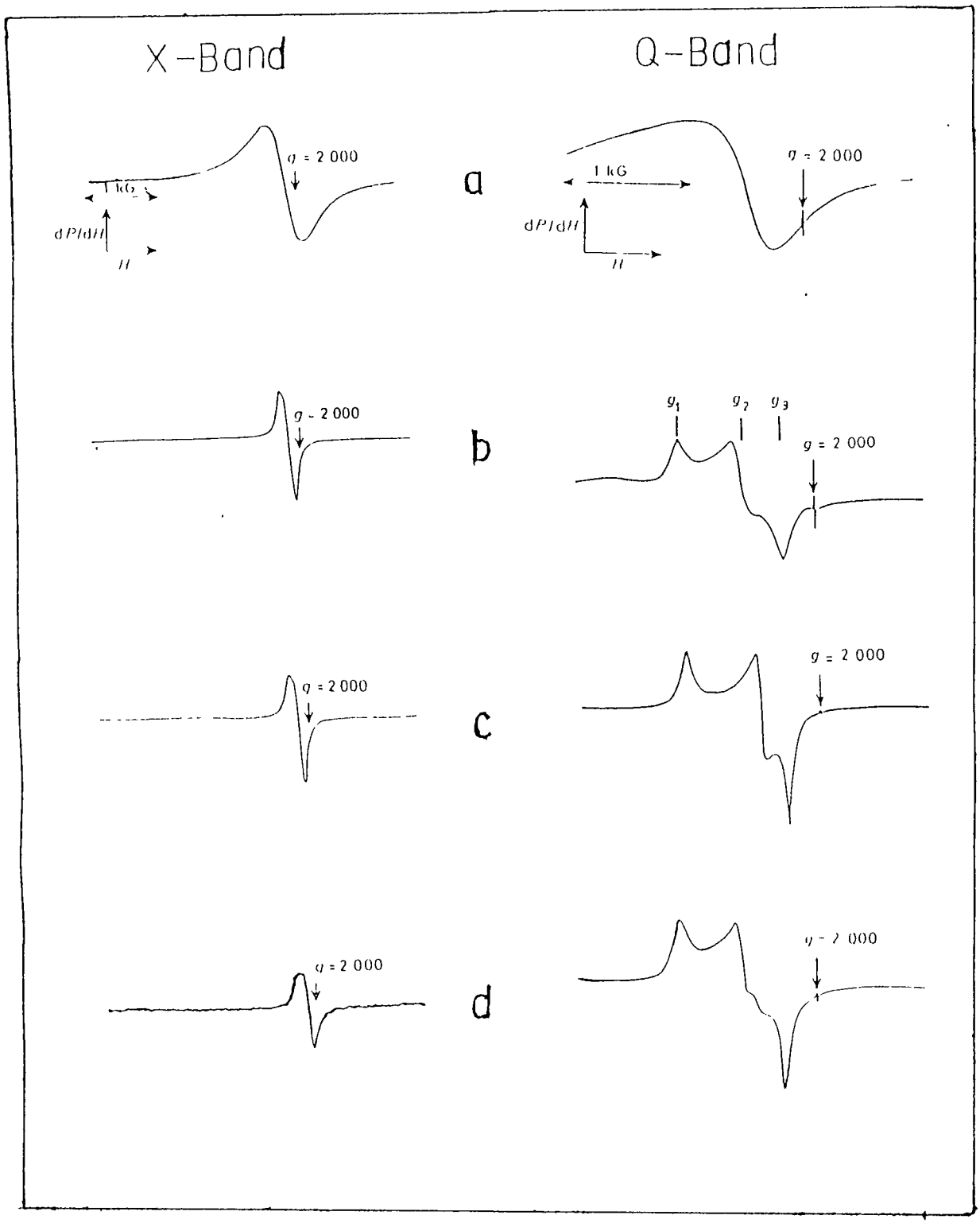

Fig. 3.6 X and Q-band EPR spectra of (a)$Y_2Cu_2O_5$, (b) $BaCuO_2$ (c) Y_2BaCuO_5 and (d) $YBa_2Cu_3O_{7-d}$ observed by Jones, et al, [Ref.14]-

others also [15,16,38,87-90] confirmed the hypothesis that a pure monophasic high-T_c superconductor, will be EPR silent.

Tyagi, et al [91] could not observe any EPR signal from the YBaCuO superconductor prepared freshly. But the same sample when exposed to the atmosphere for five days a clear signal was seen in the EPR spectrum. When the spectrum was recorded after cleaning the sample pellet by removing a thin layer from the surface, this signal was absent. Thus they concluded that any signal seen in the superconducting sample could be attributed to the post fabrication chemical or thermal treatment or break down due to exposure to the atmosphere or due to preparation techniques and that any pure superconducting phase would be EPR silent. In the case of the sample exposed to atmosphere, the observed signal shown a drop in intensity near T_c, which they attributed to change in the conductivity of the sample and the resulting increase in the screening to microwaves and magnetic field [91]. Similar conclusions were made from many other studies also [13,91-94].

No EPR signal was detected in their studies by Aguiar, et al [95] both on a superconducting $YBa_2Cu_3O_{7-d}$ sample and a non-superconducting sample obtained by annealing the same sample at 600°C. Similarly Owen, et al [44] also could not observe any EPR signal either from the superconducting $YBa_2Cu_3O_{6.9}$ or from its tetragonal counterpart $YBa_2Cu_3O_6$.

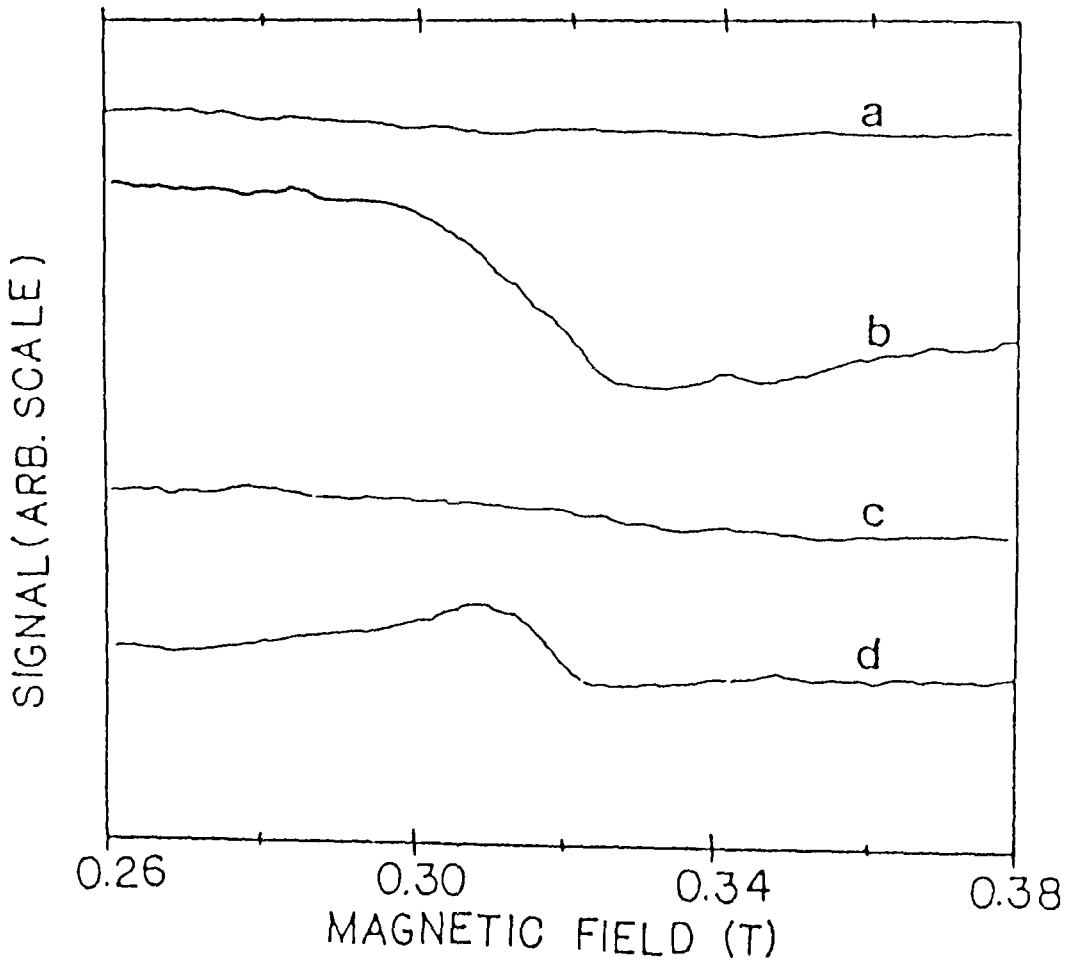

Fig. 3.7 Plots of EPR Spectra of the $YBa_2Cu_3O_{7-d}$ superconducting compound. (a) Fresh powder sample, (b) pelletized sample after exposure to atmosphere (c) after removing a thin surface layer of the sample of (b) and (d) EPR absorption in the powder removed from the surface of the sample of (b).

Studies on the lanthanum based superconducting systems also indicated the complete absence of any intrinsic Cu^{2+} EPR signal [40,44,96].

McKinnon [97] examined the $Bi_4Ca_2Sr_4Cu_4O_{16}$ superconducting compound and observed a very weak spectrum of Cu^{2+}, but is considered to be due to impurity phases, from the intensity considerations. Tagaya [27,34] also performed EPR experiments on the $BiSrCaCu_2O_x$ and Bi(Pb)-Sr-Ca-Cu-O superconducting systems. In $BiSrCaCu_2O_x$ sample, the observed EPR signal is attributed to the superparamagnetic CuO particles precipitated during the preparation [27]. The signal obtained in Bi(Pb)-Sr-Ca-Cu-O compound, in comparison with that obtained from the Ca_2CuO_3 studied, is attributed to be originating from this impurity phase formed along with the superconducting phase [34].

A search for observing the EPR signals from either the $S=\frac{1}{2}$, Cu^{2+} ions or the S=1 excited states of the Cu^{2+}-Cu^{2+} pairs in the $Bi_2Sr_2CaCu_2O_x$ high-T_c superconductor ($T_c \sim 80K$), at temperature upto 570K by Mehran et al, [22] was found unsuccessful. Sampathkumaran, et al, [98] attributed the observed absence of any Cu^{2+} EPR signals from the Bi-Sr-Ca(Y,Gd)-Cu-O superconducting system studied, to the formation of Cu^{2+}-Cu^{2+} pairs with spin singlet ground state. An extensive study was carried out on the Bismuth and Thallium

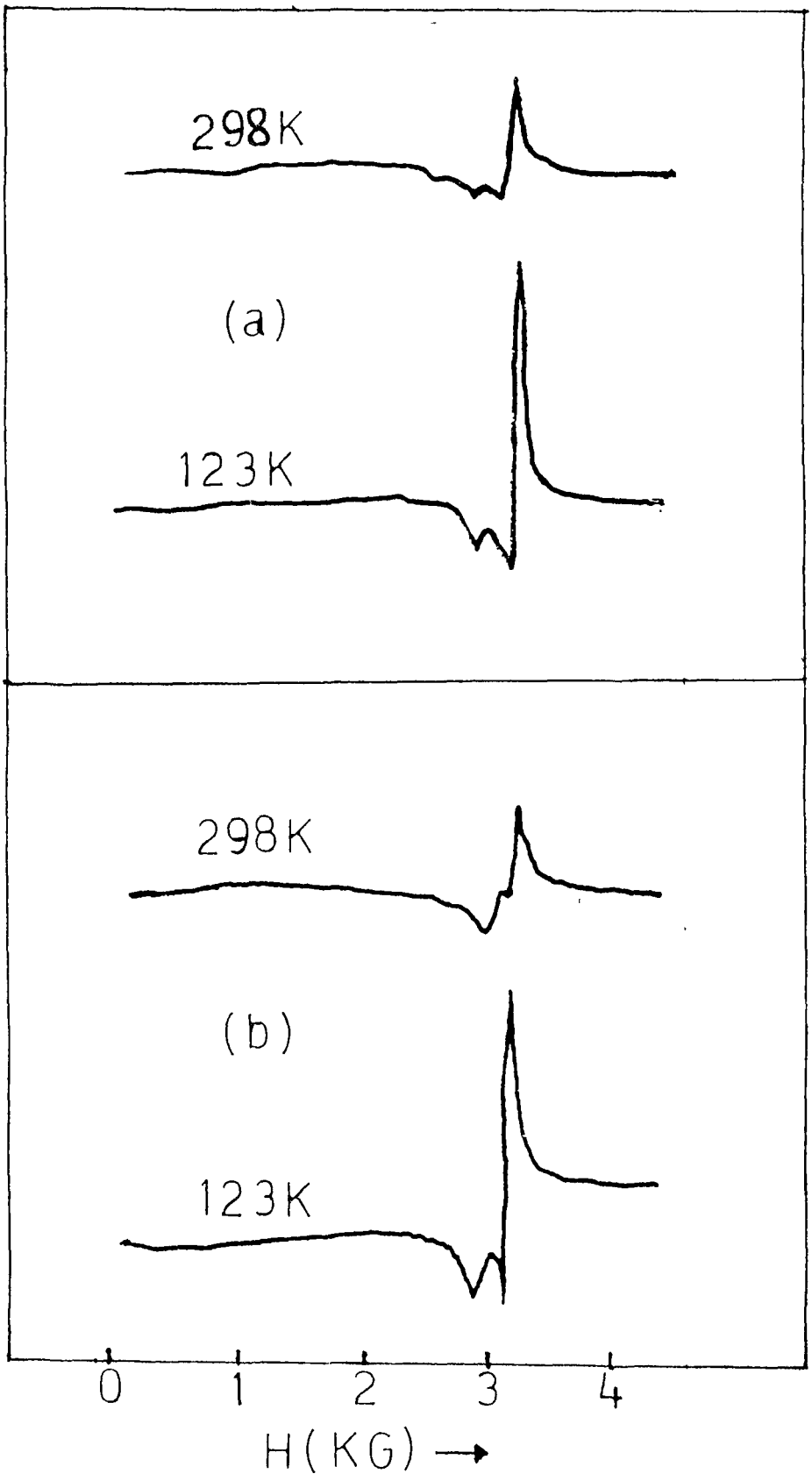

Fig. 3.8 EPR spectra of (a) $Bi_{1.6}Ph_{0.4}Sr_2Ca_3Cu_4O_y$ superconducting sample (b) Ca_2CuO_3 observed by Tagaya [Ref.34]

based superconducting systems by Edwards, et al, [99] to ascertain the EPR silence in these compounds. Of the two compositions studied in the Bi-Ca-Sr-Cu-O system, the $Bi_2CaSr_2Cu_3O_y$ was completely EPR silent, while the $Bi_2CaSr_2Cu_2O_y$ did infact yield a very weak Cu^{2+} signal, the intensity of which could only be indicative of impurity phases. The various compositions studied in the Bi(Pb)-Ca-Sr-Cu-O, Tl-Ca-Ba-Cu-O and Tl-Pb-Ca(A)-Sr-Cu-O (where A=Y or Er) superconducting systems also did not show any EPR signal.

3.5 THEORETICAL EXPLANATIONS FOR THE EPR SILENCE OF COPPER IN HTSC

Thus it appears that even though many workers still believe the existence of intrinsic Cu^{2+} EPR signal in the new copper oxide based high-T_c superconductors, the vast majority of the reports on EPR results of these compounds are in favour of the conclusion that copper in the pure superconducting phase is EPR silent. Paradoxically, cupric ions with spin $\frac{1}{2}$ and orbital non degeneracy are amongst the most amenable transition metal ions for the EPR detection. Thus it becomes a matter of accute scientific importance to understand the basic reason for this unusual EPR silence. As copper seems to be the most important and essential constituent for all the high-T_c oxides, a proper understanding of this silence may

help to elucidate the mechanism of superconductivity in these novel compounds.

It is quite surprising to note that even the simple CuO, which is the basic ingredient for all the HTSC is also EPR silent even upto temperatures much higher than its Neel temperature of 230K. Many workers [24-26] attribute this silence to the persistence of one dimensional short range antiferromagnetic order in CuO upto much higher temperatures, while others [23,97] consider it to be due to the presence of Cu^{2+}-Cu^{2+} pairs having singlet ground state and thermally inaccessible triplet excited states. Occurence of such pairs of Cu^{2+} ions with thermally accessible triplet states were realised in copper acetate monohydrate [100]. Many authors including Mehran, et al, [22] and McKinnon, et al, [97] conjectured the possibility of existence of such singlet pairs of Cu^{2+} in the high-T_c superconducting oxides also. These pairs may be considered as the basic building blocks of the short range Resonating Valence Bond (RVB) state [5,101]. According to Andersons valence bond theory, a linear Cu-O-Cu configuration can result in resonating valence bonds and the formation of canonical structures of $(Cu\text{-}O\text{-}Cu)^{2+}$ with singlet ground states and remote triplet states. The mechanism of "bond" formation is that of super exchange [22,97,101] between d-electrons on the adjacent copper ions and the p-electrons on the intervening oxygen ions. Search for Cu^{2+}-Cu^{2+} pairs in

both CuO and superconductors were found to be unsuccessful [102]. Such pairs, however will manifest themselves as peaks in the high temperature magnetic susceptibility and doublet EPR signals from the triplet S=1 excited state. But no S=1 EPR signals were seen in both CuO and superconductors at all temperatures studied. The magnetic susceptibility study by Jacobson, et al, [103] on $YBa_2Cu_3O_{7-d}$ has shown that the corrected susceptibilities increase as a function of temperatures. CuO shows a broad maximum in the susceptibility near 540K. Thus it is conjectured that the expected peaks due to S=1 triplet states in these compounds may occur at much higher temperatures. As far as high-T_c superconductors are concerned, in all these compounds, square planar copper oxide layers are reported to be present and thus the base for formation of RVB states are always ready. Thus one can anticipate superexchange not only between adjacent copper ions, but involving the entire array. Many workers including Bowden, et al, [16] and Tyagi, et al, [91] also supported this explanation based on the RVB theory, but placed it highly tentative.

Another possible mechanism suggested for the absence of EPR signals in HTSC is based on line broadening. It is important to stress that the fundamental qualitative nature which sets apart the high-T_c oxides from their related non-superconducting compounds is the itinerent nature of their

conduction (d-band) electrons. Jones, et al, [14], based on their EPR observations on the $YBa_2Cu_3O_{7-d}$ superconductor and other members of the Y-Ba-Cu-O phase diagram proposed that EPR of metallic $YBa_2Cu_3O_{7-d}$ would be difficult to observe at room temperature owing to the rapid spin relaxation expected for conduction electrons at high temperatures [104]. Here rather than a localised Cu^{2+} signal, a conduction electron spin resonance (CESR) line [99,105,106] is the more probable one. It has been shown earlier that electron relaxation occurs through the combined effects of resistivity scattering (due to the electron-phonon interaction) and spin orbit interactions. The electron spin relaxation rate is given by [107].

$$T_e^{-1} \approx \alpha (\Delta g)^2 / \tau_R$$

where Δg is the deviation of the electronic g-value from the free spin value, τ_R is the resistivity relaxation time and α is a numerical factor. The value of τ_R^{-1} can be obtained from the expression

$$\tau_R^{-1} = ne^2 \rho / m^* \approx 10^{15} S^{-1}$$

where n is the electron density, e is the electronic charge, m^* is the effective electron mass and ρ the electrical resistivity. Taking $\Delta g = 0.15$, T_e^{-1} is $2.25 \times 10^{13} S^{-1}$ at room temperature [107]

$$T_e = h / [\sqrt{3} (\pi \beta) \Delta H_{pp}]$$

where h is the Plancks constant, β is the Bohr magneton and ΔH_{pp} is the peak to peak line width of the EPR signal. This value of T_e^{-1} at room temperature would correspond to a peak

to peak line width of 1150KG, for which the CESR signal will be too broad to be detected in an EPR experiment. The possibility of a CESR signal at sufficiently low temperature cannot be ruled out, but the strong microwave absorption signal appearing in the HTSC below T_c may forbid the observation of such a signal. Interestingly, Lue [105] have described the normal state EPR spectrum of $YBa_2Cu_3O_{7-d}$ in terms of a CESR transition with associated spin waves and such signals have been reported indeed in conventional superconductors at much high temperatures [108]. Shaltiel, et al, have recently discussed the potential detection of CESR in the Bi-Ca-Sr-Cu-O family of superconductors [106]. However, by and large, CESR in metallic systems is rarely observed at room temperature. In contrast to the superconductors, the Cu^{2+} EPR signals from the semiconducting and insulating related compounds are easily observed because of the very favourable spin-spin and spin-lattice relaxation properties of the localised d-electrons in specific crystal field environments. A number of workers projected similar arguments for explaining their EPR results on HTSC [16,30,44,99,109,110]. An EPR study by Romanyukha, et al, [109] on Fe doped and undoped samples of YBaCuO superconductors, also draw similar conclusions. Based on the FLAPW band structure calculations by Massidda, et al, [111], Bowden, et al, [16] also suggested the possibility of exceptional spin-spin broadening as a more plausible explanation. They consider the Cu ions in the four

fold Cu(1) sites as Cu^{3+} ions whereas those at the five fold Cu(2) sites as Cu^{2+} ions. Further strong hybridization of the Cu-d electrons with O-p electrons occur in certain directions. For example, the d_{zy} state for the Cu(1) ions is highly localised whereas the $d_{z^2-y^2}$ is highly itinerent along the Cu(1) chains. Thus the EPR signals from HTSC compound even at room temperature may not be seen probably due to the exceptional spin-spin broadening arising from the delocalised nature of the Cu-d electrons.

Another important and probable line broadening mechanism suggested for the explanation of EPR silence of High-T_c cuprates is based on the magnetic coupling between copper spins [112,113]. Chakravarty and Orbach [112] have calculated the EPR linewidth for the antiferromagnetic La_2CuO_4 to explain the absence of EPR signal in that compound. Similar consideration should equally apply to La and Y-based superconducting system also. In these materials, the coupling between Cu ions in the Cu-O plane is well modelled by $S=\frac{1}{2}$ near neighbour quantum Heisenberg antiferromagnet (QHAF) on a square lattice with an exchange constant J of the orderof 1500K [114-116]. Calculations for the EPR line width for La_2CuO_4, which invloved a four spin correlation function, leads to values of 100KG at 400K, 34KG at 450K and 13KG at 500K. The enormous value for, room temperature EPR line width, can well explain the lack of observability of an EPR

line in La_2CuO_4, and thereby its related and similar superconducting compounds. Chakraborty and coworkers [117] have carried out a d.c magnetization measurements on the $La_2Cu_{1-x}Zn_xO_{4-y}$ system which have suggested that Zn doping suppresses T_N by reducing the correlation length for the two dimensional antiferromagnetic interaction rather than modifying the interplanar exchange term which dictates the 3-dimensional antiferromagnetic order. In their phenomenological model, the magnetic properties of $La_2Sr_xCuO_4$ can be modelled by CuO_2 layers with weak interplanar coupling. Shirane and coworkers [114] observed that at room temperature, although there is no two dimensional long range ordering, the instantaneous 2D spin correlation length exceeds 200A° in both a and c directions with an exchange constant of the order of 1500K. Calculations by Chakravarty and Orbach [114] revealed that the Cu^{2+} line width in such a case will be excessively broadened by anisotropic exchange and thus rendering this system EPR silent. Similar considerations can be extended to explain the EPR silence in the other high-T_c oxide systems also.

Aguiar, et al, [95,118] argued that only the Cu ions located in the chains, i.e., the Cu(1) sites, can contribute to the EPR signal. This is conceivable, if the Cu ions located in the planes, i.e.,the Cu(2) sites are antiferromagnetically ordered. Neutron diffraction studies

indicated such an ordering in the Cu-O planes [119] in both cases of the Y-Ba-Cu-O compound with oxygen content equal to 6.0 and 6.15. Because there is almost no change of the Cu(2) site environment in going from $YBa_2Cu_3O_6$ to $YBa_2Cu_3O_7$, it is assumed that the magnetic order in Cu(2) plane remains the same for the whole range of oxygen concentrations between six and seven. On the other hand, the environment of Cu(1) site changes dramatically on moving from $YBa_2Cu_3O_6$ to $YBa_2Cu_3O_7$, its coordination changes from linear two fold to square planar. But just counting valencies, one gets +1, +2 and +3 for the valence of the Cu ions at Cu(1) sites for $YBa_2Cu_3O_6$, $YBa_2Cu_3O_{6.5}$ and $YBa_2Cu_3O_7$ respectively. In all the three cases, it is assumed that the valency of the Cu(2) ions remains the same +2 [118]. It is interesting to note that typically Cu^{+1} compounds have a linear two fold coordination, where as Cu^{+2} and Cu^{+3} are found to have four, five or six fold coordinations. Thus normally one expects no EPR signal for both $YBa_2Cu_3O_7$ and $YBa_2Cu_3O_6$. The reasoning is supported by the observed Cu^{2+} EPR signal in the 40K superconducting phase of the $YBa_2Cu_3O_{7-d}$ and its absence in the related 90K phase. A similar explanation based on the valence state of Cu ions is projected by Tyagi et al, [91] also.

3.6 EPR STUDIES OF DOPED RARE EARTH AND TRANSITION METAL IONS IN HTSC

Of the various paramagnetic rare earth ions, Gd^{3+} is especially suitable for EPR work and so extensive research has come out on the EPR spectrum of Gd^{3+} ions in HTSC, either in the $GdBa_2Cu_3O_{7-d}$ or in the compounds with Gd^{3+} partially substituted. The free Gd^{3+} ion state is S=7/2 and is easily observable upto room temperature because of its long spin lattice relaxation time.

In most of the cases, the Gd^{3+} ion gives a single broad EPR spectrum with $g \sim 1.9$ [120-125] the line width and line shape are governed by the combined effect of exchange and dipole-dipole interactions. Nakamura,et al, [123] and Kikuchi, et al, [124] studied the EPR of Gd^{3+} signals in both superconducting and non -superconducting phases of $GdBa_2Cu_3O_{7-d}$ from 4K to room temperature. In both cases, Gd^{3+} signal at $g \sim 2$ region is obtained. Line width is found to be Lorentzian indicating the presence of exchange narrowing [126]. Kikuchi, et al, [124] did not observe any anomaly at T_c, either in width or in intensity, which show that Gd^{3+}-Cu^{2+} interaction is weak. Nakamura, et al, [123] did not observe any dependance of line shape on Gd concentration, but the line width show a proportionality to the square root of concentration which also suggested that exchange interaction is unlikely and rather dipole-dipole interaction is dominant

in these superconducting systems. On the other hand, the EPR investigation by Meharn et al, [125] observes a minimum in line width at T_c.

Schwartz, et al, [120] also observed EPR signals due to localised spin of Gd^{3+} ion, without affecting the superconductivity and suggested that the magnetic Gd^{3+} ions are only weakly coupled to the two dimensional frame work Cu-O plane. The fact that magnetic rare earth ions does not affect superconductivity has been supported by many workers [127,128]. But in a recent study by Arai, et al, [129], it was found that T_c is decreasing with increasing Gd concentration and is attributed to be indicative of strong interaction of Gd with Cu-O planes. EPR study of Gd^{3+} in $Bi_2Sr_2Ca_{0.3}Gd_{0.5}Cu_2O_y$ by sampathkumaran et al, [98] showed a signal only below 25K. The absence of any signal above this temperature is attributed to an extra path way of Gd^{3+} spin-lattice relaxation, probably through interaction with conduction electrons. Jenossy, et al, [130] examined Gd^{3+} signals from $RBa_2Cu_3O_{7-d}$ compounds with R=Y and Gd. For d=1, the dipole-dipole interaction between Gd^{3+} spins usually broaden the EPR spectrum to a width of 3000G. But for low concentrations, the spectrum consists of fine structure determined by the crystal field of the surrrounding atoms. Here the Cu^{2+}-Gd^{3+} interaction is expected to cause an exchange narrowing of the lines. A spectrum consisting of

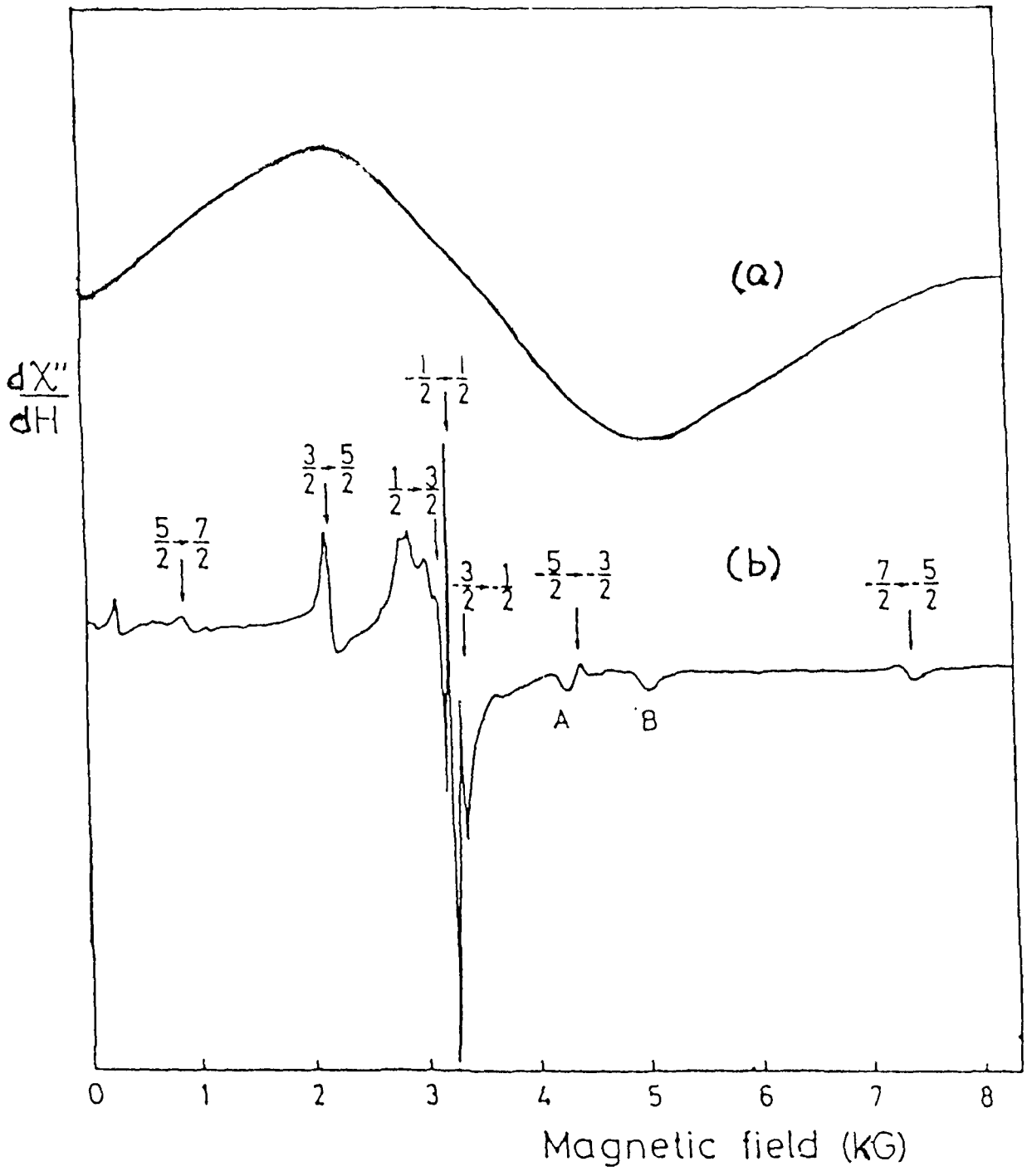

Fig. 3.9 Gd^{3+} EPR signal from (a) $GdBa_2Cu_3O_x$ superconducting sample and (b) $Y_{0.997}Gd_{0.003}Ba_2Cu_3O_{6.9}$ showing fine structure. [Ref.124,131].

seven well resolved fine structure lines of Gd^{3+} ion is obtained from the $Y_{0.999}\ Gd_{0.001}Ba_2Cu_3O_{7-d}$ which are superconducting with d<0.7 and the spectrum is shown in figure 3.9 [131].

Guskose, et al, [74] carried out a study on a series of compounds of the formula $Sm_{0.5}R_{0.5}Ba_2Cu_3O_{7-d}$ (here R=Y and most of the rare earths). For R=La, Dy and Er, the spectra at 77K consisted of a superposition of Cu^{2+} sharp signal on a very broad signal. The broad signal is considered as arising from superexchange interaction between copper ions [133]. Such a broad signal is observed for R=Eu, Tm and Lu. In the tetragonal phase of the La substituted compound, a sharp line at g=1.99 is observed and is attributed to La ions partially substituted for Ba ions. In case of Tm substituted compound, a signal with g=2.7 is observed, and is thought to be of Tm origin.

An EPR study on Fe doped $YBa_2(Cu_{1-x}Fe_x)_3O_{7-d}$ no signal either from Cu or Fe is obtained [134]. It is assumed that Fe is substituted in Cu(1) sites forming linear antiferromagnetically coupled clusters and thus not giving any signal. In the studies performed on $GdBa_2(Cu_{1-x}M_x)_3O_{7-d}$ compounds with M=Ni, Co and Fe also [121,122], no signal is observed from any of these ions except Gd^{3+}. For Ni doped compound, line width broadening have been observed due to disturbed exchange interaction of Gd. Here Ni takes Cu

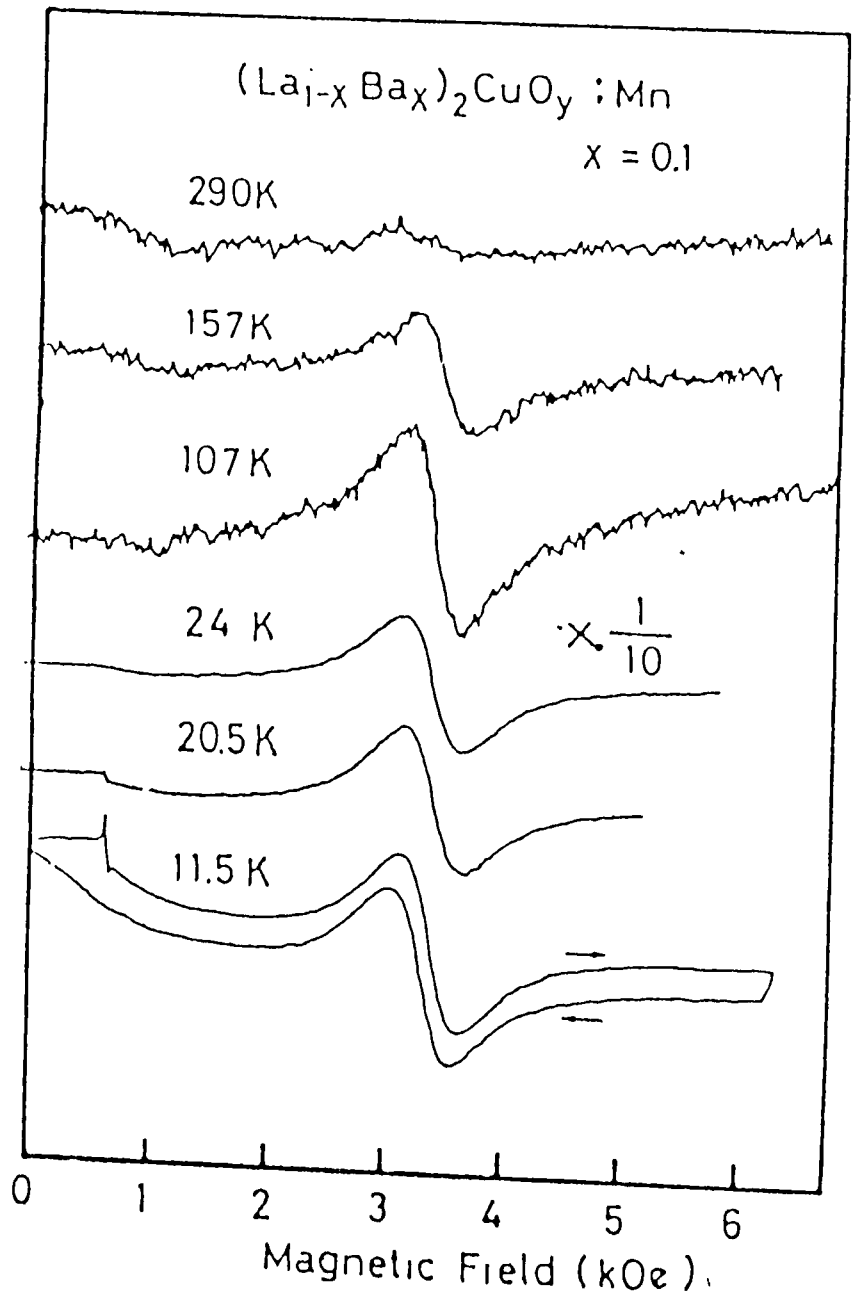

Fig. 3.10 EPR spectra of Mn^{2+} doped in $(La_{1-x}Ba_x)_2CuO_y$ superconductor at different temperatures [Ref. 136].

position in Cu-O planes. For Co and Fe doping, line width was independent of substitution as they occupy Cu sites in Cu-O chains. EPR of Mn^{2+} ions were examined, in the Mn^{2+} doped $(La_{1-x}Sr_x)_2CuO_{4-d}$ and $(La_{1-x}Ba_x)_2CuO_{4-d}$ but only a single signal with no hyperfine structure is observed in the $g \sim 2$ region at room temperature, which is typical of Mn^{2+} ions in a magnetically concentrated system [135,136]. The Mn^{2+} ions are not isolated from host Cu spins, but coupled magnetically with them. Kikuchi, et al, [136] carried out the study on both superconducting and non-superconducting Mn2+ doped $(La_{1-x}Ba_x)_2CuO_{4-d}$ and found that the behaviour of the linesin both cases are largely different. The signal from the non-superconducting compound shows strong temperature dependence of resonance field and line width as is observed by Onoda, et al, [135] also. These effects were much less in the superconducting phase. The EPR anomalies for the non-superconducting phase resumbles that observed in magnetically inhomogeneous systems such as spin glass. This similarity is considered as indicative of the fact that there occurs a magnetic slowing down associated with a progressive freezing of spins in the superconducting samples.

3.7 CONCLUSIONS

The EPR silence of copper in the new cuprate high-T_c oxides still remains as a puzzle. But studies on the EPR of rare earth and transition metal ions, which are either present

intrinsically or doped externally are much successful in understanding the various interactions between the spins in these magnetically concentrated systems. Even though it is now widely accepted that Cu^{2+} in these high-T_c superconducting compounds are EPR silent, frequent reports on the observation of Cu^{2+} EPR signals from these compounds appearing time to time seem to be quite disturbing to this conclusion. In spite of the fact that many mechanisms were suggested to explain the Cu^{2+} EPR silence, reaching a consensus on this seems to be still far away. It appears that the magnetic interactions and mechanisms remains unresolved not only of the superconductors, but even of the much simpler compound CuO, and other binary and ternary parent systems of the cuprate superconductors. A proper understanding of the magnetic complexities and EPR silence in the superconducting systems may hopefully help to elucidate the basic mechanism underlying the phenomenon of high-temperature superconductivity.

REFERENCES

1. J.G. Bednorz and K.A. Muller, Z.Phys. B **64** (1986) 189.
2. G. Aeppli, in "Ist Topsoe Summer School in Superconductivity" ed. N.H. Anderson and K. Mortenson (Riso, Denmark) (1988) 47.
3. S.W. Cheong, J.D. Thompson and Z. Fisk, Physica C **158** (1989) 109.
4. W.E. Pickett, Rev. Mod. Phys. **61** (1989) 433.
5. P.W. Anderson, Science **235** (1987) 1196.
6. R.J. Birgeneau and G.Shirane in "Physical Properties of High Temperature Superconductors" ed. D.M. Ginsberg (World Scientific, Singapore) (1989).
7. Charles. P. Poole Jr., T. Datta, H.A. Farach, "Copper Oxide Superconductors" (Wiley, New York) (1988).
8. N.E. Alekseevskii, et al, J. Low Temp. Phys. **77** (1989) 87.
9. F. Mehran, S.E. Barnes, C.C. Tsuei and T.R. McGuire,Phys. Rev. B **36** (1987) 7266.
10. J.T. Lue,Phys. Rev. B **38** (1988) 4592.
11. N.Guskose et al, Phys. Status Solidi (b) **162** (1990) L545.
12. G.Oszlanyi, G.Faigel, S.Pekker and A.Janossy, Physica C **167** (1990) 157.
13. D. Shaltiel, et al, Solid State Commun, **63** (1987) 987.
14. Ruth Jones, et al, J.Chem. Soc: Faraday Trans. **86** (1990) 675.
15. W.R. McKinnon, J.R. Morton, K.F. Preston and L.S. Selwyn, Solid State Commun, **65** (1988) 855.

16. G.J. Bowden et al, J. Phys. C **20** (1987) L545.

17. N.Guskos, et al, Phys. Stat. Solidi,(b) **165** (1991) 249.

18. S.M. Misra and L.E. Misiak, J. Phys. Condensed Matter **1** (1989) 9499.

19. R.Barucci, et al, Phys. Rev. B **37** (1988) 2313.

20. M.C.R. Symons, "Chemical and Biochemical Aspects of Electron Spin Resonance Spectroscopy",(Van Nostrand Reinhold) (1987).

21. B.G. Malstrom, R. Mosbach and T.Vanngard, Nature **183** (1959) 321.

22. F. Mehran, et al, Solid State Commun, **67** (1988) 1187.

23. M.O'Keeffe, F.S.Stone, J. Phys. Chem. Solids, **23** (1962) 261.

24. K.Kindo, M.Honda, T.Kohashi and M.Date, J. Phys. Soc. Jap. **59** (1990) 2332.

25. R.J. Singh, Alex Punnoose, Jilson Mathew, and Mohd. Umar, Intl. Conf. M^2S-HTSC III, Kanazawa, Japan, July, 1991.

26. Alex Punnoose, et al, communicated to Mod. Phys. Lett., B.

27. K.Tayaya, Jpn. J.Appl. Phys., **28** (1989) L566.

28. K. Tagaya, N.Fukuoka and S.Nakanishi, Jpn. J.Appl. Phys.,**29** (1990) 868.

29. G.J. Bowden, et al, J.Phys. C: Solid State Phys.**20** (1987) L545.

30. JiangTsu Yu and K.H. Lii, Solid State Commun, **65** (1988) 1379.

31. Jiang-Tsu Yu, Jong Gen Hwang, Chrong Chu Tsai and K.H.Lii, Solid State Commun, **70** (1989) 167.

32. Alex Punnoose, et al, Communicated to Mod. Phys. Lett. B.

33. M. Arjomand and D.J. Machin, J. Chem. Soc. Dalton Trans. (1975) 1061.

34. K. Tagaya, Jpn. J. Appl. Phys. **29** (1990) 656.

35. K Sreedhar and P.Ganguly, Inorg. Chem., **27** (1988) 2261.

36. S.B. Oseroff, et al, Phys. Rev. B **41** (1990) 1934.

37. D.C. Vier, et al, J. Appl. Phys. **69** (1991) 4872.

38. E.W. Ong, B.L Ramakrishna and Z. Iqbal, Solid State Commun, **66** (1988) 171.

39. R.Troc, Z.Bukovski, R.Horyn and Klamut, Phys. Lett. A **125** (1987) 222.

40. Zhang, et al, Solid State Commun, **63** (1987) 765.

41. F. Mehran, T.R. McGuire, J.F. Bringley and B.A. Scott, Phys. Rev. B **43** (1991) 11411.

42. H.Kikuchi and Y.Ajiro, J. Phys. Soc. Jap. **57** (1988) 2628.

43. Masashige Onoda and Masatoshi Sato, Solid State Commun, **70** (1989) 309.

44. F.J.Owens, B.L.Ramakrishna and Z.Iqbal, Physica C **156** (1988) 221.

45. F.Mehran, S.E. Barnes, E.A.Giess,T.R. McGuire, Solid State Commun, **67** (1988) 55.

46. R.Bartucci, et al, Phys. Rev. B **37** (1988) 2313.

47. N.Guskose, Th. Leventouri, Ch. Trikalinos and M.Calamioton, Phys. Stat. Solidi (b) **149** (1988) K157.
48. C.N.R. Rao, et al, Phys. Rev. B **42** (1990) 6765.
49. H.A. Farach, et al, Phys. Rev. B **41** (1990) 2046.
50. H.D.Bist, et al, Solid State Commun, **65** (1988) P899.
51. F. Mehran, et al, Phys. Rev. B **36** (1987) 740.
52. S.B.Oseroff, Solid State Commun, **64** (1987) 241.
53. T.Siegrist, Phys. Rev. B **35** (1987) 7137.
54. J.E. Gredan, A.H. O'keilly and C.V.Stager, Phys. Rev. B **35** (1987) 8780.
55. K.Kamaris, et al, Phys. Rev. Lett., **59** (1987) 919.
56. D.K. De, J. Phys. C:Solid State Phys. **21** (1988) 4481.
57. Blank, et al, Physica B ;**145** (1987) 222.
58. K.N. Shrivastava, J. Phys. C: Solid State Phys. **20** (1987) L789.
59. M.Guskose, et al, Phys. Stat. Solidi (b) **152** (1989) K9.
60. A. Abragam and B.Bleney, "Electron Paramagnetic Resonance of Transition Metal Ions,"(Clarendon press, Oxford) (1970).
61. M.D. Sastry, Physica B **151** (1988) 513.
62. F.J.Owens, Solid State Commun, **70** (1989) 173.
63. F.Mehran, et al, Solid State Commun, **66** (1988) 299.
64. C.Rettori, D.Dividov, I.Belaish and I.Felner, Phys. Rev. B **36** (1987) 4028.
65. S. Benakki, et al, J.Mater, Res. **2** (1987) 765.
66. J.Stankowski, et al, Solid State Commun, **77** (1991) 125.

67. J.Stankowski, P.Kahol, N.S.Dalal and J.S. Moodera, Phys. Rev. B **36** (1987) 7126.

68. S.K. Hoffman, B.Czyzak and J. Stankowski, Acta.Phys. Polon. A **77** (1990) 64.

69. Juh. Tzeng Lue, Phys. Rev. B **38** (1988) 4592.

70. Juh.Tzeng Lue, J. Mol. Structure, **190** (1988) 69.

71. Juh Tzeng Lue and Ping Tien Wu, Solid State Commun, **66** (1988) 55.

72. N.Guskose, et al, Phys. Stat. Solidi (b) **163** (1991) K89.

73. E.Babic, Z.Marohnic, M.Prester and N.Briniceivic, Philos. Mag. Lett., **56** (1987) 91.

74. M.Galamiotou, et al, Mod. Phys. Lett., B **5** (1991) 1287.

75. N.Guskose, et al, Mod. Phys. Lett., B **5** (1991) 969.

76. Y.Songliu, Z.Jiaqi, J.Sizhaoad and G.Weiyan, Solid State Commun, **70** (1989) 329.

77. Y. Songliu, et al, Mod. Phys. Lett., B **5** (1991) 655.

78. He Yesheng, et al, Kexue Tongbao **35** (1990) 177.

79. He Yesheng, et al, J. Phys. **1** (1988) 1055.

80. Hoydoo You, et al, Phys. Rev. B **37** (1988) 2301.

81. R. Karim, et al, J. Appl. Phys. **67** (1990) 5064.

82. Ishida Takekazu, et al, Physica C **185-189** Pt.2 (1991) 1201.

83. Y.Hayashi, et al, Jpn. J.Appl. Phys. **28** (1990) 6765.

84. Y.Hayashi, et al, Physica B **165-166** (1990) 1317.

85. J. Kondo, Y.Asai and S.Nagai: J. Phys. Soc. Jpn. **57** (1989) 4334.

86. J.Kondo, Parity **4** (1989) 30.

87. K.Kojima, K.Ohbayaski, M.Udagawa and T.Hihara, Jpn. J.Appl. Phys. **26** (1987) L766.

88. K.Bente, E.Schwarzmann and D.Siebert, Phys. Stat. Solidi (a) **111** (1989) K93.

89. R.N.De Mesquita, et al Phys. Rev. B **39** (1989) 6694.

90. D.C. Vier, et al, phys. Rev. B **36** (1987) 8888.

91. S.Tyagi, M.Barsoum, and K.V. Rao, Phys. Lett. A, **128** (1988) 225.

92. J.Flokstra, G.J.Gerritsman, D.H.A. Blank and E.G.Klien, Proc. European Workshop on High Temp. Supercond. and Pot. Appl., Geneva July (1987) 78.

93. R.Cywinski, S.H. Kilcoyne and L.N. Lomer, Solid State Commun, **67** (1988) 355.

94. J.G.Thompson, et al, Mat. Res. Bull, **22** (1987) 1715.

95. J.Albino O.De Aguiar, A.A. Menovsky, J.Venden Berg and H.B. Brom, J.Phys. C: Solid State Phys. **21** (1988) L237.

96. F.Gervais, et al, Solid State Commun, **67** (1988) 307.

97. W.R. McKinnon, J.R. Morton and G.Pleizier, Solid State commun, **66** (1988) 1093.

98. E.V. Sampathkumaran, M.D.Sastry and R.M. Kadam, Physica C **156** (1989) 267.

99. P.P.Edwards, et al, Jpn. J. Appl. Phys. **29** (1990) L258.

100. B.Bleaney and K.D. Bowers, Proc. Roy. Soc. A **124** (1952) 451.

101. S.A. Kivelson, D.S. Rokhsar and J.P.Scthna, Phys. Rev. B **35** (1987) 8865.

102. W.Que and G.Kirazenow, Solid State Commun, **64** (1987) 1053.

103. A.J. Jacobson, et al, in "Chemistry of Oxide Superconductors", C.N.R. Rao (Ed) (1988).

104. R.N. Edmonds, M.R.Harrison and P.P.Edwards, Annu. Rep. Chem. soc, Sect. C, **82** (1985) 265.

105. J.T.Lue and P.T. Wu, Solid State Commun, **66** (1988) 55.

106. D. Shaltiel, et al, Physica C **157** (1989) 240.

107. R.J. Elliott, Phys. Rev. **96** (1954) 266.

108. A.V. Narlikar and S.N. Ekbote,"Superconductivity and Superconducting materials" (South Asian, New Delhi) (1983).

109. A.A.Romanyukha, et al, Physica C **171** (1990) 276.

110. R.Janes, K.K.Singh, S.D. Burnside and P.P. Edwards, Solid State Commun, **79** (1991) 241.

111. S.Massidda, Jaejum Yu, A.J. Freeman and D.D. Koelling, Phys. Lett. (1987).

112. S.Chakravarty and R.Orbach, Phys.Rev.Lett., **64** (1990) 224.

113. A.Deville, Physica C, **153-155** (1990) 669.

114. G.Shirane, et al, Phys. Rev. Lett. **59** (1987) 1613.

115. Y.Endoh, et al, Phys. Rev. B **37** (1988) 7443.

116. G.Aeppli, et al, Phys. Rev. Lett. **62** (1989) 2052.

117. A.Chakraborty, et al, Phys. Rev. B **40** (1989) 5296.

118. J.Albino O De Aguiar, A.A. Menovsky, J.Van Den Berg and H.B. Brom, Physica C **153-155** (1988) 743.

119. J.M.Tranquada, et al, Phys. Rev. Lett. **60** (1988) 156.

120. R.M. Schwartz, et al, Phys. Rev. B **36** (1987) 8858.

121. F.Nakamura, Y.Ochiai, H.Shimizu and Y.Narahara, Physica B **165-166** (1990) 1315.

122. F.Nakamura, et al, Physica C **162-164** (1989) 1289.

123. F.Nakamura, et al, Phys. Rev. B **36** (1989) 12283.

124. H.Kikuchi, et al, J.Phys. Soc. Jap. **57** (1988) 1887.

125. F.Mehran, S.E.Barnes, C.C. Tsuei and T.R.McGuire, Phys. Rev. B **36** (1987) 7266.

126. P.W. Anderson and P.R. Weiss, Rev. mod. Phys. **25** (1953) 269.

127. E.M.Engler, J.Am. Chem. Soc. **109** (1987) 2848.

128. L.C. Porter, et al, Inorg. Chem. **26** (1987) 1645.

129. J.Arai, H.Shimizu and D.Yamaguchi, Physica C, **185-189** Pt.2 (1991) 1205.

130. A.Janossy, A. Rockenbauer and S.Pekker, Physica C, **167** (1990) 301.

131. A.Janossy, et al, Physica C, **171** (1990) 457.

132. N.Guskose, et al, Phys. Stat. Solidi (b) **162** (1990) K101.

133. B.Jezowska-Trzebiatowska, Solid State Radio Spectroscopy (Polish Acad. of Sci.) (1975) 115.

134. J.Albino O'De Aguiar, et al, Physica C **156** (1988) 571.

135. Masashige Onoda and Masatoshi Sato, Solid State Commun, **70** (1989) 309.

136. H. Kikuchi and Y. Ajiro, J. Phys. Soc. Jap. **57** (1988)2628.

[redacted]

[redacted]

[redacted]

[redacted]

4.1 INTRODUCTION

Recently, antiferromagnetic insulator CuO is investigated extensively due to the current interest in the new cuprate high-T_c superconducting oxides. In all these systems, CuO is found to be the most important ingredient. Numerous studies on the different high temperature superconducting systems have focussed attention to the role of magnetic coupling between Cu spins via oxygen atoms in the copper oxygen planes in determining the physical properties of these compounds, and is believed to be responsible for the superconducting mechanism [1,2]. Many experimental results and theoretical studies show that the high-T_c in the new ceramic superconductors is somehow linked with the magnetism of Cu-O units [1-5]. It is known that $YBa_2Cu_3O_{7-d}$ and $La_{2-x}Sr_xO_{4+y}$ order antiferromagnetically when oxygen content is low and becoming superconducting when the oxygen content is large [2-5]. In this context, it seems to be very important to study first the magnetism of the basic constituent CuO itself, in order to understand the more complicated superconducting systems.

Copper has two binary oxides, namely cuprous oxide (Cu_2O) and cupric oxide (CuO). Of these, the cuprous oxide, Cu_2O is a semiconductor and is diamagnetic corresponding to the $3d^{10}$ configuration of Cu^{1+}. On the otherhand cupric oxide, CuO is reported to be exhibiting a much complicated

magnetism [6]. Most of the essential structural and magnetic properties of this compound are still not understood well.

The Neel temperature T_N of CuO was found to be 230K where a small peak in the specific heat was observed in their measurement by Hu and Johnston [7]. Later, the specific heat measurement by Seehra et al, [8] indicated the presence of two phase transitions near 215K and 230K (See figure 4.1). But the magnetic susceptibility data of O'Keeffe and Stone did not show any distinct change either near 215K or near 230K [6]. Their susceptibility data is reproduced in figure 4.2. The susceptibility continued to rise above T_N and reaching a maximum around 600K and thereafter it remains undiminished even upto temperatures of 900-1000K. In a recent magnetic susceptibility measurement, a T_N of 453K is reported for this compound [9]. Neutron diffraction and neutron inelastic scattering studies confirmed antiferromagnetic long range ordering below 230K [10,11]. Single crystal neutron diffraction measurements revealed a magnetic structure with twice the a and c parameters of the chemical unit cell [12].

To understand the behaviour above T_N (=230K), which was thought to be the paramagnetic region, Forsyth et al, [12] measured the magnetic diffuse scattering from a powdered CuO sample upto 550K, but no significant paramagnetic scattering was observed. The broad maximum observed in the

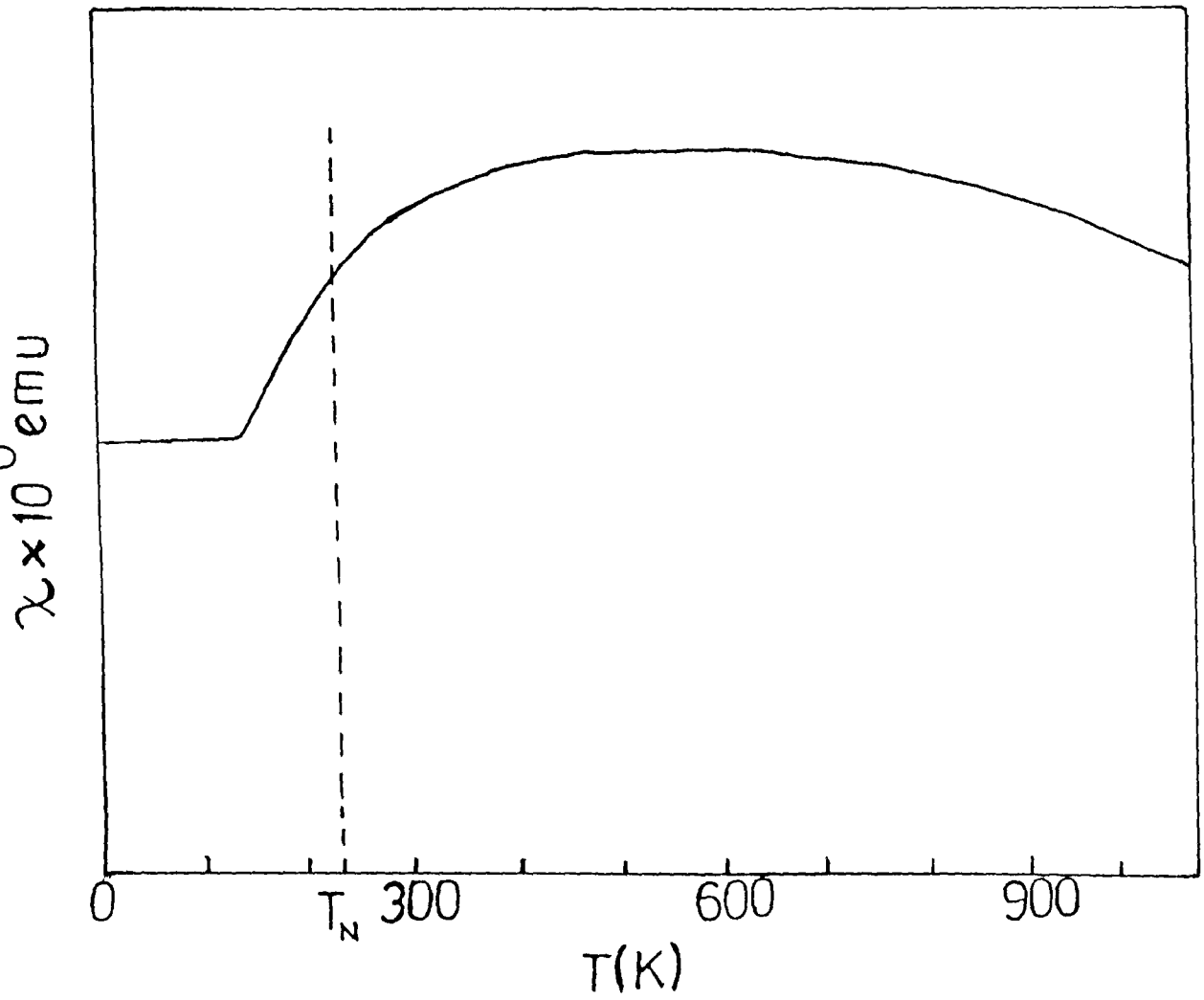

Fig. 4.1 Magnetic susceptibility of CuO [Ref.6].

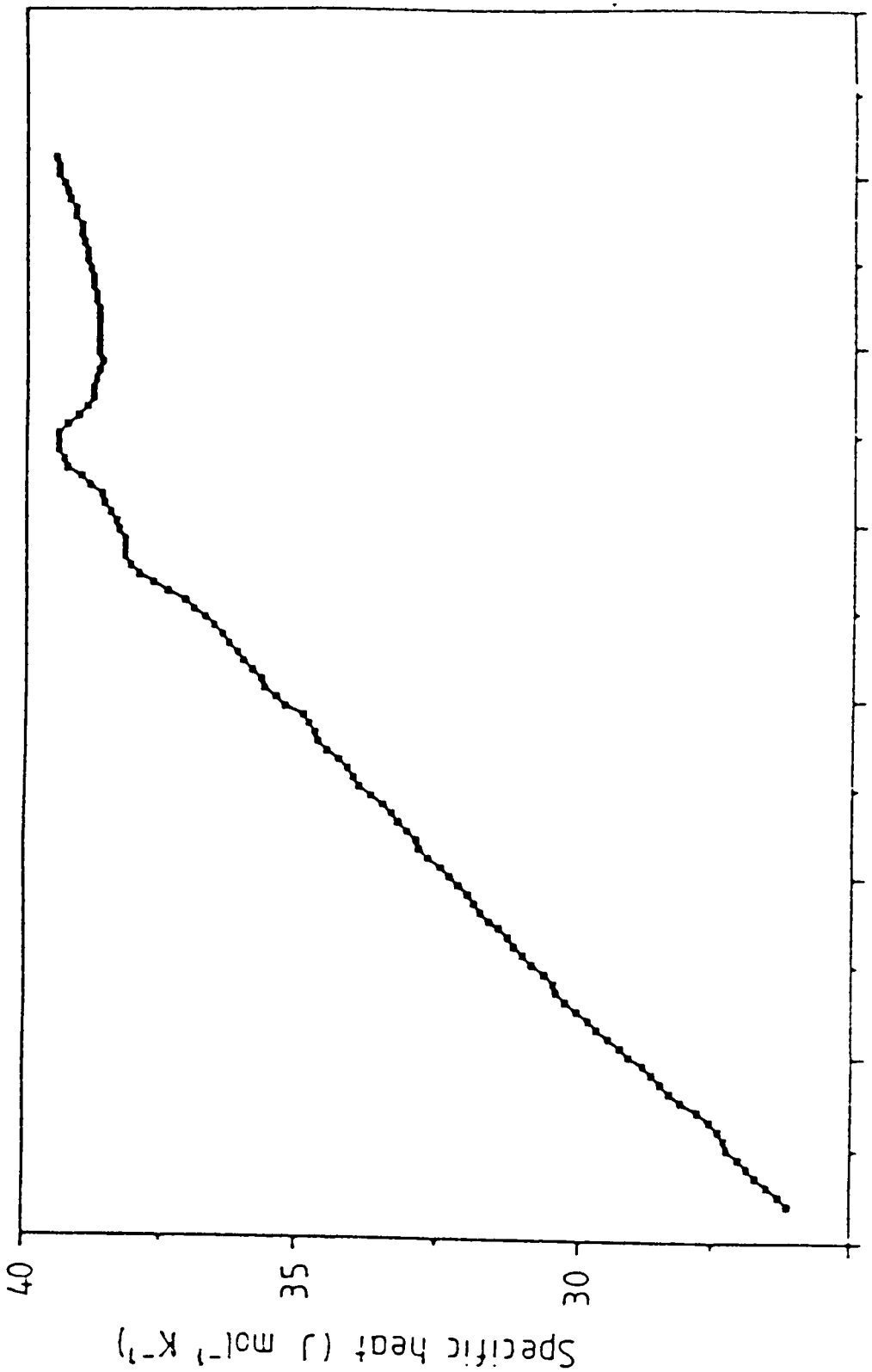

Fig. 4.2 Specific heat measurement of CuO [Ref.8].

magnetic susceptibility above T_N has been interpreted as arising due to short range fluctuating one-dimensional antiferromagnetic order [6,8]. A recent crystal structure study of CuO also implied a weaker antiferromagnetic coupling at room temperature [13]. It was surprising to note that no EPR signal due to the bulk CuO has been observed at any temperature studied [14,15]. Many authors attributed this silence to the persistance of one-dimensional short range magnetic order in CuO upto much higher temperatures above T_N [16,17]. Another explanation for the absence of EPR signals was based on Anderson's Resonating Valence Bond (RVB) theory [18,19], which attributed it to the possibility of Cu^{2+}-Cu^{2+} pair formation with spin singlet ground state [20,21]. In CuO, the exchange constant J is $730cm^{-1}$ and thus rendering the triplet state thermally inaccessible [6]. Mehran et al, examined the EPR of CuO upto 570K, but could not observe any signal either due to Cu^{2+}, spin $\frac{1}{2}$ or the Cu^{2+}-Cu^{2+} excited state spin one resonance [21]. Later Kindo, et al, [16], using a pulsed magnetic field, observed a very broad paramagnetic resonance with the g-value of about 2.0, above T_N, at the 45GHz region (shown in figure 4.3). But no resonance was observable when a standard spectrometer was used. The line width was more than one Tesla and one-dimensional spin correlation is seen from the line profile. Zero field

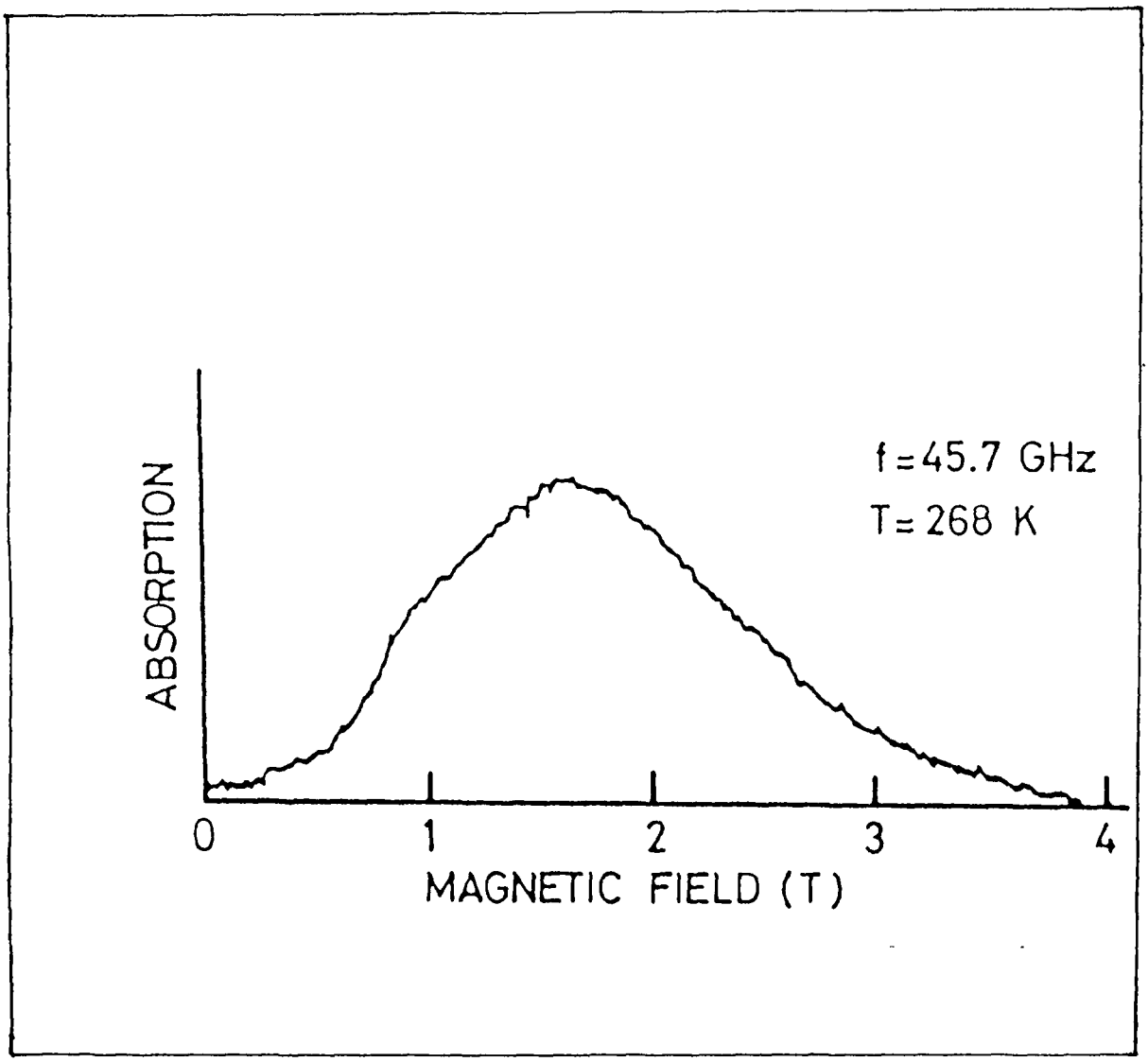

Fig. 4.3 Paramagnetic resonance of CuO at room temperature observed using pulsed magnetic field [Ref. 16].

antiferromagnetic resonance was also found from IR absorption measurements in the temperature range between 5K and 500K [16].

Thus it appears that, even though a good undestanding of the magnetic interactions in CuO below T_N=230K has been achieved, the behaviour above this seems to be extremely complicated compared to most of the other magnetic systems. In this state of affairs we planned to undertake a detailed EPR investigation in this powdered compound [22,23]. The study is further extended to thin films of CuO deposited on glass and quartz substrates [24]. The study in thin film forms is motivated by the fact that many elements have shown conventional superconductivity only in the thin film state. Transition temperature (T_c) in some transition metals have been found to rise dramatically in thin films [25]. In high-T_c oxides also, T_c is found to be much affected when converted into thin films. Here the T_c is also found to be much dependent on the post deposition annealing temperature [26]. As 950°C is the preparation temperature for most of the high-T_c superconductors, we have chosen it as the highest annealing temperature for CuO in the present study.

4.2 CRYSTAL STRUCTURE

Cupric oxide, CuO, is unique amongst the monoxides of the 3d transition elements in having a monoclinic unit cell

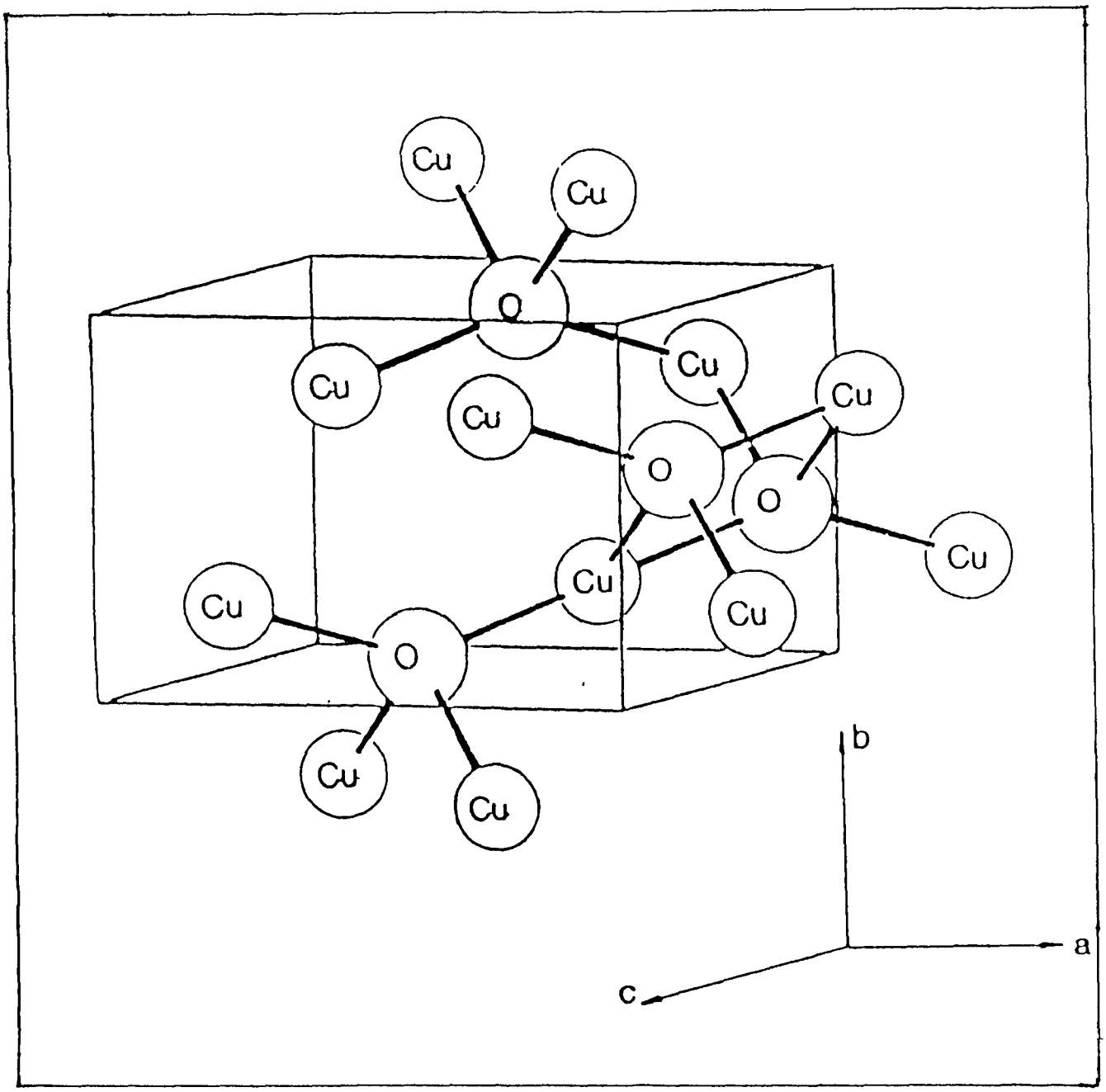

Fig. 4.4 Crystal structure of CuO [Ref.13,16,27].

with space group C2/c, while other 3d oxides such as NiO, MnO and FeO have NaCl type structures [13,16,27,28]. The unit cell parameters are a=4.6927Å , b=3.4283Å and c=5.1370Å with β=99.546° and there are four formula units per unit cell at room temperature [13]. Each copper ion is located in the plane formed by two almost equidistant pairs of oxygen neighbours. The CuO_4 units, by sharing opposite edges, formed two ribbons of parallelograms running in the (110) and ($\bar{1}$10) directions. The crystal structure of CuO is illustrated in figure 4.4.

4.3 EXPERIMENTAL DETAILS

The starting materials were either $CuCO_3Cu(OH)_2H_2O$ or CuO, supplied by s.d. fine chemicals, Bombay. The powdered sample was annealed in air at different temperatures ranging from 100°C to 950°C. The annealing temperatures were 100°C, 200°C, 300°C, 400°C, 500°C, 600°C, 700°C, 800°C, 875°C and 950°C, every time for 20 to 24 hours. The same sample was subjected to the whole heat treatments, one after the other. EPR spectra were recorded in each case after furnace colling the sample to room temperature. The films of CuO was prepared by plasma assisted reactive vapour deposition method [29] using glass and quartz substrates. The thickness of the film deposited was of the order of one micron. The films also were annealed at temperatures from

100°C to 950°C, at intervals of 50°C, every time for 20 to 24 hours. In case of thin films on glass substrates, the annealing temperatures were restricted to 700°C after which the substrate glass melted.

The EPR spectra were recorded using a JEOL, JES-RE2X (Japan) EPR spectrometer operating in the X-band with 100KHz field modulation. X-ray diffraction studies were performed on the untreated $CuCO_3Cu(OH)_2H_2O$ and after annealing it at different temperatures, using a Philips PW 1050 powder diffractometer with monochromatized Cu Kα radiation, operating at 30KV and 20mA.

The X-ray diffraction pattern of untreated $CuCO_3Cu(OH)_2H_2O$ was different from those of the annealed ones, but among the samples annealed at different temperatures, there was no difference. The XRD of CuO was identical to the pattern obtained from the annealed samples. It was safely concluded that the $CuCO_3Cu(OH)_2H_2O$ converts to CuO on annealing at temperatures above 200°C. The experiments which will be described here were repeated with EPR silent CuO as the starting material and no difference was observed. Hence forth, in our discussion, we will refer to our material as copper oxide (CuO).

4.4 RESULTS

(a) **CuO Bulk Powder**

In CuO powder samples, no EPR signals were observed, when annealed at temperatures from 100°C to 400°C. But on annealing at 500°C, two weak separate signals, one broad signal at a lower field and the other a sharp one in the high field (g=2 region) appeared for the first time. On annealing the sample further at 600°C and 700°C, the broad signal got intensified and showed a down field shift and the sharp signal almost maintained its position, but marginal gain in intensity. On further raising the annealing temperature to 800°C, the broad signal shifted towards the sharp one and subsequently coalesced. On raising the temperature to 875°C and 950°C, the single signal reduced in width but gained much in intensity. In this case, even when only a very little specimen in kept in the sample tube, a clear, strong signal was observable, with the smallest possible receiver gain of the spectrometer. The spectra of the CuO powder sample annealed at different temperatures are shown in figure 4.5. In figure 4.6 the shift of the resonance field positions of the signals is illustrated. Due to overlap of the two signals, their exact profile could not be obtained. Hence in the figure 4.6, the resonance field position of the low field signal has been represented

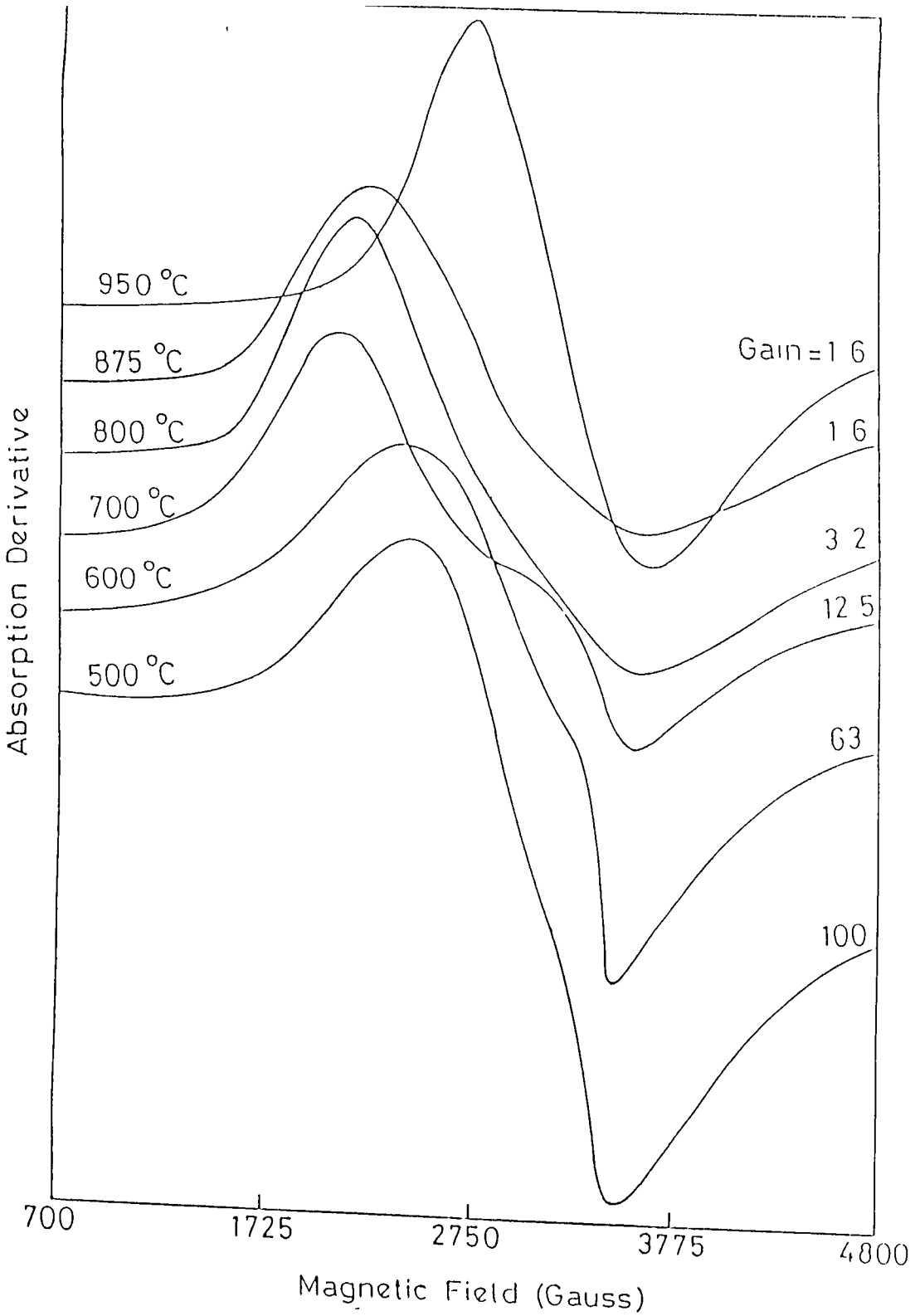

Fig. 4.5 EPR spectra of CuO annealed at different temperatures.

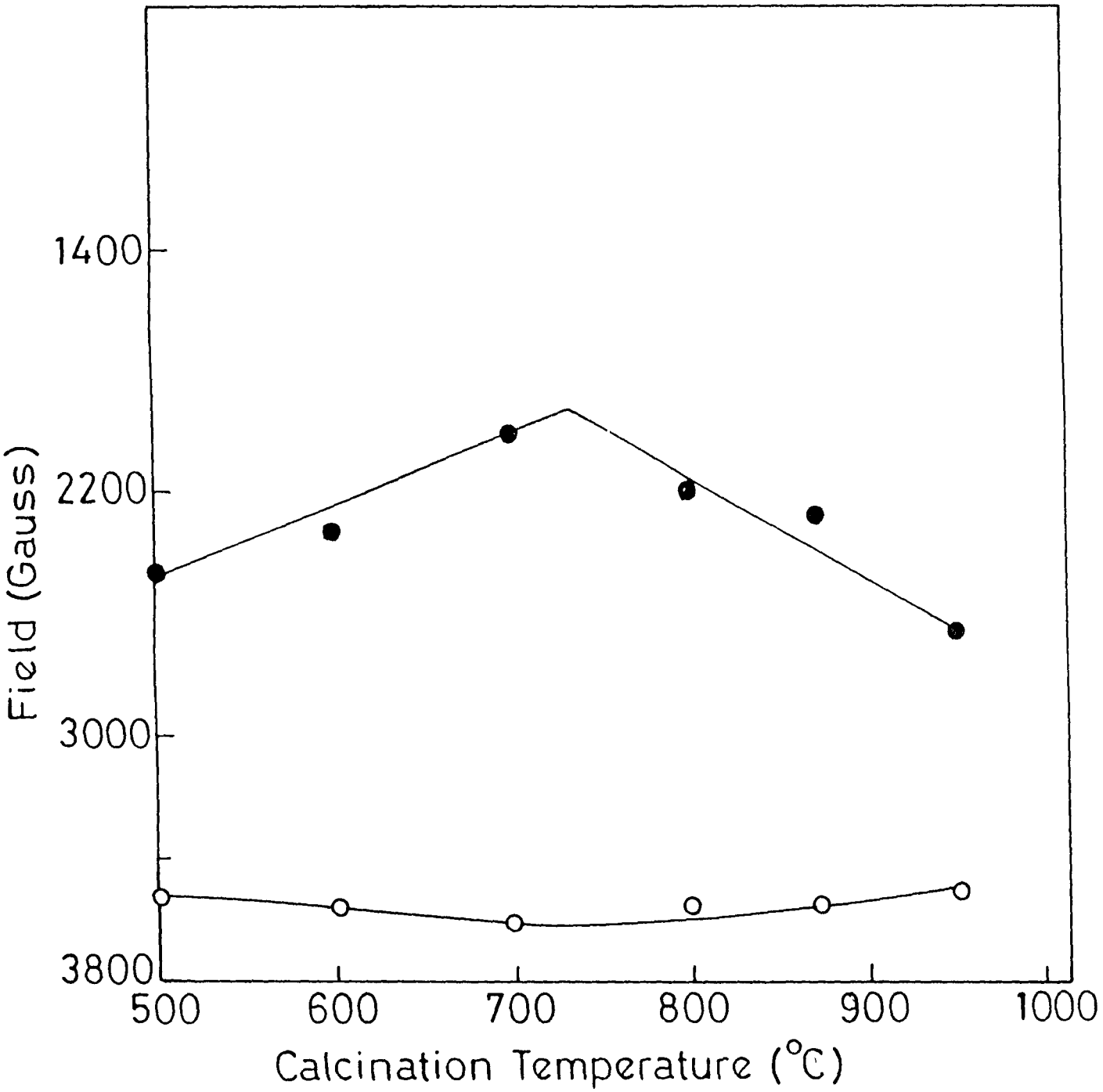

Fig.4.6 Variation of the resonance field of the signals in the EPR spectra of CuO with temperature. • for broad signal and o for sharp signal.

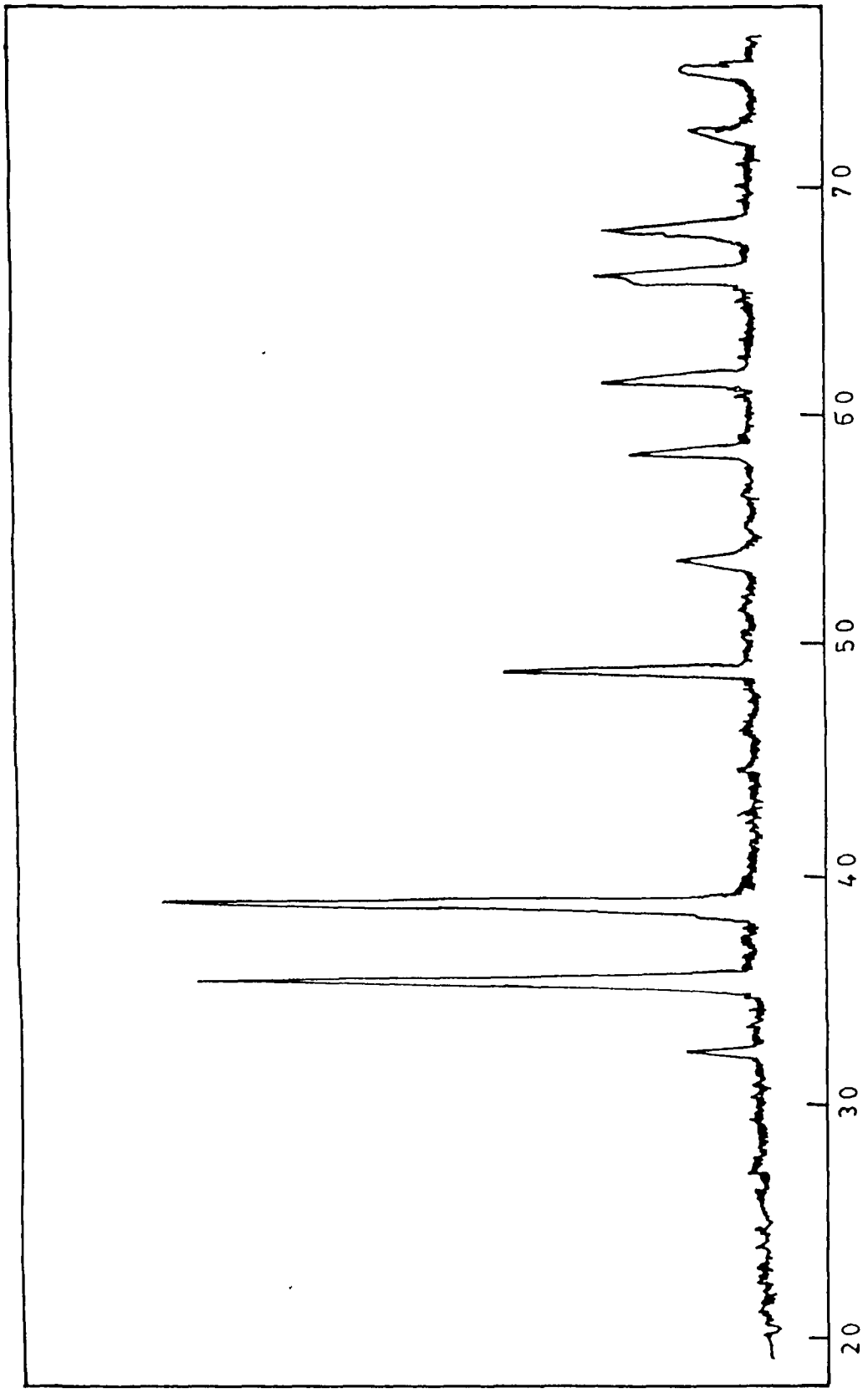

Fig. 4.7 XRD pattern of $CuCO_3Cu(OH)_2H_2O$ annealed at 950°C.

by the peak position of the upper half and that of the high field signal by the peak position of the lower half. The X-ray diffraction pattern of the untreated $CuCO_3Cu(OH)_2H_2O$ was same as reported. The XRD patterns of the sample annealed at different temperature were found identical and so the pattern of the sample annealed at 950°C is shown in figure 4.7 as a representative.

(b) **CuO Thin Films on Glass and Quartz Substrates**

In case of thin films of CuO deposited on glass substrates only signals of ordinary glass [30,31] were observed for samples annealed below 200°C (see figure 4.8(a) . On annealing at 200°C, a broad signal at a lower field and a very weak sharp signal at a little higher field ($g \sim 2$) started appearing. As the annealing temperature was raised to 300°C, the broad signal slightly intensified and shifted towards high magnetic field side and the sharp one also gained intensity but maintained its position. On further raising the temperature, the broad signal weakened and gradually shifted further and the sharp signal continued gaining intensity. At 600°C and above, the pattern changed with a very sharp signal appearing at the high field side ($g \sim 2$) accompanied by a weak four component hyperfine structured signal in the lower field side. The behaviour of the EPR signals of CuO film deposited on glass, annealed at different temperatures are shown in figure 4.8 .

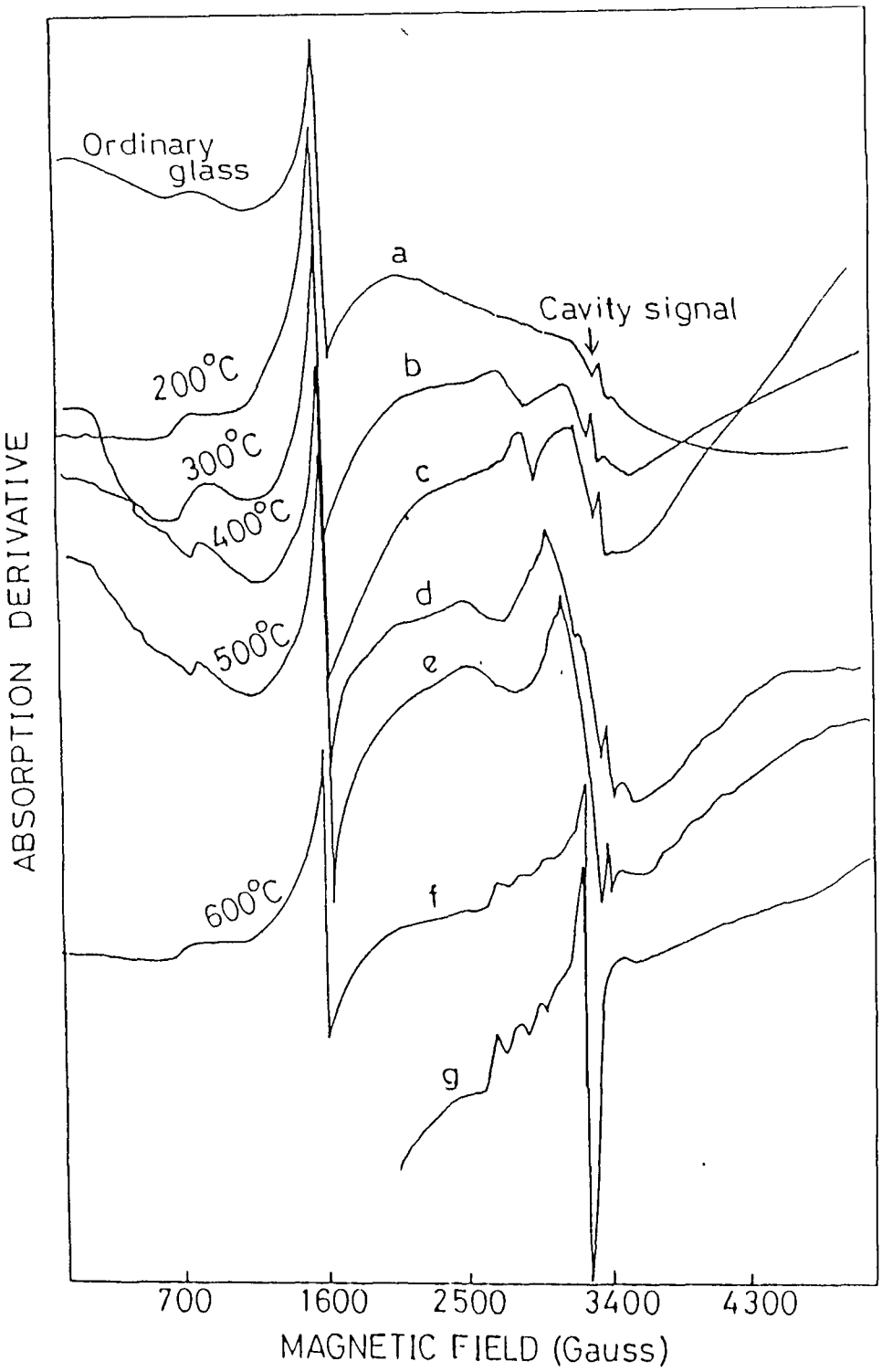

Fig. 4.8 EPR spectra of CuO thin film on glass substrate at different annealing temperatures. (a) Ordinary glass. (b to f) annealed at different temperatures indicated. (g) annealed at 700°C, shown partially. Arrow shows an unavoidable signal observed in our cavity.

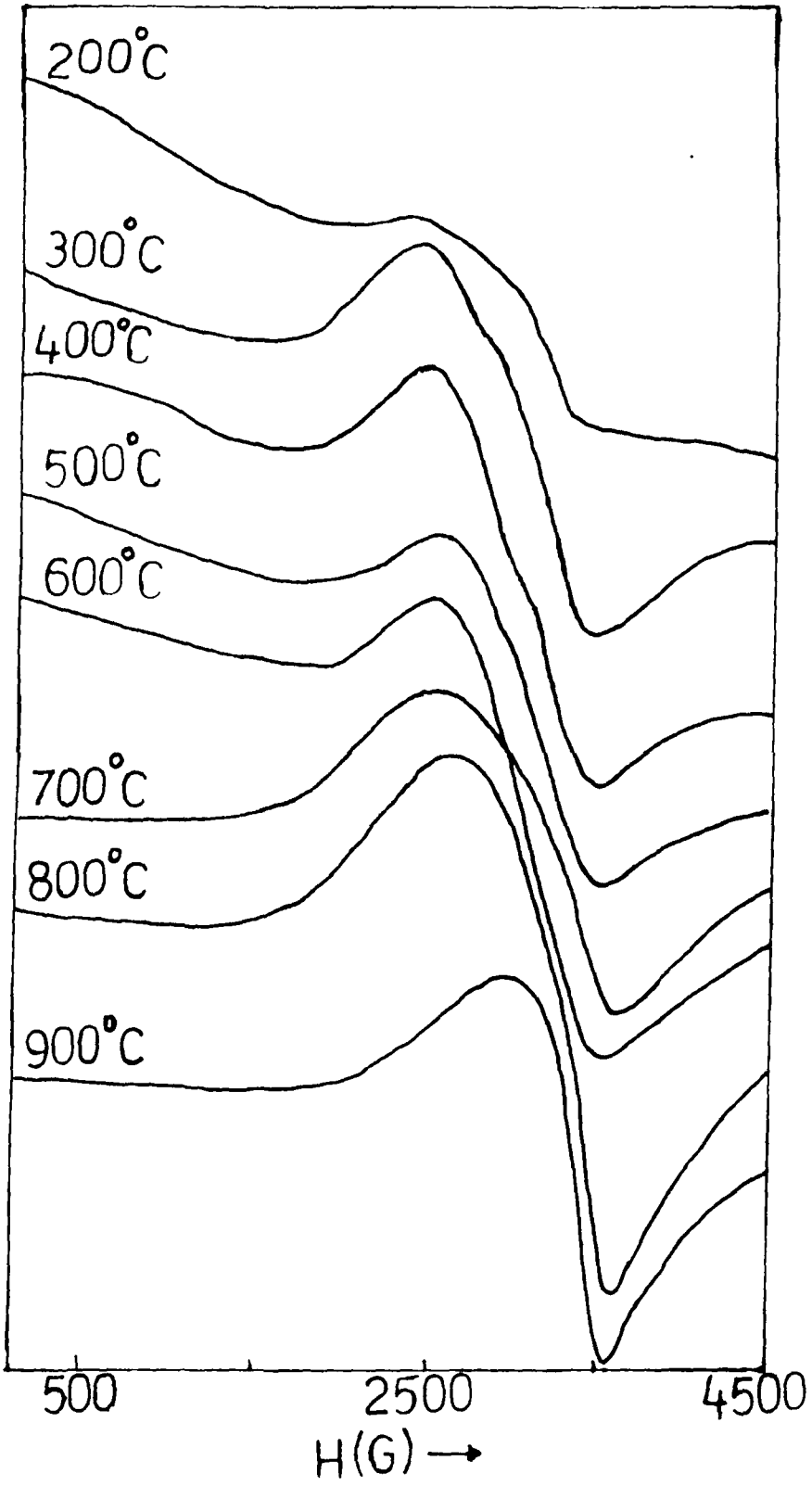

Fig. 4.9 EPR spectra of CuO film on quartz at different annealing temperatures.

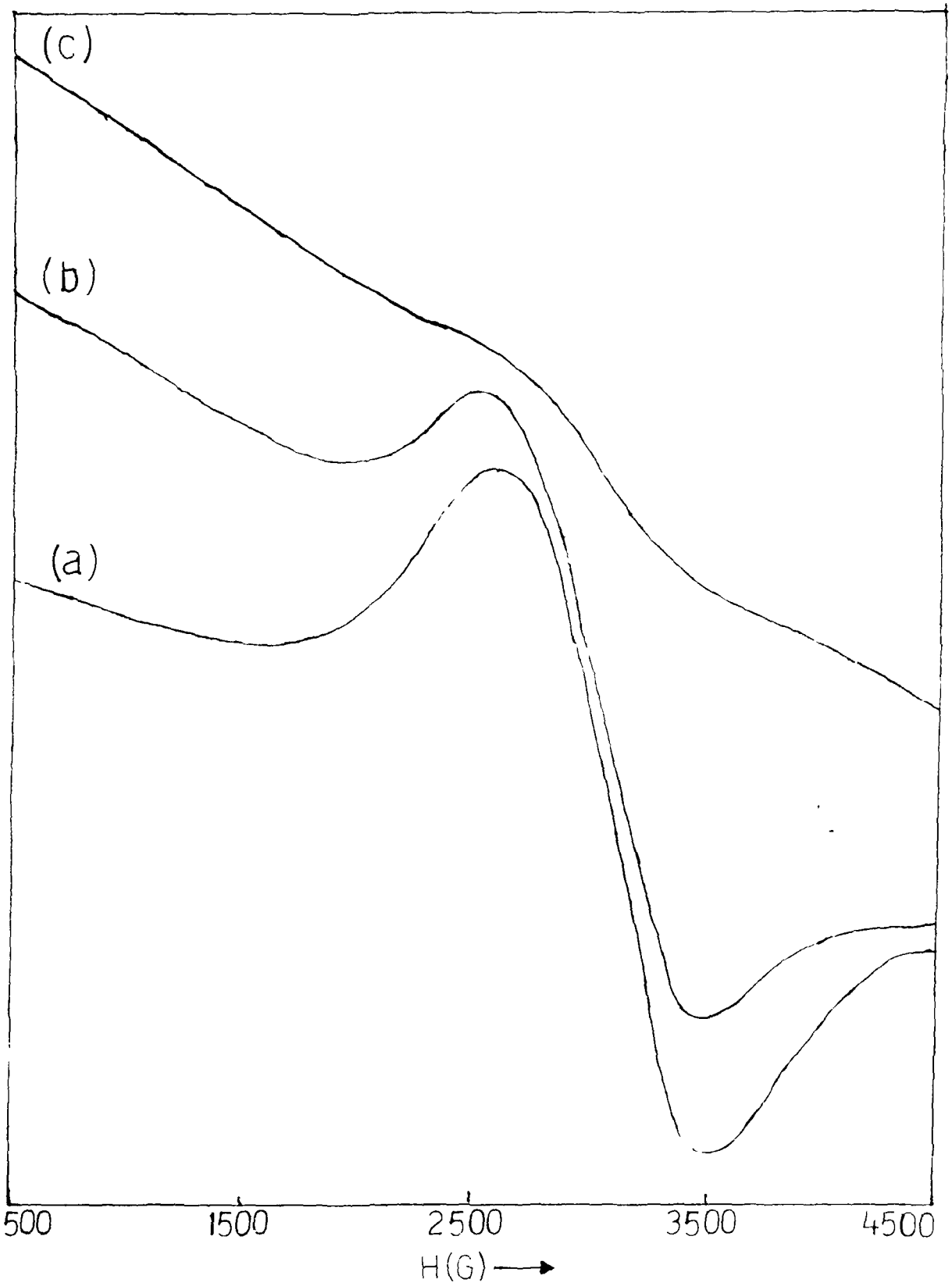

Fig. 4.10 Directional dependence of the EPR spectrum of CuO film on quartz annealed at 700°C. (a) At one typical position. (b) rotated 45° from (a). (c) rotated again through 45° from (b).

For the CuO film deposited on quartz, also, the signals first appeared at calcination temperature of 200°C and showed similar behaviour as that of CuO film on glass. Both broad and sharp signals are observed at lower calcination temperatures, which got amalgamated and sharpened on raising the temperature upto 500°C. At still higher temperatures, the single signal got intensified gradually upto 900°C. EPR spectra of CuO thin film on quartz substrates at different annealing temperatures are shown in figure 4.9.

There is one noteworthy feature. Thin film deposited on glass does not prominently display any directional dependence in the EPR spectrum. But for CuO film on quartz substrate, pronounced directional dependence of EPR spectrum was observed for calcination temperatures from 200°C to 800°C. Above 800°C, the directional dependence was completely lost. The directional dependence of the EPR spectra of CuO film on quartz is illustrated in figure 4.10.

4.5 DISCUSSIONS

(a) CuO Bulk Powder

In the present study, the observed absence of any EPR signal in CuO powder, upto the annealing temperature of 500°C is attributed to the short range magnetic order, which

is strong enough to prevent the signal from appearing [6,8,12,13,16]. On raising the annealing temperature to 500°C, the appearance of a broad signal is attributed to the weakened short range order still persisting in CuO and the sharp signal to the unassociated CuO molecules produced. On further raising the temperature to 800°C, the changes in the resonance field positions of the broad signal and the line width effects are characteristic of the destruction of the magnetic short range order in CuO, as is seen in many one dimensional magnetic systems [32-35]. The gradual intensification of the sharp upfield signal can be ascribed to the increase in the number of unassociated CuO molecules at the expense of the magnetically coupled ones. At 800°C and beyond, the merging of the two signals to a broad one indicated the vanishing of the short range order in this compound. At 950°C, the completely paramagnetic phase of CuO gives rise to a very intense single EPR signal at $g \sim 2$.

The intensity of the EPR signals of CuO at different annealing temperatures, were high enough that one cannot attribute them to be of any impurity origin. Furthermore the XRD pattern of the sample annealed at different temperatures were all found to be identical to that of CuO, which confirmed that the emitter of the signal at all annealing temperatures is CuO itself. The variation of the EPR signals of CuO observed at room temperature, with

annealing temperature needs to be explained. One possibility for this can be that CuO undergoes phase transformation on raising the annealing temperature. But this possibility can be ruled out because the XRD does not exhibits any change at any of the annealing temperature. Another plausible explanation may be that on raising the temperature, oxygen content is reduced and is not replenished fully by slow cooling of the sample. Detection of these small losses in oxygen content might be missed in XRD studies. It was pressumed that at the high temperatures of annealing, the magnetic order is destroyed, but is gained more or less on slow cooling, with every cycle of annealing and cooling, depending on the difference in oxygen content.

(b) **CuO Thin Films on Glass and Quartz Substrates**

In case of CuO films deposited on both glass and quartz substrates, the absence of signals upto 200°C is also ascribed to the persistence of the magnetic order which is strong enough to prevent the signals from appearing. Upon heating the films at and above 200°C, the magnetic interaction reduces, producing a mixture of some weakely coupled and some unassociated Cu^{2+} ions. The broad signal may be due to the weakened but still persisting magnetic order and the sharp one due to Cu^{2+} from unassociated CuO molecules.

Compared to bulk CuO, the early appearence of signals at 200°C can be ascribed to the easy breaking of the magnetic coupling in thin film form due to its two dimensional distribution. It is known that the binding energy of atoms and molecules in films are, on average, lower than that in the bulk,due to various kinds of defects and internal stresses present in the film structure. In the bulk powder, the dependence of the EPR signals with temperature was doubted to be due to the losses in oxygen content. In the thin films, such losses in oxygen content may be more easy to attain,due to their bidimensionality.

Upon raising the annealing temperature from 200°C to 500°C, the shift of the broad signal indicate the gradual destruction of the magnetic short range order. In case of CuO film on glass substrate, the substrate glass started softening at 600°C and so at this temperature and above, the Cu^{2+} ions formed by breaking the magnetic order in CuO, enters into suitable sites in the glass substrate and give rise to spectra similar to that reported for CuO dpoed in glass [30,31]. It is known that there are two different sites in glass as that of network formers and network modifiers. The two signals, one structured with four components and the other single sharp one observed in our study at and above 600°C, is also can be attributed to CuO entered in these two different glass sites as has been

reported else where also [30,31]. For the film on quartz, above 600°C the single signal shows an increase in width, which indicates the presence of strong dipolar interaction.

For CuO film on quartz, upto 800°C, there was strong directional dependence. This is attributed to the presence of orientational order of the film spread over the quartz substrate. At still higher temperatures, this regular orientation is upset by thermal motion resulting into the directionally independent EPR spectrum.

4.6 CONCLUSIONS

In both CuO bulk powder and thin films, even though the Neel temperature is 230K, strong short range magnetic order seems to persist upto much higher temperatures, in accordance with the observations from other studies. In bulk powder, the complete destruction of the magnetic order takesplace when annealed at temperatures of 700°C to 800°C. Above this a single intense signal due to purely paramagnetic Cu^{2+} is observed. The dependence of the EPR signals of CuO and thus the magnetic order in it, with annealing temperature indicates that the oxygen content may be changing.

In CuO films on both glass and quartz, the early appearence of the signals much earlier compared to that

(500°C) of CuO powder is attributed to the easy breaking of the magnetic order in them due to their bidimensionality. The complete destruction of the short range order takes place in films at around 500°C. For the CuO film on quartz, prominent directional dependence is observed which vanishes above 800°C. This is attributed to the orientational ordering between CuO film and quartz.

Thus it appears that the complicated magnetic interactions in CuO persists upto much higher temperatures. Similar complicated behaviours can be expected in many of its related compounds, obtained by reacting it with other oxides, including high-T_c superconductors. Thus it seems to be interesting to investigate the magnetic interactions in CuO and its binary and ternary oxides for a better understanding of the magnetism in the high-T_c cuprates.

REFERENCES

1. See for example, several Papers Presented in the Intl. Conf. High-T_c Supercond. Bangalore, India, Jan 1990.
2. D.Vaknin, et al, Phys. Rev. Lett. **58** (1987) 2802.
3. Y.J. Uemura, et al, Phys. Rev. Lett. **59** (1987) 1045.
4. J.W. Lynn, et al, Phys. Rev. Lett. **60** (1988) 2781.
5. W.H.Li, et al, Phys. Rev. B **38** (1988) 9844.
6. M. O'Keeffe and F.S.Stone, J. Phys. Chem. Solids **23** (1962) 261.
7. Jih-Heng Hu and Johnston H.L., J.Am.Chem.Soc. **75** (1953) 2471.
8. M.S.Seehra, Z.Feng and R.Gopalakrishnan, J. Phys. C: Solid State Phys. **21** (1988) L1051.
9. Y.Yamada, K.Sugawara and Y.Shiohara, Proc. of the ISS Conf. Tsukuba (1989) 547.
10. B.N. Brockhouse, Phys. Rev. A **94** (1954) 781.
11. B.X.Yang, J.M.Tranquada and G.Shirane, Phys. Rev. B **38** (1988) 174.
12. J.B. Forsyth, P.J. Brown and B.M.Wanklyn, J. Phys. C: Solid State, Phys. **21** (1988) 2917.
13. S. Asbrink and A. Waskowska, J. Phys: Condens. Matter **3** (1991) 8173.
14. F.Mehran and P.W.Anderson, Solid State Commun, **71** (1989) 29.

15. McKinnon, J.R.Morton and C.Pleizier, Solid State Commun, **66** (1988) 1093.

16. K.Kindo, M.Honda, T.Kohashi and M.Date J. Phys. Soc. Jpn. **59** (1990) 2332.

17. K.Tagaya, Jpn. J. Appl. Phys. **28** (1989) L566.

18. P.W. Anderson, Mat. Res. Bull. **8** (1973) 153.

19. P.W. Anderson, Science **235** (1987) 1196.

20. S.A. Kivelson, D.S. Rokhsar and J.P.Sethna, Phys. Rev. B **35** (1987) 8865.

21. F.Mehran, et al, Solid State Commun, **67** (1988) 1187.

22. R.J.Singh, Alex Punnoose, Jilson Mathew and Mohd. Umar Third Intl. Conf. on Mat. and Mech. of Superconductivity-High-T_c Supcond. [M^2S-HTSC III] Kanazawa, Japan, July (1991).

23. Alex Punnoose, et al, Phys. Lett. A (Communicated)

24. Alex Punnoose, et al, Mod. Phys. Lett. B (Communicated).

25. C.P.Poole Jr, T.Datta, H.A.Farach, "Copper Oxide Superconductors", (Wiley, NY) (1988).

26. Z.Ivanov, et al, Mod. Phys. Lett. B **3** (1989) 785.

27. H.Hagemann, et al, Solid State Commun, **73** (1990) 447.

28. S.Ashrink and L.J.Norby, Acta. Cryst. B **26** (1970) 8

29. M.Sohma and K.Kawaguchi, Solid State Commun, **79** (1991) 47.

30. R.H. Sands, Phys. Rev. **99** (1955) 1222.

31. T.Castner, et al, J. Chem. Phys. **32** (1960) 668.

32. F.J. Owens, C.P.Poole Jr., and H.A. Farach, "Magnetic Resonance of Phase Transitions",(Academic, New York) (1979).

33. K. Nagata and Y.Tazuke, J. Phys. Soc. Jpn. **32** (1972) 337.

34. K.Nagata, J. Phys. Soc. Jpn. **40** (1976) 1209.

35. Y.Tazuke and K.Nagata, J. Phys. Soc. Jpn. **38** (1975) 1003.

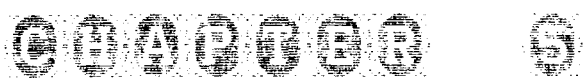

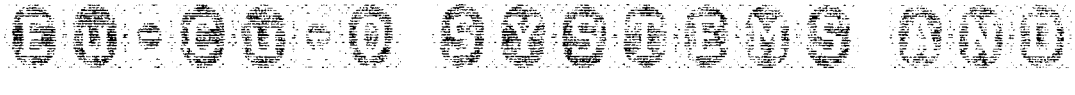

5.1 INTRODUCTION

Even though a great deal of work has been reported on the EPR of high-T_c superconductors, no systematic EPR study has been carried out in the parent compounds of the high-T_c cuprates, and their binary, ternary etc., combinations. A detailed study on these simpler systems may help to understand the magnetic properties and mechanism of the much more complex high-T_c superconductors. There have been many theoretical suggestions and experimental indications that mangentism plays an important role in the underlying superconducting mechanism in these compounds [1-5]. EPR is supposed to be a powerful technique to study these complicated magnetic properties. Most of the EPR investigations on the high-T_c superconductors indicated that the copper ions in these compounds are EPR silent as is mentioned in chapter 3. Even the basic constituent CuO also was reported to be EPR silent in the literature [6,7]. But recently we were able to observe strong EPR signals from this compound by subjecting the sample to successive heat treatments at much elevated temperatures [8,9], which we have discussed in chapter 4. This prompted us to monitor the EPR spectrum of the binary mixtures of BaO-CuO and Eu_2O_3-CuO which are parent systems of the Eu-Ba-Cu-O (123) superconductor, with a view to see how the EPR signal in CuO at each calcination temperature is modified by the addition

of BaO and Eu_2O_3 to it. The studies on the BaO-CuO and Eu_2O_3-CuO systems, are also important, as many phases in these systems were found to be present in the high-T_c superconducting compounds as impurities and giving extrinsic signals in their EPR spectra. To ascertain the EPR silence of the high-T_c superconductors, EPR is monitored in $EuBa_2Cu_3O_{7-d}$ superconductor prepared in our laboratory.

5.2 EXPERIMENTAL DETAILS

(a) **Ba-Cu-O system**

High purity samples of $BaCO_3$ and $CuCO_3Cu(OH)_2H_2O$ were the starting materials. In a few cases BaO and CuO were also used, but no change was seen in the observed EPR results. The BaO-CuO mixture was prepared from the starting materials, in a ratio to ensure equal number of Cu and Ba atoms within the mixture. The mixture is calcined at different temperatures from 100°C to 950°C, every time for 20 to 24 hours with two intermittent grindings. The calcination temperatures were 100,200,300,400,500,600,700, 800,900 and 950°C. The same sample was subjected to the entire heat treatments one after the other. EPR spectrum of the sample was recorded at room temperature after furnace cooling the sample from each calcination temperatures. The spectra were recorded on a JEOL, JES-RE2X (Japan) EPR

spectrometer, working in the X-band with 100KHz field modulation.

For resistance measurements, the samples were pelletised (1.2cm in diameter and 1mm in thickness) and sintered (for 8 to 10 hours) at their respective calcination temperatures. Resistance measurements were performed on each of these pellets under similar conditions using a multimeter (DM-9, PLA), with silver paste acting as electrodes. Powder X-ray diffraction measurements were performed on samples calcined at 500°C and 800°C on a Philips PW 1050 powder diffractometer with monochromatized Cu Kα radiation, operated at 30KV and 20mA. Reflectance spectra in the visible region were also recorded in these two samples using a Philips (Pye Unicam PU 8800) UV/Vis spectrophotometer.

(b) **Eu-Cu-O system**

High purity samples of Eu_2O_3 and $CuCO_3Cu(OH)_2H_2O$ (and some times CuO also) were mixed in the ratio Eu:Cu=1:3 and is intimately ground in a pestle and mortar. It is then successively calcined at different temperatures ranging from 100°C to 1000°C, each time for 20 to 24 hours with two intermittent grindings. Here also the calcination temperatures were the same as that of BaO-CuO system. EPR spectra were recorded on these samples at room temperature

after slow cooling from each calcination temperatures.

(c) **Eu-Ba-Cu-O Superconductor**

For the $EuBa_2Cu_3O_{7-d}$ superconductor the starting materials were Eu_2O_3, $BaCO_3$ and $CuCO_3Cu(OH)_2H_2O$. They were mixed in the proper ratio and the mixture is calcined for several hours at 900°C. It is then pelletized and sintered at 950°C for 10 to 12 hours. Conductivity measurements were performed using a four probe set up and T_c is found to be 90K. EPR is examined on a few pieces of the superconducting pellet at room temperature.

5.3 RESULTS

(a) **EPR and Resistance Studies of Ba-Cu-O System**

For the BaO-CuO mixture, no detectable signal was observed when calcined at temperatures below 300°C. But on calcining at 300°C, two seperate signals, a broad signal at a lower field and a sharp upfield signal, were observed for the first time. They got intensified on raising the calcination temperatures to 400°C and 500°C. At 600°C the broad signal disappeared leaving only a weak sharp signal. On calcining the sample at 700°C, in addition to the sharp signal, a new broad signal appeared in the lowfield side, which intensified and broadened on further raising the temperature. At 900°C, only one very strong and sharp

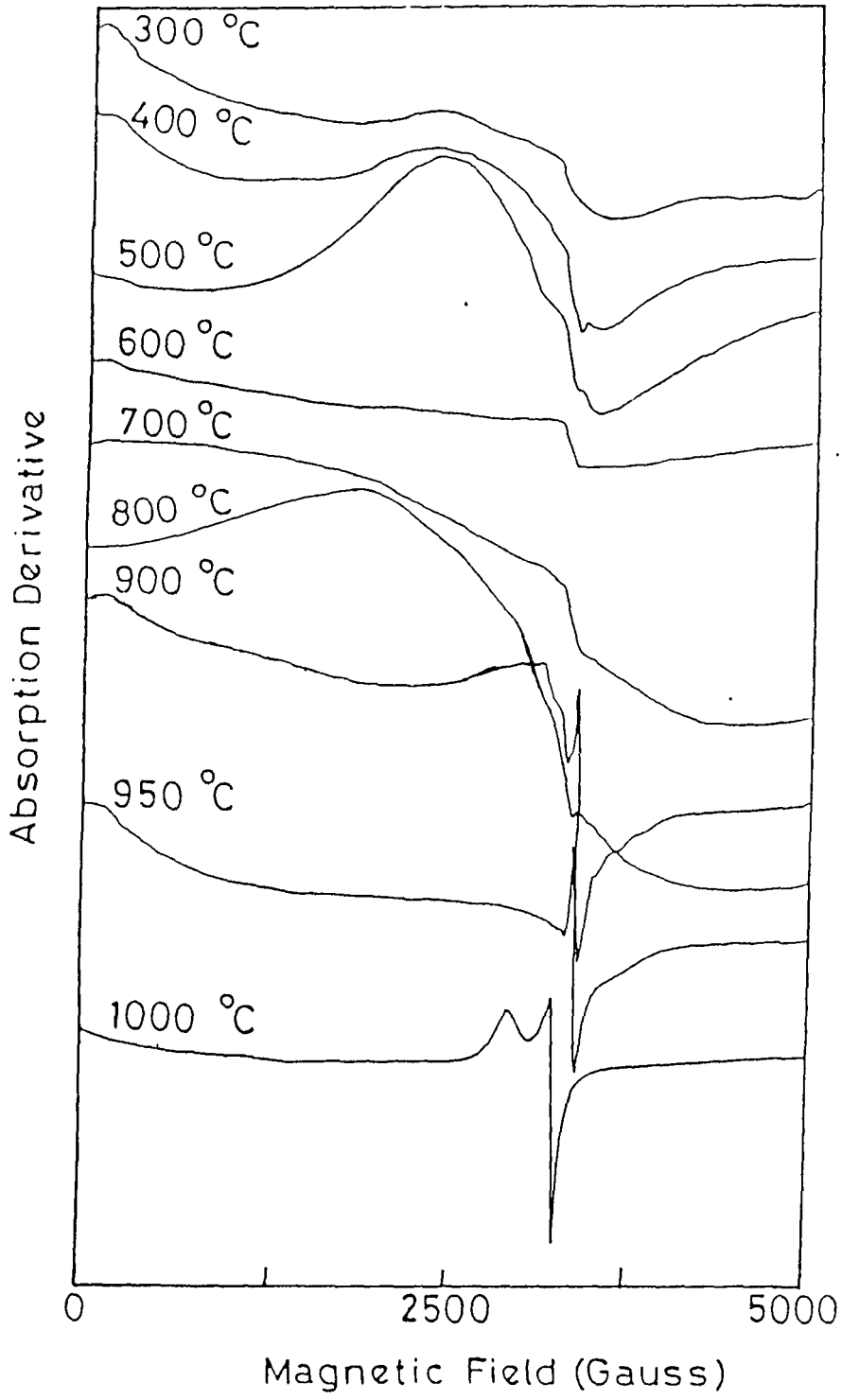

Fig. 5.1 EPR spectra of BaO-CuO system at various calcination temperatures.

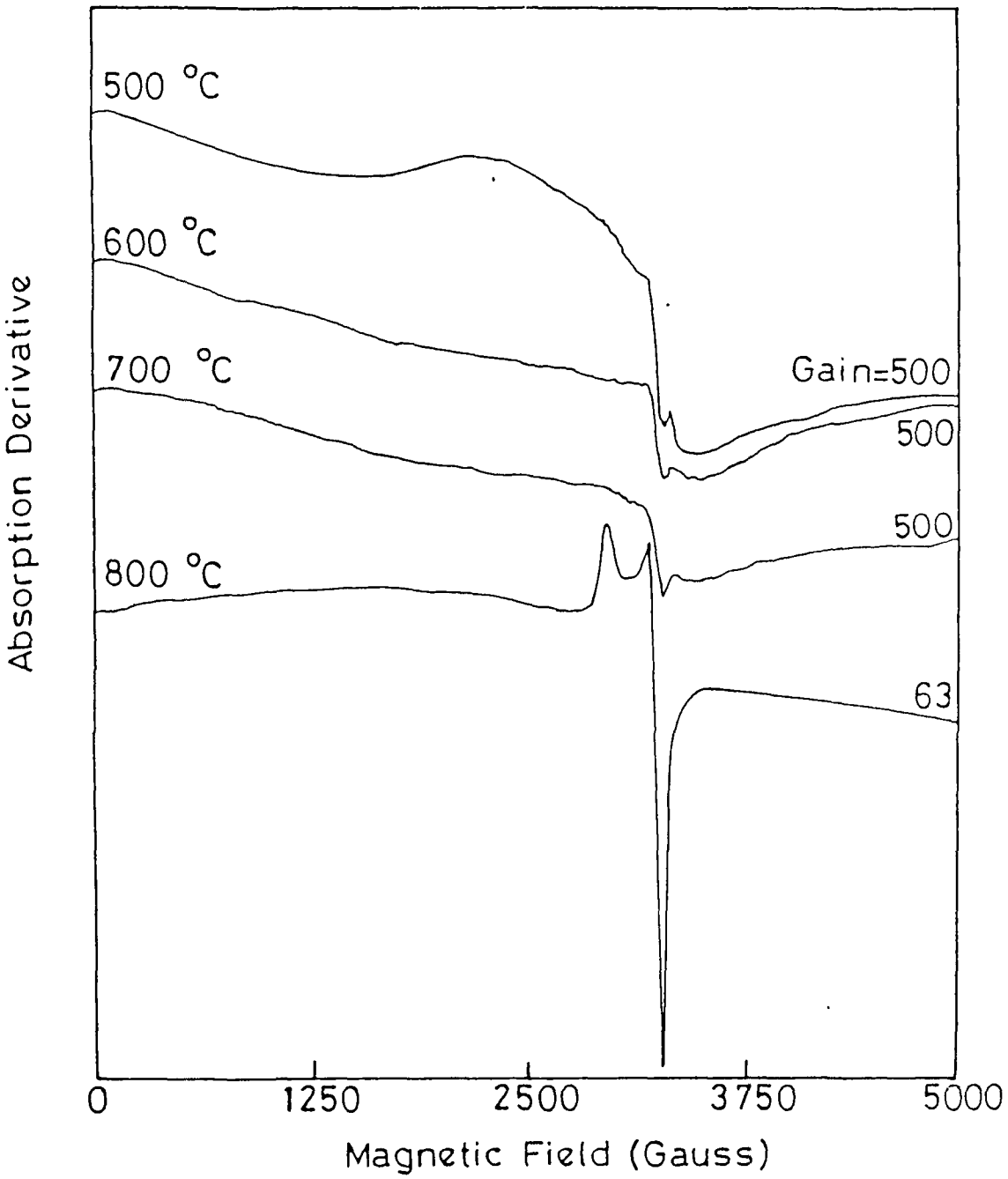

Fig. 5.2 EPR spectra of BaO-CuO mixture quenched from different calcination temperatures.

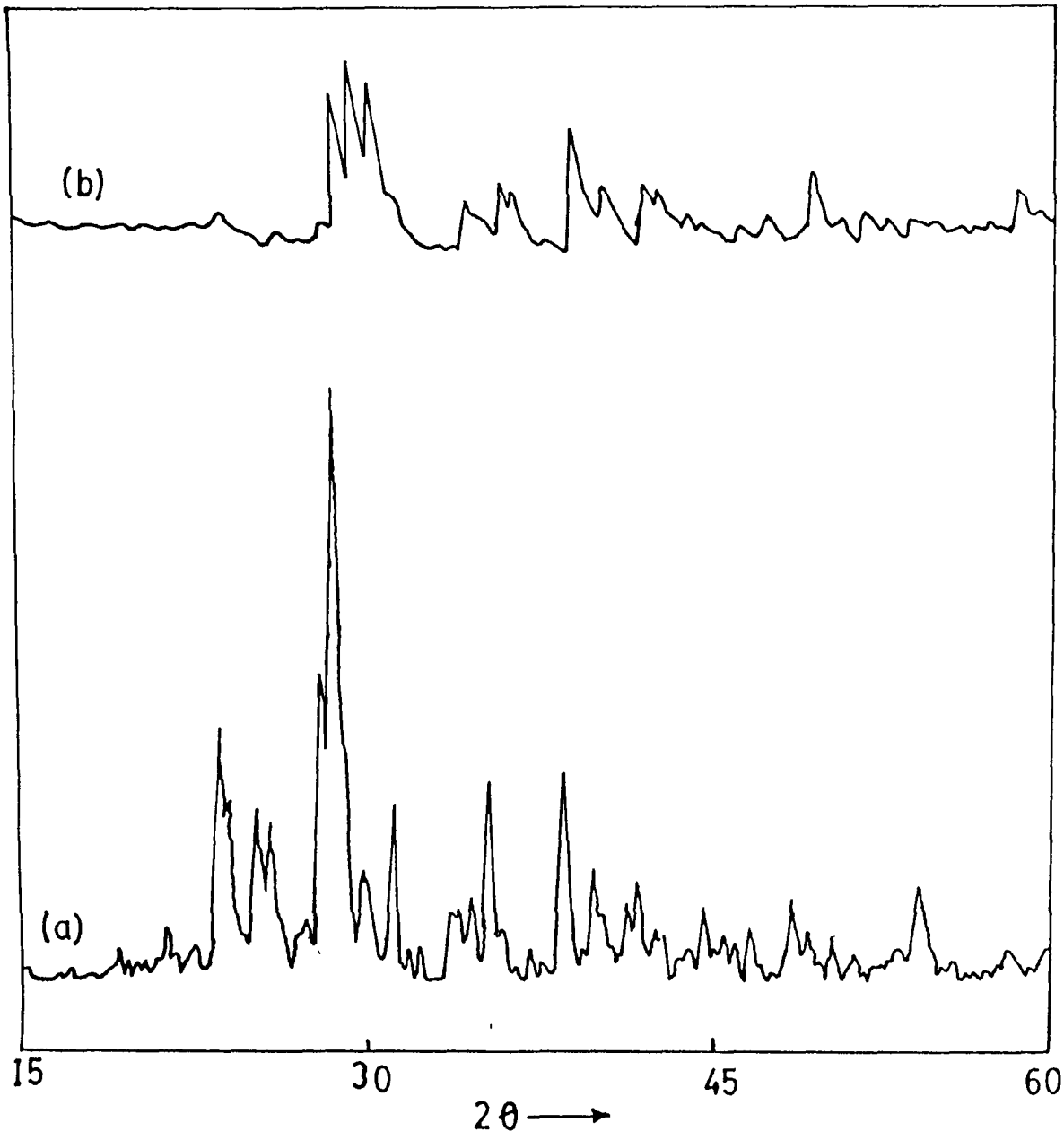

Fig. 5.3 XRD of BaO-CuO mixture calcined at (a) 500°C and (b)800°C.

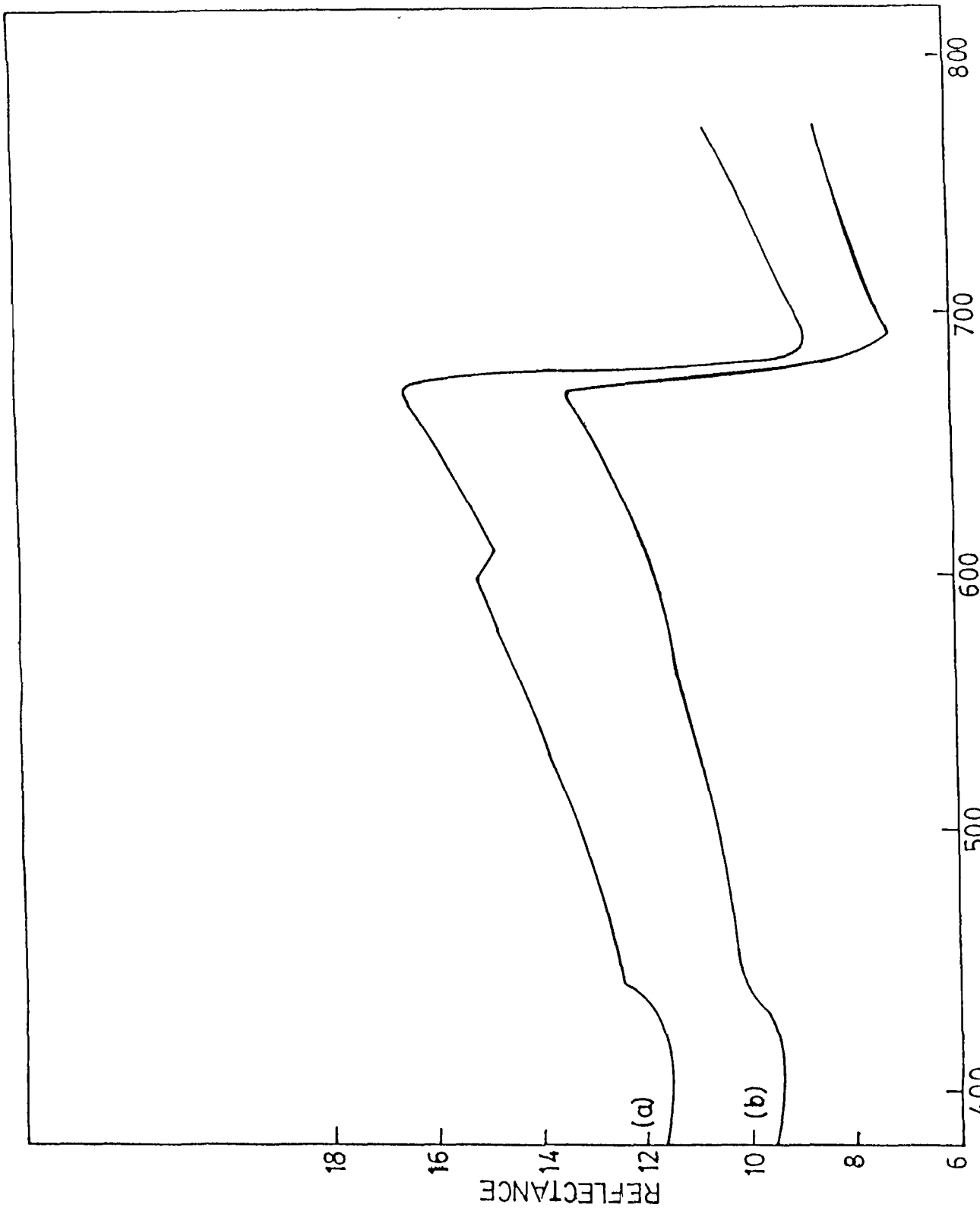

Fig. 5.4 Reflectance spectra of BaO-CuO combination at (a) 500°C and (b) 800°C.

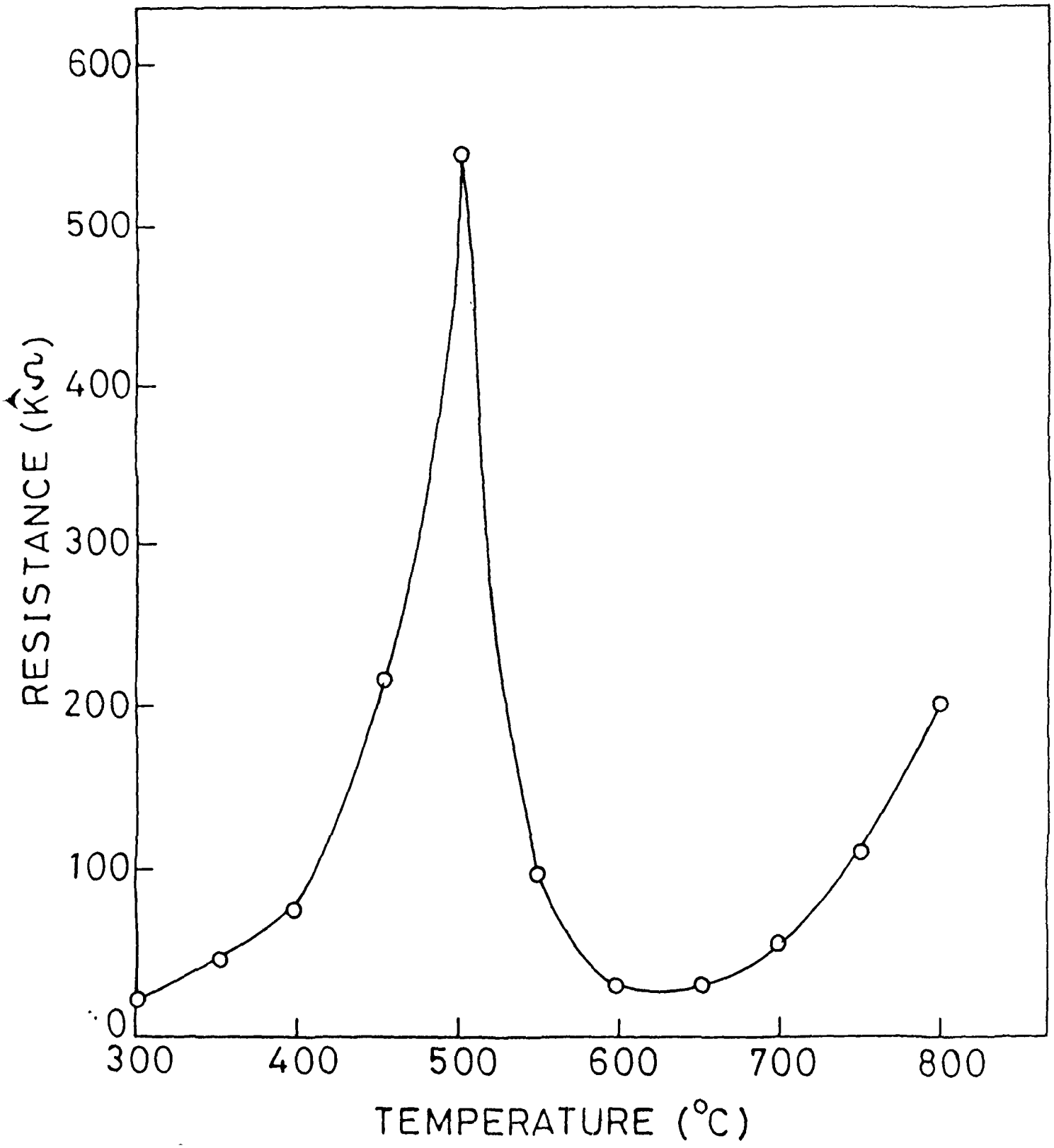

Fig. 5.5 Plot of Resistance vs calcination temperature of the pellets prepared from the BaO-CuO mixture.

signal is observed. At 950°C the spectrum consisted of two well resolved intense signals with their positions in the neighbourhood of the earlier sharp signal. The spectra of the sample calcined at various temperatures are shown in figure 5.1.

EPR spectra were also recorded on a few samples obtained by quenching the samples from each calcination temperature. In this case, the broad signal was found to be either appreciably reduced in intensity or totally absent as shown in figure 5.2. To ascertain any phase formation upon rising the calcination temperature, XRD patterns and reflectance spectra of the sample calcined at 500°C and 800°C were also taken and are shown in figures 5.3 and 5.4 respectively. Resistance measurements were performed on the pellets of the sample calcined at different temperature. The pellets were sintered at their corresponding calcination temperatures before measuring their resistance. The resistance shown an increase with the calcination temperature upto 500°C as shown in figure 5.5.

(b) **EPR Studies of Eu-Cu-O System**

In the case of Eu_2O_3-CuO binary combination, the first appearence of the signals is observed at calcination temperature of 200°C. The spectrum consisted of a broad signal at a lower field and a sharper signal in the high field side. The general behaviour of the signals in the

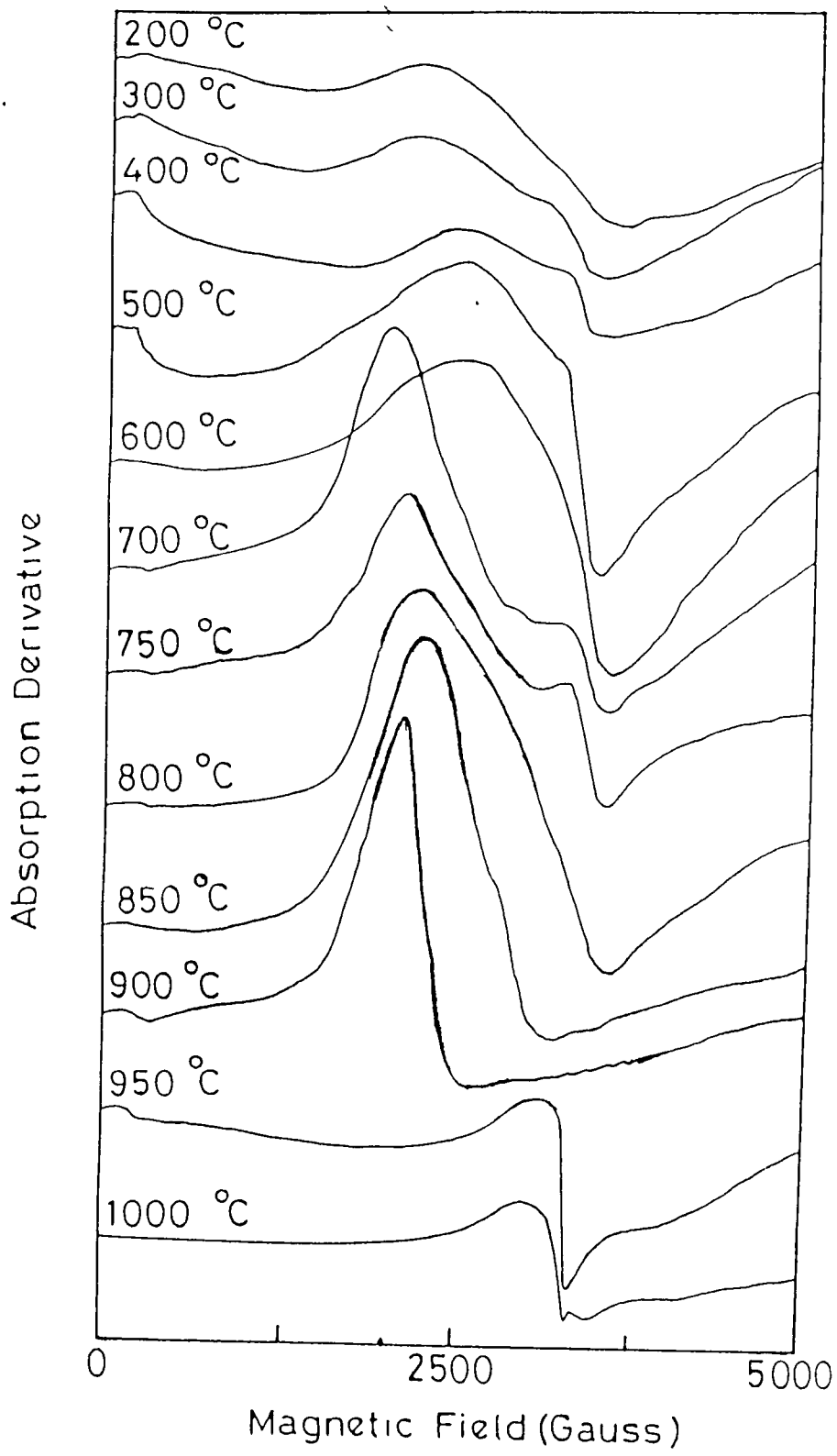

Fig. 5.6 EPR spectra of Eu_2O_3-CuO at different calcination temperatures.

lower calcination temperatures remained almost same as that of the Ba-Cu-O system. Both the broad and sharp signals which appeared at calcination temperature of 200°C, got intensified upto 500°C with the broad signal showing a gradual shift towards the sharp upfield signal. At 600°C, they got mixed and appears to be a single, broad, composite signal. Further calcination at 700°C, initiated the emergence of a new signal at a much lower field which gradually got intensified at still higher calcination temperatures, nullifying the earlier observed signal. At calcination temperatures of 800°C and 900°C, only the strong signal in the low field is observed with hardly any signal in the g~2 region. At 950°C and 1000°C, the signal pattern completely changed with a single signal in the low field side is found. The variation of the EPR signals of Eu_2O_3-CuO binary system is shown in figure 5.6.

(c) **EPR Study of Eu-Ba-Cu-O Superconductor**

For the preparation of $EuBa_2Cu_3O_{7-d}$ superconductor, the usual procedure of mixing Eu_2O_3, $CuCO_3Cu(OH)_2H_2O$ and $BaCO_3$ in the proper ratio, calcining it at 900°C and sintering the pelletized sample at 950°C, followed by slow cooling to room temperature, is adopted. From the conductivity measurements T_c was found to be 90K indicating that the procedure adopted by us is not defective. EPR spectra were monitored on different pieces of the

superconducting pellet and no appreciable signal is observed in all the cases.

It should be pointed out that in all these systems studied and presented here, for the entire temperature range, several samples were prepared and from each sample various portions were examined. There were minor changes in the spectra from sample to sample, but on the whole, there was convincing reproducibility.

5.4 DISCUSSIONS

(a) **Ba-Cu-O System**

In chapter 4, it was found that the CuO powder is EPR silent, when annealed below 500°C. This was attributed to the persistence of strong short range magnetic order in the compound [10-13]. In CuO, the appearence of the broad low field signal and a sharp upfield signal, when annealed at 500°C, is attributed to the weakening of this short range order. Upon annealing at still higher temperatures upto 800°C the signals got intensified, came closer and gradually amalgamated. The broad signal was ascribed to the presence of weakened short range order and the sharp one to Cu^{2+} from unassociated CuO molecules. The vanishing of the broad signal at 800°C has shown complete destruction of the magnetic order in CuO. Above 800°C, the purely paramagnetic

phase of CuO gives rise to a single strong signal at g~2, characteristic of Cu^{2+}.

In BaO-CuO combination also, the absence of any signal below 300°C is again ascribed to the short range magnetic order in CuO. On calcining at 300°C and above, the magnetic interaction weakens, resulting into the emergence of two separate signals. The broad signal is due to the weakened magnetic order and the sharp one due to the Cu^{2+} from the unassocated CuO molecules. At 600°C, the observed absence of any broad lowfield signal indicates vanishing of the remnants of the short range magnetic order and the sharp signal at g~2 may be due to the Cu^{2+} from the completely paramagnetic CuO. In case of BaO-CuO mixture, the early appearence of the signals at 300°C compared to that of CuO (500°C) and the destruction of magnetic order at 600°C in contrast to 800°C for CuO seem to be quite significant. This can be understood in terms of dilution effect of BaO in the CuO chains. On calcining the mixture at higher temperatures, the magnetic coupling in CuO vanishes, but during relaxation on cooling, the CuO chains get interspersed by BaO molecules. This effectively reduces the coupling strength.

When the calcination temperature is raised to 700°C, the emergence of a broad signal in the lowfield suggests the

formation of some new phase. On raising the calcination temperature to 800°C, the further intensification and broadening of this signal indicate that the new formation which started at 700°C, continued at higher temperatures also. The broadening of this signal is indicative of some spin ordering associated with the phase, as has been observed elsewhere also [14-17]. At calcination temperatures of 900°C and 950°C, the observation of the sharp signals at $g \sim 2$ can be attributed to the paramagnetic Cu^{2+} ions.

At calcination temperatures below 700°C, the changes in the EPR spectra are expected to be governed only by the dilution effect of BaO on CuO chains and the consequent weakening of the magnetic interaction. No phase formation is thought to be realised in this range as is suggested from other studies also [18]. To ascertain the formation of new phases at higher calcination temperatures, X-ray diffraction patterns and reflectance spectra were taken for the sample calcined at 500°C and 800°C. Phases of the samples have not been identified, but X-ray diffraction patterns and reflectance spectra provide convincing evidence that on going from 500°C to 800°C, phase formation has certainly taken place. The close resemblence of the X-ray diffraction pattern and EPR spectrum of the sample calcined at 800°C, with that of the $BaCuO_2$ reported earlier [15-19] suggest

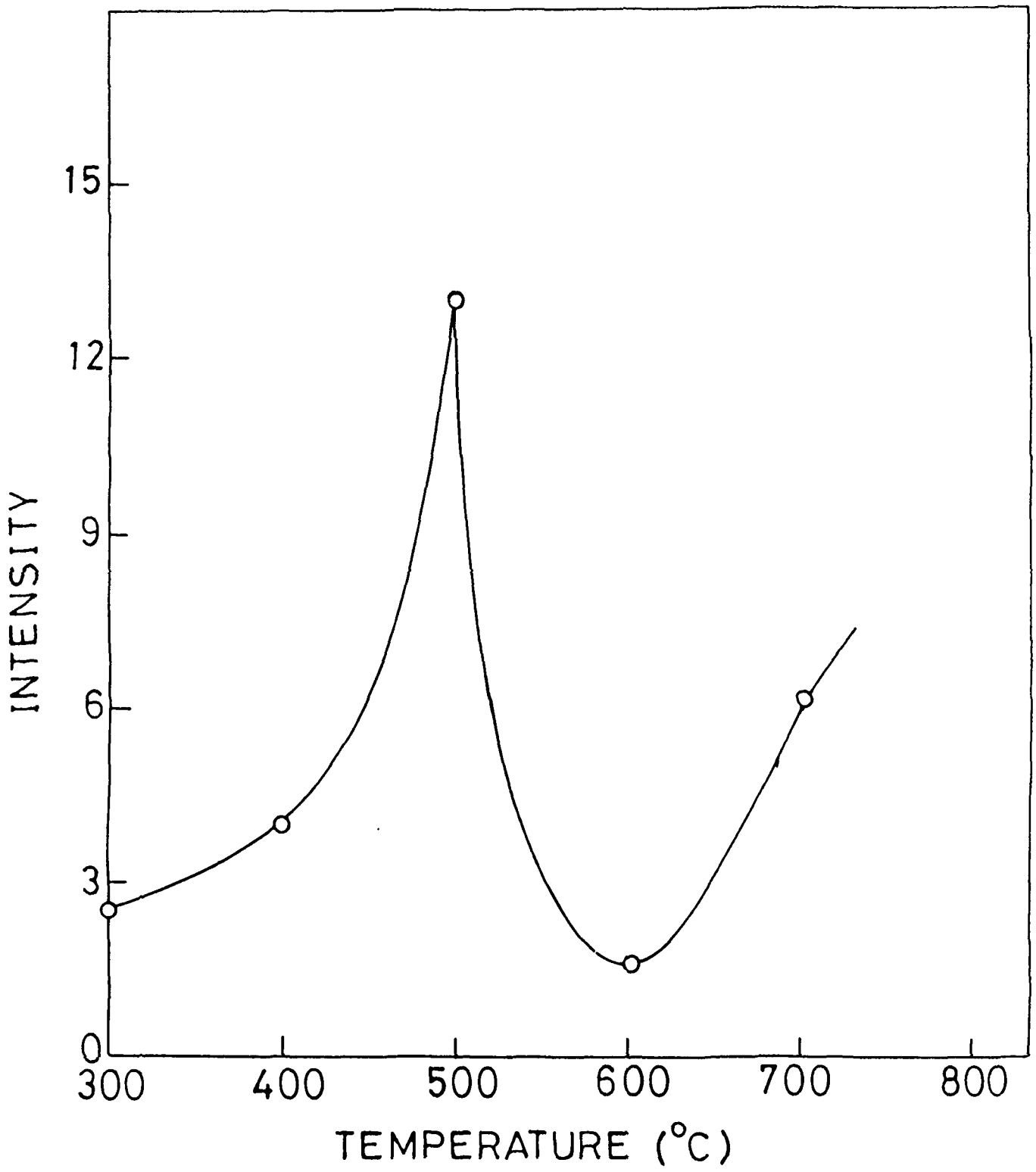

Fig. 5.7 Variation of the intensity of the broad signal in the EPR spectra of BaO-CuO system with calcination temperatures.

that the phase formed at 800°C in our experiment also is $BaCuO_2$.

In quenched samples, the observed reduction in the intensity of the broad signal at 500°C and its complete absence at 600°C and 700°C supports our assignment of the broad signal to weak short range magnetic order in the compound. In case of rapid quenching no time is allowed for regaining the magnetic coupling which was destroyed at high temperatures. We have attributed broad signal observed in the slow cooled samples at calcination temperatures of 300°C, 400°C and 500°C to weakened magnetic order in CuO. The absence of this broad signal at 600°C was suggested to be indicative of the complete destruction of the magnetic order. To ascertain transition from the magnetically ordered phase to the paramagnetic phase, resistance measurements were also performed on pellets prepared from samples calcined at these temperatures. The variation of the resistance with calcination temperature is shown in figure 5.5. Variation of the intensity of the observed broad signal (taken in arbitrary units) with calcination temperatures (shown in figure 5.7) follows the same pattern as that of resistance. The similarity of the two curves suggests that the increase in electrical resistance upto 500°C is due to the contribution from spin disordered scattering as observed in many magnetic systems [20,21].

This result thus supports the EPR observation of a phase transition in the Ba-Cu-O system at calcination temperature of around 600°C.

(b) **Eu-Cu-O System**

In this system also, the observed absence of any EPR signal upto the calcination temperature of 200°C is attributed to the persistence of the short range order in CuO [10-13]. The appearence of a broad lowfield signal and a sharp upfield signal on calcining at 200°C and their intensification and mixing up of the signals at higher temperatures indicate weakening of the order. The broad signal is due to the weakly coupled Cu ions and the sharp one due to Cu^{2+} from unassociated CuO molecules. The vanishing of the broad signal at 600°C indicate the destruction of the short range magnetic order in CuO. On raising the calcination temperature to 700°C and above, the emergence and gradual intensification of a broad signal at a lower field and the weakening and subsequent absence of the signal at $g\sim2$ indicates the formation of a new phase associated with magnetic ordering. The complete absence of this signal at 900°C and 950°C and the appearance of the signal at $g\sim2$, may be due to vanishing of this ordering, so that only a single signal due to paramagnetic Cu^{2+} is observed.

(c) $EuBa_2Cu_3O_{7-d}$ Superconductor

In the EPR study at room temperature carried out on the superconducting pellets of $EuBa_2Cu_3O_{7-d}$, the observed absence of any signal is in support of the hypothesis that copper in the high-T_c superconductors is EPR silent. In the Ba-Cu-O and Eu-Cu-O binary systems studied, phases associated with magnetic ordering are found to form at higher calcination temperatures. In superconducting phases also such magnetic ordering might have been formed which are strong enough to prevent any EPR signals as is explained by many others also [22-25].

5.5 CONCLUSIONS

In CuO bulk powder, no EPR signal was observed, when annealed below 500°C, which is attributed to strong short range magnetic order persisting in this compound. At 500°C and above, the appearence of a broad low field signal and a sharp upfield signal were thought to be indicative of the weakening of this short range order. Above 800°C, the vanishing of the broad signal, leaving a strong single signal in the g=2 region indicated complete destruction of the magnetic order in CuO. But in Ba-Cu-O system, the first appearence of the signals at 300°C, which is much earlier compared to that of CuO, indicates early weakening of the magnetic order in CuO due to the dilution effect of BaO on

CuO chains. The absence of the broad signal at 600°C shows the destruction of the magnetic order in CuO. This is also confirmed from the resistance measurements. Above 600°C, EPR as well as X-ray results indicate the formation of some new phases associated with spin orderings.

At lower calcination temperatures, Eu-Cu-O system also exhibited similar behaviours. In this case the signals were first observed when calcined at 200°C. At higher calcination temperatures the gradual shift and subsequent amalgamation of the signals at 600°C, indicate complete destruction of the short range order persisted in CuO. In Eu-Cu-O system also, above 600°C, the EPR spectra indicated formation of new phases, probably associated with magnetic ordering. In both BaO-CuO and Cu_2O_3-CuO mixtures, in the calcination temperature range of 900 to 950°C, strong signal at g_N2 were observed and are attributed to unassociated Cu^{2+}. In the high-T_c superconductor, $EuBa_2Cu_3O_{7-d}$ studied, no EPR signal could be detected. This is in support of the hypothesis that copper in high-T_c cuprates is EPR silent.

REFERENCES

1. W.E. Pickett, Rev. Mod. Phys. **61** (1989) 433.
2. S.W. Cheong, J.D. Thompson and Z.Fisk, Physica, **158C** (1989) 109.
3. J.M. Tranquada, et al, Phys. Rev. Lett., **60** (1988) 156.
4. S.B. Oseroff, et al, Phys. Rev. B **41** (1990) 1934.
5. R.J. Bigeneau and G.Shirane in "Physical Properties of High Temperature Superconductors", ed. D.M. Ginsberg (World Scientific, Singapore) (1989).
6. F. Mehran and P.W. Anderson, Solid State Commun, **71** (1989) 29.
7. W.R. McKinnon, J.R. Morton and C.Pleizier, Solid State Commun, **66** (1988) 1093.
8. Alex Punnoose, et al, Phys. Lett. A (communicated).
9. R.J. Singh, Alex Punnoose, Jilson Mathew and Mohd. Umar, Third. Intl. Conf. on Mat. and Mech. of Superconductivity High-T_c Supercond. [M^2S-HTSC III] Kanazawa, Japan, July (1991).
10. M. O'Keeffe and F.S. Stone, J. Phys. Chem. Solids **23** (1962) 261.
11. M.S. Seehra, Z.Feng and R.Gopalakrishnan, J. Phys. C: Solid State Phys. **21** (1988) 1051.
12. J.B. Forsyth, P.J. Brown and B.M.Wanklyn, J. Phys. C: Solid State Phys. **21** (1988) 2917.
13. S.Asbrink and A.Washowska, J.Phys.: Condens. Matter **3** (1991) 8173.

14. Mitsuhiro Motokawa, et al, J. Phys. Soc. Jpn. **54** (1985) 4767.

15. Jiang-Tsu Yu and K.H. Lii, Solid State Commun, **65** (1988) 1379.

16. M.Arjomand and D.J. Machin, J.C.S. Dalton, (1975) 1061.

17. Ruth Jones, et al, J.C.S.Faraday Trans. **86** (1990) 675.

18. U. Anselmi-Tamburini, et al, J. Phys. Chem. Solids **52** (1991) 715.

19. G.J. Bowden, et al, J. Phys. C: Solid State Phys. **20** (1987) L545.

20. M.E.Fisher and J.S. Langer, Phys. Rev. Lett., **20** (1968) 665.

21. D.S. Simons and M.B. Salamon, Phys. Rev. Lett., **26** (1971) 750.

22. S.Chakravarty and R.Orbach, Phys. Rev. Lett., **64** (1990) 224.

23. A. Deville, et al, Physica C, **153-155** (1990) 669.

24. G.Shirane, et al, Phys. Rev. Lett., **59** (1987) 1613.

25. A. Chakraborty, et al, Phys. Rev. B **40** (1989) 5296.

LIST OF PUBLICATIONS

1. "AF Origin of High-T_c Superconductivity": R.J. Singh, **Alex Punnoose**, Jilson Mathew and Mohd. Umar.
   Third Intl. Conf. Mat. and Mech. of Superconductivity-High-T_c Superconductors [M^2S-HTSC III], Kanazawa, Japan, July 22-26 (1991).

2. "A Mechanism of High-T_c Superconductivity": R.J. Singh, **Alex Punnoose**, Jilson Mathew and Mohd. Umar.
   Symposium H, Materials Research Society Fall Meeting, Boston, USA, Dec. 2-6, (1991).

3. "Magnetism of CuO and Superconductors": **Alex Punnoose**, Jilson Mathew, B.P. Maurya, Mohd. Umar and R.J. Singh.
   Communicated to Phys. Lett. A.

4. "EPR Studies of CuO Bulk powder and Thin films": **Alex Punnoose**, Jilson Mathew, B.P. Maurya, Mohd. Umar and R.J. Singh.
   Submitted after corrections to Mod. Phys. Lett. B.

5. "EPR Study of CuO Thin Films": **Alex Punnoose**, Jilson Mathew, Mohd. Umar and R.J. Singh.
   Materials Research Society, Spring Meeting, San Fransisco, USA, April 27- May 1 (1992).

6. "Magnetic Phase Transition in BaO-CuO System": **Alex Punnoose**, Jilson Mathew, Mohd. Umar and R.J. Singh.
   Materials Research Society, Spring Meeting, San Francisco, USA, April 27-May 1, (1992).

7. "Four Spin Cyclic Exchange Mechanism of High-T_c Superconductivity": **Alex Punnoose**, Jilson Mathew, Mohd. Umar and R.J. Singh.
   Condensed Matter and Materials Physics Conference [CMMP-91] Birmingham, UK, Dec. 17-19 (1991).

8. "EPR and Resistance Studies of BaO-CuO System": **Alex Punnoose**, Jilson Mathew, B.P. Maurya, Mohd. Umar and R.J. Singh.
   Submitted after revision to Mod. Phys. Lett. B.

9. "Four Spin Cyclic Exchange: Mechanism of High Temperature Superconductivity": R.J. Singh, **Alex Punnoose**, Jilson Mathew, B.P. Maurya, Mohd. Umar and M.I. Haque.
   Communicated to Phys. Rev. B.

10. "Four Spin Cyclic Exchange in Parent Binary Systems of 123 Superconductor": **Alex Punnoose**, Jilson Mathew, B.P. Maurya, Mohd. Umar and R.J. Singh.
    Third World Congress on Superconductivity, Munich, Germany, Sept. 14-18, (1992). [to be held].